

**ANALYSIS OF SMALL BIOMOLECULES
BY ESI- AND MALDI- MASS SPECTROMETRY**

**ANALYSIS OF SMALL BIOMOLECULES
BY ESI- AND MALDI- MASS SPECTROMETRY**

By

Rashidah Mohd Pilus, B. Sc.

A Thesis

Submitted to the School of Graduate Studies

In Partial Fulfillment of the Requirements

for the Degree

Master of Science

McMaster University

© Copyright by Rashidah Mohd Pilus, February 2004

MASTER OF SCIENCE
(Chemistry)

McMaster University
Hamilton, Ontario

TITLE : Analysis of small biomolecules ESI- and MALDI-
 Mass Spectrometry

AUTHOR : Rashidah Mohd Pilus (McMaster by University)

SUPERVISOR : Dr. Johan K. Terlouw

NUMBER OF PAGES : xii, 95

ABSTRACT

This thesis describes the use of mass spectrometric methods based upon electrospray ionization, ESI, and (matrix-assisted) laser desorption/ionization, (MA)LDI, for the quantitative analysis of small biomolecules. Structure analysis when required, was obtained through tandem mass spectrometry (MS/MS).

The Girard type reagent, 4-hydrazino-4-oxobutyl tris(2,4,6-trimethoxy)phenyl phosphonium bromide, in combination with the solid phase derivatization technique, is used to selectively prepare a pre-ionized malondialdehyde derivative to be analyzed by MALDI or LDI. The in situ derivatization and isolation minimize interferences from other components in biological samples. The combination of pre-ionization and aromatic functionalities allows for laser induced ionization without the need of matrix. The combination of these techniques provides an avenue for development of automation to produce a high throughput method of analysis.

Chapter 3 involves the study of the complexation of diols to the oxovanadium ion. The oxovanadium (IV) complex of ethylene glycol is used as a reference to study the complexation of other diols and amines with the vanadyl ion. The ES spectra of various diols studied produce intense signals for the mixed and the analyte complexes, indicating effective complexation of the analytes with the vanadyl ion.

Oxovanadium (IV) is observed to be more selective for complexation to diols than amines. This eliminates the possibility of interference from N-containing ligands to the detection of diols by the reference complex. The electrospray spectrum is used for quantitation and the tandem mass spectrometry spectrum for structure confirmation. The MS/MS spectrum also assists the identification of the diols by the structural differences within their isomers. The equilibrium constant of a set of diols was determined and its calibration curve were constructed. This study produces an alternative method to detect and quantify diols in aqueous solutions and blood samples.

ACKNOWLEDGEMENTS

I would like to acknowledge the people who have been instrumental to the completion of my graduate studies. First and foremost, I would like to thank my supervisor, Dr. Johan K. Terlouw : without your persistence and encouragement, it would have been difficult for me to accomplish my goals. You are an excellent professor and dedicated to your students and their achievements. Thank you for the opportunity I had working with you.

Thank you Dr. Jack Rosenfeld for the knowledge and experience gained while working with you on the project of Chapter 2 and for making it very interesting. Thank you Dr. Bain for your offers of time and assistance whenever I need them in my courses, for the preparation of my thesis and my defense. To Anna Trikoupis : my deepest appreciation for your continuous assistance and especially for your friendship during my stay in Canada. My gratitude also extends to Dr. Kirk Green, for providing thorough training on the sophisticated mass spectrometers and Tadek Olech, for technical assistance, and Gina Dimopolous, Lisa Heydorn, Zahra Jama, Richard Lee and Cathy Wong for their support all throughout the programme.

Finally, I would like to acknowledge the contribution of my loved ones back home in Malaysia. To my parents : I am grateful for your unconditional love and for being with me throughout everything. To my siblings : I greatly appreciate your continuous support.

To my wonderful husband : your love and sacrifices during the long time I have been abroad make me very grateful. Thank you for your patience in waiting for me to complete my studies before returning home.

TABLE OF CONTENTS

Abstract.....	iii	
Acknowledgements.....	iv	
Table of Contents.....	v	
List of Figures.....	vi	
List of Abbreviations.....	x	
CHAPTER 1		
Introduction		
1.1 Introduction and scope of this thesis.....	1	
1.2 Electrospray Ionization (ESI).....	2	
1.3 Tandem mass Spectrometry.....	7	
1.4 Matrix Assisted Laser Desorption/Ionization (MALDI).....	9	
1.5 Quadrupole Mass Analyzer.....	12	
1.6 Time-of-Flight Mass Analyzer.....	14	
1.7 Solid Phase Analytical Derivatization (SPAD).....	16	
CHAPTER 2		
Analytical Derivatization with Quarternized functional groups: Enhancing the Sensitivity and Selectivity of the Mass Spectrometric analysis of Malondialdehyde.....		21
CHAPTER 3		
Analysis of Diols in aqueous solutions by their Oxovanadium (VO ⁺⁺) complexes using Electrospray Mass Spectrometry.....		43
Summary.....	95	

LIST OF FIGURES

Page	
4	Figure 1.1 Schematic diagram illustrating the charged droplet formation from the Taylor cone during electrospray in the atmospheric pressure region of the ion source
12	Figure 1.2 Schematic diagram of the ESI-Quadrupole instrument equipped with a Z-spray ion inlet
13	Figure 1.3 Schematic diagram of the quadrupole mass analyzer separating masses. Opposite pairs of the rods are connected electrically but are of opposite polarity, DC voltage = U . A radiofrequency (R_f) AC voltage ($V_0 \cos \omega t$) is superimposed on this DC voltage, where $\omega = 2\pi f$. During a mass scan, the AC and DC fields are ramped but the ratio of DC/AC (i.e. U/V_0) is kept constant
15	Figure 1.4 Schematic diagram illustrating the operation of the time-of-flight mass analyzer
31	Figure 2.1 MALDI spectra produced from an experiment using DHB as the matrix (item A) and an experiment without any matrix applied (item B).
33	Figure 2.2 Limit of detection of MDA determined from experiments with BZA (top) and MMDA (bottom) as the internal standard
34	Figure 2.3 MALDI spectra of a mixture containing derivatized MDA (m/z 687 and 669) and BzA (m/z 721).
35	Figure 2.4 The calibration curve for the MDA analysis with BzA as internal standard
36	Figure 2.5 MALDI spectra of a mixture containing underivatized HTMPP (m/z 633), derivatized MDA (m/z 669 & 687), MMDA (m/z 683 & 701) and the remaining acetal (m/z 733)
37	Figure 2.6 The calibration curve for the MDA analysis with MMDA as internal standard.
52	Figure 3.1. a) ES spectrum of VO : EG [1:2] in solution. b) ES spectrum of VO : EG-d ₄ [1:2] in solution.

- 53 **Figure 3.2.** a) MS/MS spectrum (Ar,10eV) of the [2M] complex of EG, $(VO(EG_d)_2H^+)$; b) MS/MS spectrum of the [2M] complex of EG-d₄, $(VO(EG_{d-4})_2H^+)$
- 56 **Figure 3.3.** a) ES spectrum of VO : EG : 1,2-propanediol [1:2:1] solution. b) MS/MS spectrum of the mixed complex $VO(EG_d)L_dH^+$ with L = 1,2-propanediol. c) MS/MS spectrum of the mixed complex $VO(EG_{d-4})L_dH^+$ with L = 1,2-propanediol
- 59 **Figure 3.4.** a) ES spectrum of VO:EG:2R,3R(-)-butanediol [1:2:1] solution. b) ES spectrum of VO:EG:meso-2,3-butanediol [1:2:1] solution
- 60 **Figure 3.5.** a) MS/MS spectrum of the mixed complex of VO : EG : 2R,3R(-)-butanediol [1:2:1] solution. b) MS/MS spectrum of the mixed complex of VO : EG : *meso*-2,3-butanediol [1:2:1] solution. MS/MS spectra acquired with Ar at a collision energy of 10eV
- 61 **Figure 3.6.** a) MS/MS spectrum of the mixed complex of VO : EG : 2R,3R(-)-butanediol [1:2:1] solution. b) MS/MS spectrum of the mixed complex of VO : EG : *meso*-2,3-butanediol [1:2:1] solution. MS/MS acquired with Ar at a collision energy of 15eV
- 62 **Figure 3.7.** MS/MS spectrum of the mixed complex of VO : EG-d₄ : 2R,3R(-)-butanediol [1:2:1] solution at a collision energy of 10eV
- 64 **Figure 3.8.** a) MS/MS spectrum of the mixed complex of a cis-1,2-cyclopentanediol [1:2:1] solution. b) MSMS spectrum of the mixed complex of a trans-1,2-cyclopentanediol [1:2:1] solution MSMS spectra acquired with Ar at a collision energy of 15 eV.
- 65 **Figure 3.9.** MS/MS spectrum of the mixed complex $VO(EG_{d-4})L_dH^+$ with L = trans-1,2-cyclopentanediol. MS/MS spectrum acquired with Ar at a collision energy of 15eV
- 67 **Figure 3.10.** a) MS/MS spectrum of the mixed complex of a cis-1,2-cyclohexanediol [1:2:1] solution. b) MS/MS spectrum of the mixed complex of a trans-1,2-cyclohexanediol [1:2:1] solution. MS/MS spectra acquired with Ar at a collision energy of 15 eV.
- 68 **Figure 3.11** MS/MS spectrum of the mixed complex of $VO(EG_{d-4})L_dH^+$ with L = trans-1,2-cyclohexanediol. MS/MS spectrum acquired with Ar at a collision energy of 15eV.

- 70 **Figure 3.12** . a) ES spectrum of a VO : EG : trehalose [1:2:1] solution. b) ES spectrum of a VO : EG-d₄ trehalose [1:2:1] solution.
- 71 **Figure 3.13**. MS/MS spectrum of the mixed complex of VO : EG : trehalose (top); MS/MS spectrum of the mixed complex of VO : EG-d₄: trehalose (bottom). MS/MS spectra acquired with Ar at a collision energy of 15 eV
- 73 **Figure 3.14** ES spectra of VO : EG : ethanolamine [1:2:1] (top) and VO : EG-d₄: ethanolamine [1:2:1] (bottom).
- 74 **Figure 3.15** ES spectra of VO:EG:ethylenediamine [1:2:1](top) and VO:EG-d₄ : ethylenediamine [1:2:1] (bottom).
- 75 **Figure 3.16** ES spectra of VO:EG:dimethylethylenediamine [1:2:1] (top) and of VO:EG-d₄: dimethylethylenediamine [1:2:1] (bottom).
- 77 **Figure 3.17**. The formation constant K_1 for the mixed complex at m/z 204 and K_2 for the [2M] complex of 1,2-propanediol at m/z 218 as a function of time
- 78 **Figure 3.18**. The formation constant K_1 for the mixed complex at m/z 218 and K_2 for the [2M] complex of 2*R*,3*R*-(-)-2,3-butanediol at m/z 246 as a function of the reaction time
- 79 **Figure 3.19**. The formation constant K_1 for the mixed complex at m/z 230 and K_2 for the [2M] complex of cis-1,2-cyclopentanediol at m/z 270 as a function of the reaction time.
- 80 **Figure 3.20**. The formation constant K_1 for the mixed complex at m/z 244 and K_2 for the [2M] complex of cis-1,2-cyclohexanediol at m/z 298 as a function of time.
- 81 **Figure 3.21**. The formation constant K_1 for the mixed complex at m/z 244 and K_2 for the [2M] complex of trans-1,2-cyclohexanediol at m/z 298 as a function of time.
- 83 **Figure 3.22**. Partial ES spectra of the VO:EG reagent as a function of its concentration : top spectrum : 2.5×10^{-5} M; middle : 2.5×10^{-4} M; bottom : 2.5×10^{-3} M.

- 84 **Figure 3.23.** Partial ES spectra showing the complex ions $\text{VO}(\text{EG}_d)_2\text{H}^+$, $\text{VO}(\text{EG}_d)\text{L}_d\text{H}^+$ and $\text{VO}(\text{L}_d)_2\text{H}^+$ at a 1,2-propanediol to reagent ratio of 0.1 : 1 and a VO : EG concentration of 2.5×10^{-4} M (top spectrum) and 2.5×10^{-3} M (bottom spectrum).
- 85 **Figure 3.24** Partial ES spectrum showing the complex ions $\text{VO}(\text{EG}_d)_2\text{H}^+$, $\text{VO}(\text{EG}_d)\text{L}_d\text{H}^+$ and $\text{VO}(\text{L}_d)_2\text{H}^+$ at a VO : EG concentration of 2.5×10^{-4} M and a mol ratio of 1,2-propanediol to reagent of 0.2 : 1.
- 87 **Figure 3.25.** Plots of the intensity ratios of the mixed complex to the reagent complex and the diol [2M] complex to the mixed complex versus the diol to reagent mol ratio
- 88 **Figure 3.26.** Calibration curve for 1,2-propanediol : [218/204] - diol [2M] complex to mixed complex, [204/190] - mixed complex to EG [2M] complex.
- 89 **Figure 3.27.** Calibration curve for meso-2,3-butanediol: [246/218] - diol [2M] complex to mixed complex, [218/190] - mixed complex to EG [2M] complex.
- 91 **Figure 3.28** a) Calibration curve for cis-1,2-cyclopentanediol : [270/230] - diol [2M] complex to mixed complex, [230/190] - mixed complex to EG [2M] complex; b) Calibration curve for cis-1,2-cyclohexanediol: [298/244] - diol [2M] complex to mixed complex, [244/190] - mixed complex to EG [2M] complex.

LIST OF ABBREVIATIONS

MALDI	=	matrix assisted laser desorption ionization
LDI	=	laser desorption ionization
ESI	=	electrospray ionization
ES	=	electrospray
MS	=	mass spectrometry
ES/MS	=	electrospray mass spectrometry
GC/MS	=	gas chromatography mass spectrometry
MS/MS	=	tandem mass spectrometry
LC/MS	=	liquid chromatography mass spectrometry
CID	=	collision induced dissociation
MS1	=	first quadrupole in the quadrupole instrument
MS2	=	second quadrupole in the quadrupole instrument
eV	=	electron Volt (1 eV=23.061 kcal/mol or 96.487 kJ/mol)
RF	=	radio frequency
M	=	matrix
TOF	=	time-of-flight
ESPT	=	excited state proton transfer
UV	=	ultra violet
DC	=	direct current
AC	=	alternating current
SPE	=	solid phase extraction
XAD2	=	polystyrene divinylbenzene
SPAD	=	solid phase analytical derivatization
m/z	=	mass to charge ratio
HTMPP	=	4-hydrazino-4-oxobutyl tris(2,4,6- trimethoxyphenyl) phosphonium bromide
MDA	=	malondialdehyde
PA	=	proton affinity
q	=	charge
r,R	=	radius
MMDA	=	methyl malondialdehyde
HPLC	=	high performance liquid chromatography
CE	=	capillary electrophoresis
BzA	=	benzaldehyde
DHB	=	2,5- dihydroxybenzoic acid
LOD	=	limit of detection
LOQ	=	limit of quantitation
LLOQ	=	lower limit of quantitation
S/N	=	signal to noise
RSD	=	relative standard deviation

SD	=	standard deviation
CV	=	coefficient of variation
FDA	=	food and drug association
QC	=	quality control
PAHs	=	polycyclic aromatic hydrocarbons
VO	=	oxovanadium
EG	=	ethylene glycol
d	=	deprotonated
FA	=	formic acid
1M	=	oxovanadium complex containing one ligand
2M	=	oxovanadium complex containing two ligands
K_{eq}	=	equilibrium constant

Chapter 1

1.1 Introduction and scope of this thesis

The work described in this thesis concerns the development of methods based on mass spectrometry and additional separation techniques for the detection and analysis of small polar molecules of biological interest.

Chapter 2 describes a methodology based on solid phase derivatization and mass spectrometry to obtain a high throughput technique for the analysis of malondialdehyde. The inclusion of a selective and sensitive reagent in the study eliminates the use of a matrix in MALDI, hence enhances the speed of the analysis and the opportunity to develop a fully automated methodology. The selectivity of the reagent and the elimination of the matrix greatly reduces the interferences often associated with the analysis of biological samples with the MALDI technique.

The application of this technique, which is initially developed for the study of malondialdehyde, could be extended to provide a fast and reliable procedure for the analysis of other aldehydes present in biological matrices in order to measure the extent of oxidative stress. The quantitative analysis of all aldehydes related to oxidative stress is essential to measure the severity of cell damage.

Chapter 3 presents a mass spectrometric technique to detect and characterize the structure of diols through the formation of their oxovanadium complexes. The competition for complexation studied in this Chapter shows the tendency for oxovanadium to potentially complex to larger diol ligands as compared to ethylene glycol, whose complex serves as the reference. This study also shows the high preference of the oxovanadium ion for O-donor to N-donor ligands in acidic solution.

The tandem mass spectrometry experiments described in this Chapter provide information on the structural differences between the isomers of the diols and hence provide a complementary method of identification.

In both studies, the mass spectrometric technique applied involves “soft” ionization, by electrospray ionization (ESI) or matrix assisted laser desorption ionization (MALDI). The soft ionization technique gains its name from the way ions are formed and

results in a high intensity of quasi molecular ions and few fragments. These two methods are also capable of transferring the analyte from the condensed phase to the gas phase. In addition, the ionic nature of the reagent used in the MALDI study of malondialdehyde eliminates the use of the matrix and results in the application of laser desorption ionization (LDI). The solid phase analytical derivatization technique, which contributes to the selectivity and the speed of the analysis, will be discussed in section 1.7.

1.2 Electrospray ionization (ESI)

Electrospray is a gentle ionization technique that even allows non-covalent biomolecular complexes to remain intact while ionized. This technique enables the transfer of ions from a solution to the gas phase where they are accelerated and subsequently analyzed according to their m/z values. ESI gains wide application as almost half of the chemical and biochemical processes studied involve ions in solution.

Ionization takes place in the source at atmospheric pressure and it is rapid and sensitive towards a wide range of analytes, from low molecular weight polar compounds (less than 200 Da) to biopolymers beyond 100 kDa. The ions produced include singly and multiply charged inorganic ions, like Li^+ or Na^+ alkali ions and Mg^{2+} or Ca^{2+} alkali earth ions, as well as singly and doubly charged transition metal ions and their complexes with mono- and poly-dentate ligands such as those described in Chapter 3. ESI also analyzes anions of organic and inorganic acid such as NO_3^- , Cl^- , H_2PO_4^- and protonated bases such as amines, alkaloids and peptides. Generally, compounds of less than 1000 Da produce singly charged protonated molecules $(\text{M}+\text{H})^+$ in the positive ion mode, while high mass biopolymers produce a series of multiply charged ions. The solvents used are polar, be they protic solvents like water, methanol, ethanol, or aprotic such as acetone, acetonitrile and dimethylsulfoxide.

The overall mechanism of ion formation in the electrospray process consists of two major parts: i) the formation of gas-phase ions from the ions in solution at atmospheric pressure, and ii) the transfer of the gas-phase ions from the atmospheric pressure region to the vacuum section of the mass analyzer.

a) The formation of gas-phase ions by electrospray

The transfer of ions from the solution to the gas-phase is a highly endothermic process. This is because the ion undergoes a strong interaction with a number of solvent molecules, which form a solvation sphere around the ion. The transfer process involves the application of an electric field to initiate the formation of charged aerosols, hence the term electrospray. The three steps involved in the production of gas-phase ions from the ions in the solution are i) the production of charged droplets at the electrospray capillary tip, ii) the shrinkage of these charged droplets by solvent evaporation and droplet disintegration, iii) the actual mechanism by which gas-phase ions are produced from the very small and highly charged droplets.

1. Production of charged droplets at the ES capillary tip

An electric field applied to the capillary creates a potential between + 500 to + 4500 V. A voltage of 2-3 kV is usually applied to the metal capillary, which is typically 0.2 mm o.d. and 0.1 mm i.d. The capillary is located at about 1-3 cm from the counter electrode, which consists of a metal plate with an orifice leading to the mass analyzer. The electrospray capillary tip is very thin, hence the electric field that surrounds it is very high, almost 10^6 V/m. The value of the electric field at the tip relative to the large and planar counter electrode is defined as:

$$E_c = 2V_c / (r_c \ln (4d/r_c)) \quad 1$$

where V_c , r_c , and d represent the applied potential, the capillary outer radius, and the distance between the capillary tip to the counter electrode, respectively. The most important parameter is r_c , which is inversely proportional to the electric field created. The voltage required is critically dependent on the inner diameter of the capillary and the solvent that makes up the solution. Basically, capillaries with larger inner diameter, and solvents with higher boiling point, require a higher voltage. A typical solution used in the capillary consists of a polar solvent in which the analyte is dissolved at a concentration of 10^{-5} - 10^{-3} mol/L.

In the positive ion mode, the capillary is set as the positive electrode. Under the influence of the electric field created, the positive ions in the solution move downfield

towards the counter electrode, thereby forming a meniscus at the tip of the capillary. The negative ions, on the other hand, drift away from the meniscus of the liquid. The mutual repulsion between the positive ions gathered at the meniscus overcomes the surface tension of the liquid and the surface begins to expand, allowing the positive ions together with the liquid to move further downfield. This leads to a cone formation, the so-called Taylor cone [1], and if the applied field is sufficiently high, a fine jet emerges from the cone tip, which breaks into small charged droplets. The electric field that leads to the instability of the Taylor cone, the onset of the ES process, is represented by the equation:

$$E_{ON} = (2\gamma\cos\theta/\epsilon_0 r_c)^{1/2} \quad 2$$

where θ , γ , ϵ_0 , r_c represent the respective half angle of the Taylor cone, the surface tension, the permittivity of vacuum, and the radius of the capillary. The voltage required on the capillary to create this electric field is given by:

$$V_{ON} = (r_c\gamma\cos\theta/2\epsilon_0)^{1/2} \ln(4d/r_c) \quad 3$$

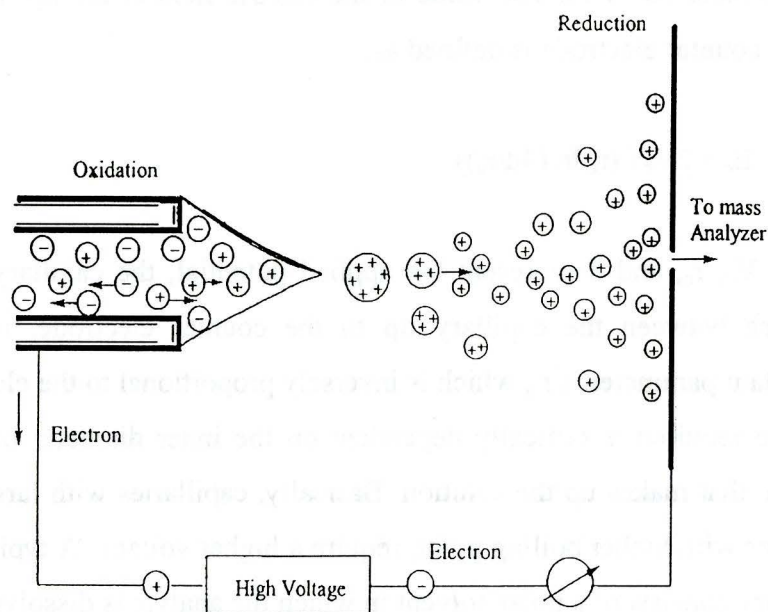


Figure 1.1 Schematic diagram illustrating the charged droplet formation from the Taylor cone during electrostatic spray ionization in the atmospheric pressure region of the ion source

From this equation, it is obvious that solvents with a high surface tension, such as water, require a higher voltage in order to stretch into a Taylor cone and a jet.

The droplets formed are positively charged due to the high concentration of positive ions at the surface of the cone. These droplets drift through the air downfield towards the counter electrode. This mode of charging, which produces ions drifting in a certain direction under the influence of an electric field, is called the electrophoretic mechanism [2,3,4].

2. Solvent evaporation leading to droplet shrinkage and Coulomb fission

The charged droplets produced are exposed to the ambient air while drifting to the counter electrode. The thermal energy of the ambient air causes the solvent to evaporate. Solvent evaporation leads to shrinkage of the droplets and increases the electric field on their surface. The decrease in radius (R) of the droplets at constant charge (q) results in an increasing repulsion between the positive ions at their surface. When this repulsion reaches the so-called Rayleigh stability limit, where the repulsion overcomes the surface tension, the droplet undergoes fission, at :

$$q_{RY} = 8\pi(\epsilon_0\gamma R^3)^{1/2} \quad 4$$

It is experimentally observed [5] that the droplets undergo fission when they are close to the Rayleigh limit. The fragmentation is usually referred to as Coulombic fission. Droplets that have relieved the Coulombic stress through jet fission will continue to evaporate solvent molecules until they reach the Rayleigh stability limit again and undergo another jet fission, which is also known as Coulomb explosion.

3. The formation of gas-phase ions from small, highly charged droplets

There are two mechanisms proposed for the formation of the gas-phase ions. The first mechanism is called the “charge residue” method. It was discovered by the first investigators of the ES/MS method, Dole and co-workers [6]. This mechanism indicates

that repeated Coulombic fission occurs to the extent that only one ion remains per droplet. Solvent evaporation from such a droplet leads to the gas-phase ion formation.

The second mechanism is proposed by Iribarne and Thomson [7,8]. It predicts that when the radii of the droplets reduce to a certain size, direct ion emission from the droplets becomes possible. This process is called “ion evaporation”.

A comparison between experimental results and the predictions derived from the two theories has been discussed. It appears that there are some discrepancies between experiment and either of the theories [9]. The formation of gaseous ions in both theories is distinctly different only for certain conditions. Both theories assume that droplets with radii $R > 10$ nm release their coulombic stress by Rayleigh fission; according to the ion evaporation theory, droplets with $R \approx 10$ nm and smaller release their coulombic stress by ion emission, while the charge residue theory believes fission continues beyond this size. However, neither theory addresses the microscopic droplets, where $R < 1$ nm. The more recent study of Locertales et. al. [10], however, presents experimental evidence in support of the ion evaporation theory.

b) Transfer of the gas-phase ions from atmospheric pressure to the vacuum section of the mass analyzer

In principle, an electrical field in the electrospray can be generated by grounding the sprayer and connecting the source to a high voltage or by connecting both to a separate power supply set at different voltages. Selection of either of these options depends on the type of mass analyzer and the method chosen for the transportation of ions from the atmospheric pressure source region into the vacuum of the mass analyzer. In quadrupole mass spectrometry, the ion source can be at ground potential and the sprayer at up to ± 5 kV [11,12].

The short flight path and the high collision rate affect the focusing of the ions in an atmospheric pressure ion source. In electrospray mass spectrometry, the assistance of a high-velocity gas flow is normally used to take care of aerosol formation [11,13], while the electric field does the droplet charging. Charged droplets generated by electrospray spread out in a wide angle at the capillary tip, hence a fast coaxial gas flow is used to keep the droplets in a narrower beam. The function of this nebulizing gas, together with the focusing gas (the curtain gas), is to increase the number of ions transported into the

vacuum of the mass analyzer region. The dimension and the geometry of the sampling orifice (the cone electrode in the Quattro Ultima instrument), as well as the location of the tube guiding the curtain gas are important for ion sampling efficiency. A correct combination of gas flow and electric field helps the guiding of the ions to the orifice.

The vacuum system design

In the quadrupole mass analyzer, a multi-stage vacuum system is created. Ions are drawn from the atmospheric pressure ionization chamber (760 Torr) through the sampling orifice into the first chamber, the pressure of which is lower, ca.1 Torr. Part of the expanding beam of ions and gases is taken into the second chamber, which is pumped down to 10^{-4} Torr or less. Most of the gases are pumped away in the second chamber before the ions are guided into the mass analyzer region, which is maintained at a pressure of 10^{-5} Torr.

In the Quattro Ultima instrument, which uses a Z-spray inlet/ion source (see section 1.5), the ions first pass through an initial skimmer orifice positioned at a right angle to the direction of the spray. The ions move to the first skimmer under the influence of an electric field and also the reduced pressure in the region behind the skimmer. Next, the beam of ions is bend again, towards a second skimmer, the 'extraction cone', and then it enters the mass analyzer. Excess solvent gases and involatiles leave the source region through the exhaust.

1.3 Tandem mass spectrometry

The information content of the primary ESI mass spectra is often not adequate for structure elucidation, particularly of large molecules. The number of possible isomers goes up exponentially with the increase in molecule size. For organic mixture analysis, an increasing mixture complexity raises the probability that more than one component contributes to an individual mass peak.

Tandem mass spectrometry, for which the acronym MS/MS is often used, involves the coupling of two or more mass analyzers with the capability to fragment, at their interface, a mass selected ion present in the regular ESI mass spectrum. In this way,

characteristic product ions are obtained, which are mass-separated in the second mass analyzer. An obvious advantage of this technique is the speed at which a compound can be identified; Liquid chromatography - mass spectrometry (LC/MS) is limited by the time required for chromatographic separation (usually many minutes), while MS/MS requires only an additional ion transit time of about 10^{-5} - 10^{-3} sec from the regular ionization, separation and detection time of 10^{-5} - 10^{-2} sec [14]. The second advantage of MS/MS is the reduction in interference signals that may arise from other components of a mixture. This is significant for structural elucidation. Generally, there are two types of MS/MS instruments; the one uses mass analyzers arranged in tandem, while the other stores the ions before the collision process, as for example in the ion-trap [15].

The collision or target gases routinely used in tandem mass spectrometry are helium, argon, nitrogen and oxygen. In a collision experiment, the center-of-mass kinetic energy, E_{cm} , represents the *maximum* amount of energy that can be converted into internal energy of the ion : $E_{cm} = E_{lab}m_t / (m_t + m_i)$, where E_{lab} is the ion's translational energy and m_i and m_t represent the respective masses of ion and target gas. Thus, the amount of energy transferred to the ion is dependent on its translational energy and the mass of the collision gas [16a]. The larger the E_{cm} value, the more high-energy dissociation reactions are observable.

High-energy dissociation reactions are typically observed with He under single collision conditions in magnetic sector instruments where the ion's translational energy is high (keV). In collision experiments with a quadrupole-type instrument, E_{lab} is much lower, 10-100 eV, so that only the dissociations of low energy requirement are observed. However, the hexapole collision cell refocuses scattered ions efficiently so that high collision gas pressures can be used. Under these conditions multiple collisions take place so that (almost) all of the precursor ions are induced to dissociate [16b].

In a triple quadrupole instrument, a hexapole is placed between the two quadrupoles. The hexapole functions as a collision induced dissociation (CID) chamber when a collision gas, usually Argon, is introduced. The hexapole does not act as mass filter but it provides a non-mass selective ion containment for the low-energy collision processes. The RF voltage applied to the hexapole focuses ions scattered by the collision process. A relatively high collision gas pressure ensures that the ions undergo many collisions. This, in combination with the strong focusing field of the hexapole, results in a

high yield of product ions generated by collision induced dissociation. The selectivity of an MS/MS experiment depends on the mass resolution in the two stages of mass analysis [17]. The tandem quadrupole provides unit mass resolution in both stages.

The scan modes routinely available in MS/MS experiments with quadrupoles are daughter ion, parent ion and constant neutral loss scans. In daughter ion (or product ion) scanning, a known precursor ion selected by the first quadrupole, MS1, undergoes collision induced dissociation in the hexapole. The m/z values of the fragment formed are scanned by the second quadrupole, MS2. This method is usually applied to obtain structural information. Parent ion (or precursor ion) scanning involves scanning of MS1 over a mass range for ions which produce a specific daughter ion in MS2. The parent ion that produces a daughter ion at the specified mass in MS2 will yield a response at the detector. This method is selective in that only parent ions that produce the known daughter ion will be observed. This type of scan is usually performed to confirm the structural information derived from the daughter ion scan. Constant neutral loss scanning involves monitoring the loss of a known neutral fragment in both MS1 and MS2 quadrupoles. MS1 is scanned for a specific mass range, and then MS2 is scanned for the mass range minus the "off-set mass" of the specified fragment. This type of scanning is also selective in that only parent ions that lose a specific neutral will be detected. This method is used to screen mixtures of a specific class of compounds which all lose a common neutral.

1.4 Matrix assisted laser desorption / ionization (MALDI)

The ionization method used for the analysis of malondialdehyde is MALDI in combination with LDI. This method is often used in the analysis of non-volatile, thermally labile and large molecules such as proteins, peptides, sugars and polymers.

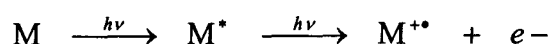
Initially, laser desorption ionization was used where laser pulses with a strength of 10^6 - 10^{10} W/cm² were applied directly to the sample, at a pulse width of 1-100 ns. One problem with this approach is that the laser wavelength may not lie within the light absorption spectrum of the analyte, resulting in a low yield of ions. In the commonly used N₂ UV laser, the energy imparted to the analyte is only about 4 eV, but twice as much

energy is required to ionize a common (bio)organic molecule. Hence, a matrix is often required to absorb most of the energy imparted by the laser and transfer it to the analyte to increase its desorption and ionization efficiency. Moreover, the energy imparted by the laser may sometimes be too strong for the analyte, which results in its decomposition rather than its ablation. These setbacks have revolutionized the application of a matrix in LDI, hence termed MALDI. However, as shown in Chapter 2, an ionic and hydrophobic reagent of fairly high mass makes it possible to use LDI as efficiently as MALDI.

Basically, the (MA)LDI set up used consists of three main components: a MALDI ion source, a time-of-flight (TOF) mass analyzer, and a multichannel plate detector. Factors influencing the MALDI process are the matrix, the laser wavelength, and the laser pulse width. The basic step in MALDI analysis is the sample preparation in which a matrix is added to the sample, usually in a ratio of 1000 : 1 and only 1 μ L of this mixture is used for the analysis. The 1 μ L is deposited on the MALDI target plate and allowed to co-crystallize to dryness before being introduced to the ionization chamber of the mass spectrometer. The ionization chamber is kept under high vacuum during the experiment. In this study, a N₂ UV laser with a wavelength of 337 nm is used for the ionization process. The pulse width is 4ns, each pulse having an energy of 180 microjoules.

Mechanism of ion formation in MALDI experiments

The most straightforward explanation for the formation of ions by laser excitation of an absorbed organic analyte involves multiphoton ionization of a single matrix molecule. This process has been proposed to be the primary ionization step in MALDI and the resulting matrix radical cation is the initiator for the formation of analyte ions [18]. In the simplest process, two laser photons excite a matrix molecule from the ground state to above its ionization energy :



There is also evidence that more than one excited matrix molecule, M*, is needed to generate ions, matrix or analyte, in MALDI [19], by the following sequence:



However, excited-state proton transfer (ESPT) is the most frequently proposed MALDI ionization process [20]. It requires only one photon to yield an excited matrix molecule, which is presumed to become more acidic than its ground state. As a result, the acidic labile proton is transferred to a neighbouring matrix or analyte molecule, which becomes protonated. Such excited-state acidity has been documented in aromatic hydroxyl and amine groups.

Another mechanism concerns the liberation of pre-formed ions by the laser pulse. This mechanism is most relevant for compounds that are ionic in character. For many ionic compounds, such as the phosphonium ion containing reagent of Chapter 2, the adduct ion is detected rather than the protonated compound.

Molecular dynamics simulations show that the UV MALDI plume can be described as a very rapid, even explosive, solid-to-gas phase transition [21]. It is predicted that at this stage secondary ion-molecule reactions occur and of particular importance are proton-transfer, cationization and electron-transfer reactions.

In the matrix-matrix reaction in the plume, the matrix radical cation may react with another matrix molecule to form a protonated matrix ion and a radical, which subsequently captures a free electron to form the even electron $(M-H)^-$. In the matrix-analyte reaction, the protonated matrix may react with the analyte A to produce the protonated analyte. These reactions are shown below:



1.5 The quadrupole mass analyzer

The quadrupole mass analyzer is used in combination with ESI for the study of the oxovanadium complexes of Chapter 3. The main function of the mass analyzer is to separate ions produced in the ion source according to their mass to charge ratio (m/z). The Z-spray inlet/ion source of the instrument consists of a sampling cone, an ion block and two RF lenses. The mass separation process is carried out by two quadrupoles. These are separated by a hexapole, which acts as the collision induced dissociation (CID) chamber and operates in the RF mode only. A schematic diagram is shown in Figure 1.2.

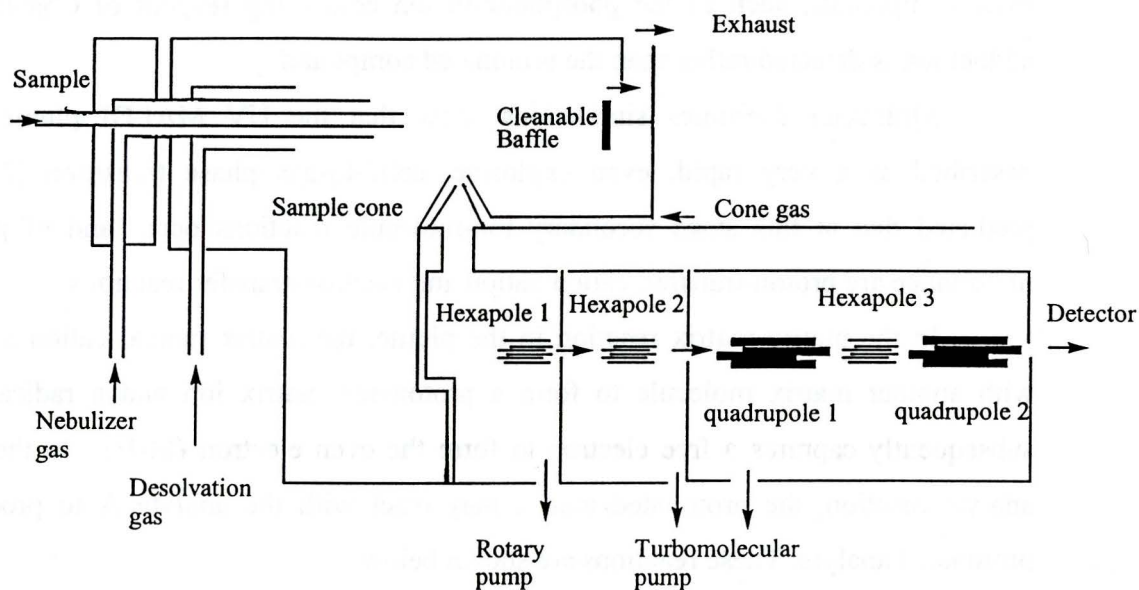


Figure 1.2 Schematic diagram of the ESI-Quadrupole instrument equipped with a Z-spray ion inlet

Ions emerging from the atmospheric pressure ionization chamber are drawn into the sampling cone by the charge on the cone and the reduced pressure (ca. 1 Torr) behind it. Next, two hexapole RF lenses are used to focus the ions into the mass analyzer section.

A positive voltage applied to the hexapoles forces the ions to remain close to the axis of the beam.

The first RF lens causes ions that have entered the source block to turn through a further 90° to become aligned with the quadrupoles. The second RF lens, which carries a small voltage, is located in the second chamber, where the pressure is $\sim 10^{-4}$ Torr. This set up enables the ions to pass through to the analyzer region as a tightly focussed beam.

The ions then move into the mass analyzer region, whose pressure is at 10^{-5} Torr. The analyzer consists of four parallel cylindrical rods acting as the electrodes of the mass filter, see Figure 1.3.

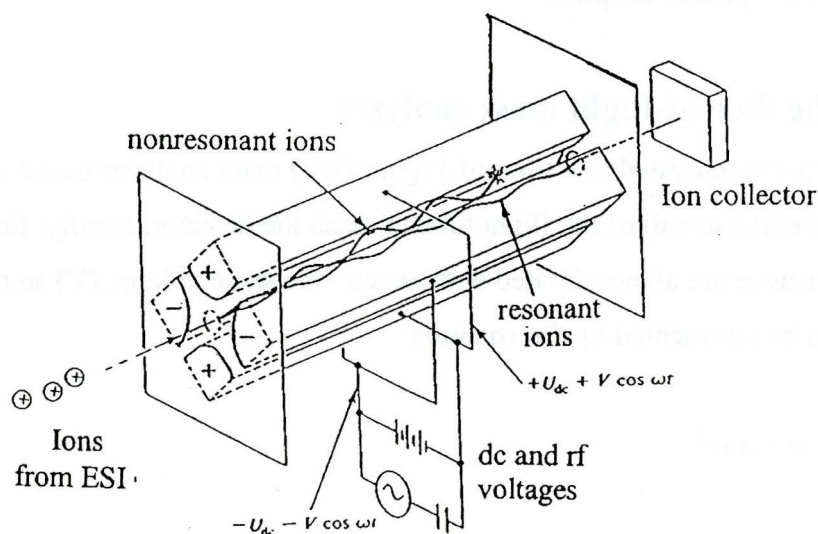


Figure 1.3 Schematic diagram of the quadrupole mass analyzer separating masses. Opposite pairs of the rods are connected electrically but are of opposite polarity, DC voltage = U . A radiofrequency (R_f) AC voltage ($V_0 \cos \omega t$) is superimposed on this DC voltage, where $\omega = 2\pi f$. During a mass scan, the AC and DC fields are ramped but the ratio of DC/AC (i.e. U/V_0) is kept constant.

Ions are accelerated and focused into the space between the rods by the RF lenses. Opposite rods in a quadrupole are connected electronically, to the positive and negative terminal of a variable direct current (DC) source. The rods are also supplied with a

variable RF (radio frequency) alternating current (AC) potential, so that a two dimensional quadrupole field is created. Simultaneous application of the AC and DC potentials to the rods affects the movement of ions by causing them to oscillate between the rods. The oscillation path is related to the mass to charge ratio of the ions: ions with a stable trajectory remain between the rods and pass to the detector.

In practice, the RF to DC ratio is set at the lower end of the mass range specified. While maintaining the ratio, the voltages are increased to enable rapid scanning of a range of masses, which yields a mass spectrum.

Once the mass analyzer has separated the ions, the beam of ions is converted into an electrical signal at the detector and recorded. The detector used in the Quattro Ultima instrument is a photomultiplier.

1.6 The time-of-flight mass analyzer

Ions are separated in a time-of-flight (TOF) mass analyzer based on the time they take to travel the length of the flight tube to reach the detector. Ideally, the ions produced in the ion source are all accelerated with exactly the same voltage (V) so that their kinetic energy can be represented by the equation:

$$eV = \frac{1}{2} mv^2 \tag{5}$$

where v is the velocity and m is the mass of the ion. Since velocity v is equal to the length of the tube, L , over time t :

$$eV = \frac{1}{2} m(L/t)^2 \tag{6}$$

the time is then dependent on the mass of the individual ion:

$$t = (m/2eV)^{1/2} L \tag{7}$$

In practice, the ions do not all have exactly the same kinetic energy and neither do they start their flight down the tube at exactly the same time. This creates spatial and

temporal distributions and as a result, ions of equal mass reach the detector at slightly different times. To overcome this limitation, which affects the mass resolution, a reflectron is fitted into the instrument, see Figure 1.4.

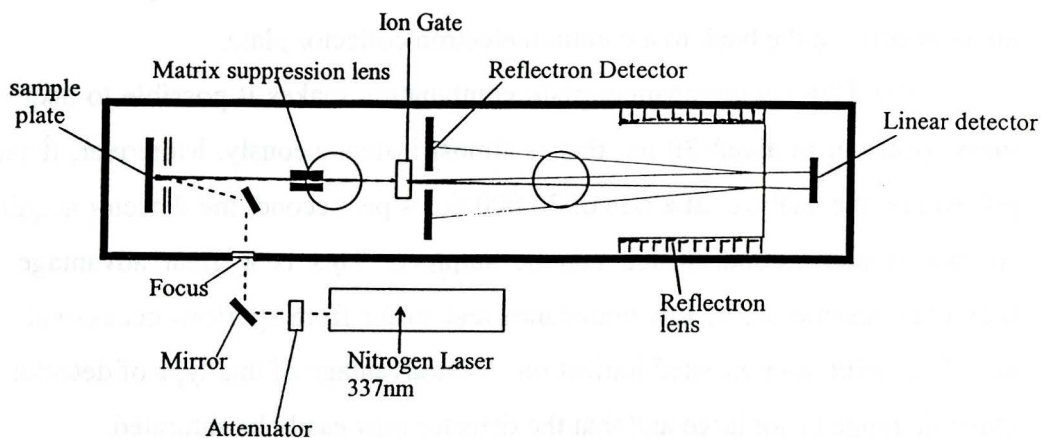


Figure 1.4 Schematic diagram illustrating the operation of the time-of-flight mass analyzer

The time-of-flight mass analyzer operates in two modes : the linear and the reflectron mode. In the reflectron mode, ions of equal mass but different velocities penetrate the reflectron to a different extent. An ion with a higher energy, hence a higher velocity, will penetrate the reflectron field further. It therefore takes a longer time as compared to an ion with a lower velocity, to traverse the reflectron. This traveling time difference causes both ions to emerge at the field free region and also the detector at the same time. The reflectron assists in so-called ‘energy focusing’ by decelerating and re-accelerating ions in the reverse direction, leading to a higher resolution. Other methods that have been introduced to improve resolution in the MALDI include time-lag focusing and the use of an orthogonal accelerator.

The ions are separated according to their mass to charge ratio (m/z) and this value together with the measured ion abundance produces a mass spectrum. In a time-of-flight instrument, the detector used is the microchannel plate detector, which is an array type detector.

Typically, when dealing with the separation of ions in the mass range of 1-3000 Daltons by a TOF analyzer, all of the ions reach the detector within ca. 30 μ s. The spatial distribution of the ions is fairly broad, while ions of adjacent m/z values are separated in time by 20-30 nanoseconds. These parameters make the microchannel plate collector the detector of choice. A microchannel plate detector is basically an assemblage (“array”) of a great many single point detectors \square microchannel electron multipliers \square , all of which are connected at the back to a common electron collector plate.

The TOF / microchannel plate combination makes it possible to acquire the full mass spectrum in about 30 μ s, that is almost instantaneously. Moreover, if the ions are pulsed into the analyzer at a rate of 30,000 times per second, the detector acquires 30,000 spectra in one second, which can be summed. This is a great advantage when the individual spectra are of low abundance and suffer from spurious occasional “electronic noise”, as with laser-assisted ionization. A disadvantage of this type of detector is that the dynamic range is not large and that the detector may easily be saturated.

1.7 Solid phase analytical derivatization (SPAD)

Solid phase extraction (SPE) is a method of sample preparation that concentrates and purifies analytes from solution by sorption onto a solid phase cartridge, followed by elution of the analyte with a solvent appropriate for instrumental analysis. The derivatization of the analytes is usually carried out after the extraction process. Solid phase derivatization is an extended technique resulting from the successful application of the solid phase extraction. Solid phase derivatization involves the introduction of a reagent capable of derivatizing the analyte of interest on the solid phase for isolation through elution by a specific solvent. The work of Zhou et. al. [22] outlines the application of the silica based solid phase reagent for derivatization in chromatography.

Traditionally, sample preparation consists of sample dissolution, purification and liquid-liquid extraction. The disadvantage of liquid-liquid extraction is the use of a large volume of organic solvent, cumbersome glassware, cost and time. Furthermore, this technique often creates emulsions with aqueous samples that are difficult to extract. This

method is also not easily automated. Solid phase extraction was invented in the mid-1970s as an alternative technique to overcome these limitations.

Solid phase derivatization greatly reduces the sample preparation time, up to six fold [23,24], by combining the extraction, purification and derivatization processes in one in-situ derivatization step that serves the purpose of all these processes.

Solid phase reagents can be prepared with many types of matrices including silica, alumina, and organic polymers. Zhou et al. describe three types of immobilization procedures: i) physical adsorption of the reagent onto the solid matrix, ii) covalent attachment of a reactive tag through a chemical bond with silanols on a silica surface, and iii) covalent attachment of a reactive tag to an organic polymer coating on a silica surface.

With physical adsorption of the reagent to the silica surface, the SPE column becomes the derivatizing agent, and the derivatization takes place when the analyte passes through the column. In the second approach, the reagent is attached directly to the surface of the silica and can bind the analyte directly. An example of this approach is the isolation of aldehydes from air using SPE. The reaction involves a hydrazone derivative that is chemically attached to the silica sorbent.

Polymeric sorbents

Water soluble analytes require a more hydrophobic sorbent with a greater surface area for complete retention. The sorbent used in the solid phase analytical derivatization technique applied in Chapter 2 is a polymeric sorbent, the XAD2 resin. It consists of styrene-divinylbenzene copolymers. Carbon and polymeric sorbents may also be used for polar metabolites of drugs and environmental pollutants. They typically have large surface areas (600-1200 m²/g) and hence a greater capacity for sorption due to a higher carbon percentage and a more hydrophobic surface. Another advantage of the aromatic sorbents is their selective interaction with aromatic ring analytes by a specific π - π interaction. The aromatic rings of the matrix network permit electron-donor interaction between the sorbent and π bonds of the solute. This may further increase the analyte-sorbent interaction and increase the energy of sorption. Because both the graphitized carbon and the styrene-divinylbenzene structures contain aromatic rings, they may selectively isolate aromatic compounds [25]. In the study of this thesis, the XAD2 resin

with the attached “aromatic” reagent, 4-hydrazino-4-oxobutyl tris(2,4,6-trimethoxy phenyl) phosphonium bromide, successfully retains the water soluble malondialdehyde.

The mechanism of retention in solid phase derivatization involves non-polar van der Waals interactions, dispersion or partitioning. Intermolecular forces that do not involve ions and are essentially non-polar, are collectively known as van der Waals forces. It is a weak intermolecular force that exists even in real gases. The partitioning process refers to the separation of the solute by utilizing the difference in partition coefficient between the two phases. A very large interface area between the stationary and the mobile phase allows for a rapid attainment of the equilibrium distribution of the solute between the two phases. This is usually achieved by having the mobile phase adsorbed to the solid phase with such tenacity that it will not migrate over to the solid phase. The solute flows freely within these phases without being retained by adsorption, hence participates in a partition between the two phases [26]. Dispersion on the other hand, results from mass interactions and is shown to be exponentially related to the molecular weight. The density of the dispersing solute indicates the nature of the diluting solvent. However, the property of solute or solvent that conditions the magnitude of the dispersion forces during interaction is hard to determine. Generally, dispersion is more pronounced as more partitioning steps occur: thus it increases with increasing migration distance [27].

Elution of analytes from reversed-phase sorbents is a rather simple process. A non-polar solvent needs to be used to disrupt the van der Waals forces that retain the analyte. Three common solvents that are quite compatible with reversed-phase sorbents are methanol, acetonitrile and ethyl acetate. In the case that a hydrophobic solute present does not effectively elute with these solvents, a methylene chloride - ethyl acetate mixture may be applied.

References

1. G.I. Taylor. Proc. R. Soc. London A. A280 (1964) 383.
2. D.P.H. Smith. IEEE Trans. Ind. Appl. IA-22 (1986) 527.
3. I. Hayati, A.I. Bailey, T.F. Tadros. J. Colloid Interface Sci. 117 (1987) 205.

4. J. Fernandez de la Mora, I.G. Locertales. *J. Fluid Mech.* 243 (1994) 561.
5. L. Rayleigh. *The Theory of Sound*. Dover. New York. 1945.
6. M. Dole, L.L. Mack, R.L. Hines, R.C. Mobley, L.D. Ferguson, M.B. Alice. *J. Chem. Phys.* 49 (1968) 2240.
7. J.V. Iribane, B.A. Thomson. *J. Chem. Phys.* 64 (1976) 2287.
8. J.V. Iribane, B.A. Thomson, *J. Chem. Phys.* 71 (1979) 4451.
9. R.B.Cole. *Electrospray Ionization Mass Spectrometry : Fundamentals, Instrumentation, and Applications*. John Wiley & Sons. New York. 1997. p. 32.
10. J. Fernandez de la Mora, I.G. Locertales. *J. Chem. Phys.* 103 (1995) 5041.
11. A.P. Bruins, T.R. Covey, J.D. Henion. *Anal. Chem.* 60 (1988) 1948.
12. M. Yamashita, J.B. Fenn. *J. Phys. Chem.* 88 (1984) 4451.
13. J.F. Banks, J.P. Quinn, C.M. Whitehouse. *Anal. Chem.* 66 (1994) 3688.
14. F.W. McLafferty, F.M. Bockhoff. *Anal. Chem.* 50 (1978) 69.
15. R.E. March, J.F.J. Todd. *Practical aspects of Ion trap Mass Spectrometry*. 1. CRC Press. New York. 1995.
16. a) K.L. Schey, H.I. Kenttamaa, V.H. Wysocki, R.G. Cooks. *Int. J. Mass Spectrom. Ion Process.* 90 (1989) 71; b) P.H. Dawson, D.J. Douglas. *Tandem Mass Spectrometry*. John Wiley & Sons. New York. 1983. p. 125.
17. R.A. Yost, C.G. Enke. *Tandem Mass Spectrometry*. John Wiley & Sons. New York. 1983. p. 175.
18. H. Ehring, M. Karas, F. Hillenkamp. *Org. Mass Spectrom.* 27 (1992) 427.
19. R. Zenobi, R. Knochenmuss. *Mass Spectrom. Rev.* 17 (1998) 337.
20. M. Karas, D. Bachmann, F. Hillenkamp, U. Bahr. *Int. J. Mass Spectrom. Ion Proc.* 78 (1987) 53.
21. A. Vertes, G. Irinyi, R. Gijbels. *Anal. Chem.* 65 (1993) 2389.
22. F.X. Zhoul, J.M. Thorne, I.S. Krull. *Trends. Anal. Chem.* 11 (1992) 80.
23. S.M. Breckenbridge, X. Yin, J.M. Rosenfeld, Y.H. Yu. *J. Chromatog. B.* 694 (1997) 289.
24. J.M. Rosenfeld. *J. Chromatog. A.* 843 (1999) 19.
25. E.M. Thurman, M.S. Mills. *Solid-Phase Extraction*. 147. John Wiley & Sons. New York. 1998.

26. J.C. Giddings, R.A. Keller. *Chromatography*. Chapman & Hall, Ltd. London. 1961.
p. 92.
27. R.P.W. Scott. *J. Chromatog.* 122 (1976) 35.

Chapter 2

Analytical derivatization with quaternized functional groups: Enhancing the sensitivity and selectivity of the mass spectrometric analysis of malondialdehyde.

Preamble and summary

Mass spectrometry is one of the most sensitive and specific instrumental techniques available to the analytical chemist. It is also one of the most expensive techniques and so high sample throughput is important economically. Equally important, such throughput is essential in the study of numerous biomedical and environmental problems. In these areas of investigation there is a requirement not just to improve the figures of merit of an analytical method but also to improve the chemistry of sample preparation with a particular focus on automation. Additionally, because high sensitivity techniques require less sample they permit a finer spatial resolution of analytes within tissues and permit a more accurate time resolution of kinetics particularly in small animals that are important models in drug development.

In this study we describe a combination of a phosphonium reagent and solid phase analytical derivatization (SPAD) that is used to prepare pre-ionized derivatives that also contain aromatic functionalities. A newly developed reagent, 4-hydrazino-4-oxobutyl tris (2,4,6 trimethoxyphenyl) phosphonium bromide (HTMPP), is a Girard type reagent that combines within one reagent the phosphonium group as the positive charge with hydrazine as a functionality reactive towards carbonyls [1]. The quaternized phosphonium has three methoxyphenyl groups which render it lipophilic. Pre-ionization enhances sensitivity in the positive ionization mode of mass spectrometric techniques. The combination of pre-ionization with the aromatic functionalities allows for laser induced ionization without the need of matrix. The use of SPAD provides an avenue for development of automation.

The technique was applied to the determination of malondialdehyde in aqueous solution. HTMPP was sorbed onto a solid phase of a styrene-divinylbenzene macroreticular cross-linked co-polymer by precipitation from ethanol by the addition of water. Aqueous solutions of analyte were added and the mixture was agitated by ultrasonication. Subsequent to isolation of the solid phase by aspiration or filtration, the derivatized analytes were eluted from the surface with an organic solvent. A small aliquot was analyzed by electro-spray ionization [1] and matrix assisted laser induced ionization (MALDI). In addition, laser induced ionization experiments were performed without the use of a matrix.

Malondialdehyde (MDA), $\text{HC(=O)CH}_2\text{C(H)=O}$, is the product of the reaction between reactive oxygen species and polyunsaturated fatty acids. It is believed to be a marker of oxidative stress. The molecule is highly water soluble, volatile and contains no functionality that permits detection at high sensitivity. In most analyses MDA is typically derivatized to less volatile, chromophoric or electrophoric products which are then analyzed by high performance liquid chromatography or gas chromatography. In the SPAD process, MDA was simultaneously sorbed and derivatized directly from the water onto the surface of the impregnated resin from which it was recovered as the monohydrazone derivative. Since a similar derivatization was not found for SPAD with the common Girard P reagent, the results imply that the highly lipophilic nature of the HTMPP is an important factor in this sorption/derivatization process. The limit of detection by MALDI is 1 picomol/ μL . Moreover, the derivative could be detected at equal sensitivity in the presence and absence of matrix using the MALDI instrumentation. Ionization in the absence of the matrix suggests that derivatization with HTMPP would provide carbonyl specific detection since any non-derivatized material would not be ionized. This would limit interferences that might be expected to be found in biological samples such as peptides or oligosaccharides.

Introduction

Low molecular mass compounds play an important role in the fields of biochemistry, biotechnology and medicine. They are mainly the substrates and products of enzyme-catalyzed reactions, intermediate metabolites, pharmaceutical substances or

the end products of biotechnological processes. The objective of the work described in this Chapter is to provide an alternative to their often difficult analysis due to i) an inherent low concentration ii) a complex biological matrix that causes interference and iii) a limited availability of adequate analytical methods. In addition, the target analytes have to be isolated and purified prior to analysis by multiple and time-consuming steps.

The hydrophilic nature and the lack of basic sites in certain compounds have presented problems for their analysis when the detection is based upon protonation in mass spectrometric techniques such as matrix-assisted laser desorption/ionization (MALDI) and electrospray ionization (ESI). In order to overcome this problem, several investigators have applied specific pre-ionized functional groups that increase the signal intensity and thus the detection [2]. In this study, the additional functional group also decreases the hydrophilic character of the derivative so that direct isolation through solid phase derivatization becomes feasible. Derivatization has other advantages in the analysis of low-molecular mass compounds using MALDI/MS [3] such as a decrease in the volatility of the analyte and a shift towards higher mass, far apart from the interference of matrix derived signals. The derivatizing reagent applied in this study is selective towards a carbonyl group. A highly selective and sensitive derivatizing reagent allows for an unambiguous identification of a class of compounds in a mixture, and a measurement without the use of the additional matrix substance. The derivatization process is carried out on solid phase, thus enabling in-situ selective derivatization, isolation, and pre-concentration of the derivative.

MALDI/MS has been extensively used for the analysis of small biomolecules and biopolymers due to its soft ionization properties [4]. The advantages of MALDI/MS are its high sensitivity, allowing the detection down to the picomol range of some underivatized oligosaccharides such as those found in glycoproteins [5,6], and a high tolerance against impurities such as salts and buffers. The application of internal standards consisting of isotopically labeled analogues enables quantitation work using MALDI/MS [7,8,9]. In spite of these advantages, a further improvement of the technique is required for the analysis of low molecular mass analytes at low concentration. As mentioned above, the derivatization with a quaternary ion moiety greatly enhances the signal strength and hence the sensitivity of the technique. At the same time it reduces the

loss of volatile analytes such as malondialdehyde and biomolecules during drying, crystallization, and especially in the high vacuum of the instrument prior to analysis. Internal standards too are applied to measure the level of sensitivity, reproducibility and accuracy of the analysis by MALDI/MS technique.

Malondialdehyde, $\text{HC(=O)CH}_2\text{C(H)=O}$, is the product of the reaction between reactive oxygen and polyunsaturated fatty acids. During lipid peroxidation, a multitude of degradation products is formed. However, MDA is the most commonly quantified molecule as the marker of oxidative stress or oxidative injury on the lipid membranes and there has been a continuous development of analytical methods associated with determining this molecule [10,11]. MDA is capable of inhibiting the activity of certain enzymes and it interacts with lipoproteins, causing oxidative stress that leads to neurodegenerative and cardiovascular diseases [12,13]. In biological matrices MDA exists both as the free molecule and bound, mainly to SH or NH_2 groups of proteins and nucleic acids [14].

The reference methods for the analysis of MDA are based on the technique of Gas Chromatography-Mass Spectrometry (GC/MS). Those using isotopic-dilution with the deuterated isotopomer $\text{HC(=O)CD}_2\text{C(H)=O}$ as the internal standard offer the best guarantee of specificity, sensitivity and reproducibility [14,15]. The use of isotope-labeled molecules as internal standard in mass spectrometry offers the possibility of validating other proposed internal standards that differ from the analyte in structure, stability and reactivity. However, isotope-labeled molecules have their limitations : they may be expensive and difficult to synthesize, and are detectable only by GC/MS and other standard MS methods which are not always available [12,14,16].

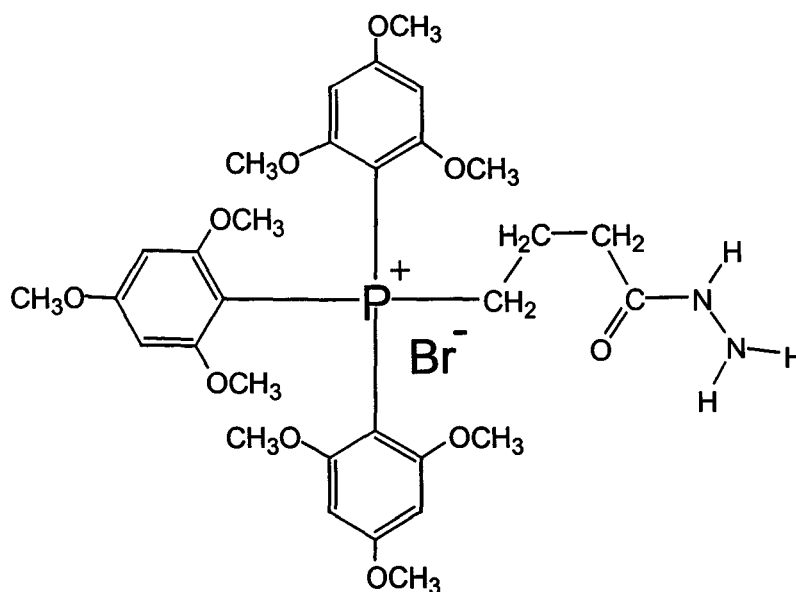
Bull and Marnet [17] have evaluated the use of the methyl analogue of malondialdehyde, $\text{HC(=O)CH(CH}_3\text{)C(H)=O}$, (MMDA) as an internal standard for malondialdehyde analyses with High Performance Liquid Chromatography (HPLC). They have since successfully applied this internal standard to other methods, including Capillary Electrophoresis (CE) [12]. MMDA is structurally close to MDA, easily obtainable from a commercially available compound, detectable by methods other than mass spectrometry and MMDA is not present in biological matrices. The use of benzaldehyde (BzA) as an

internal standard [18] in this study also reflects its absence in biological matrices as well as its availability for comparison.

Experimental

Chemicals and Reagents

The derivatizing reagent, 4-hydrazino-4-oxobutyl [tris(2,4,6-trimethoxyphenyl)] phosphonium bromide, (HTMPP), whose structure is shown below, was supplied by Glaxo Research and Development Ltd (UK). The precursors for the internal standards, viz. malonaldehyde bis(dimethylacetal) (1,1,3,3-tetramethoxypropane) and 2-methyl-3-ethoxyprop-2-enal (3-ethoxymethacrolein), were purchased from Aldrich Chemicals.



All other reagents and solvents were of analytical grade and purchased from Fisher Scientific and Lancaster Synthesis. The matrix solution used contained 10 mg of 2,5-dihydroxybenzoic acid (DHB) in 1 mL of ethanol.

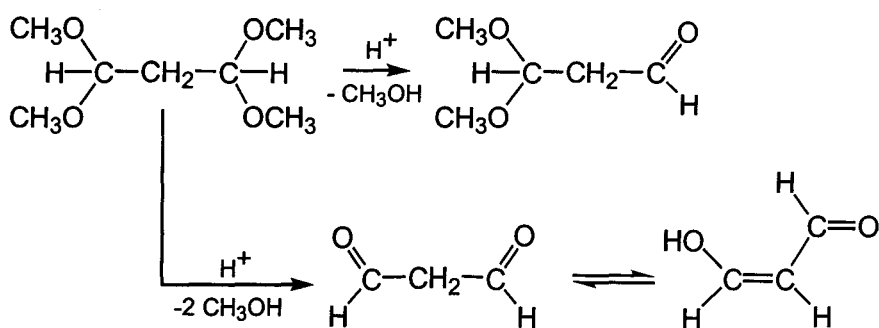
Internal standards

Aldehydes that were used as an internal standard are benzaldehyde (BzA) and methyl-malondialdehyde (MMDA). The samples for the MALDI experiments were

prepared by mixing 20 μL of the HTMPP stock solution (1mM) with 10 μL of the internal standard solution (1mM) and 10 μL of an MDA solution, whose concentration was varied from 1mM to 0.015 mM [19]. A calibration curve of analyte and internal standard intensity ratio against the molarity of the analyte was plotted from the data acquired and the intercept of the curve was used to determine the limit of detection (LOD) value. The internal standards were used to measure the level of accuracy and precision of the MALDI/MS analysis.

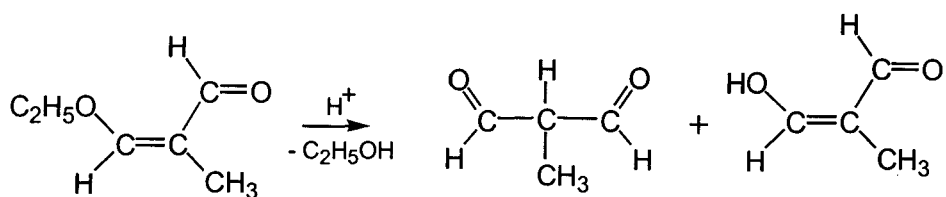
Synthesis of internal standards

The 1 mM malondialdehyde standard solution was prepared by acid hydrolysis of the (bis)acetal in 0.1 M HCl at room temperature for 2 hours as the compound is not commercially available due to its instability. It was generated as follows [13,20,21]:



Scheme 1. Formation of MDA from the acid hydrolysis of tetramethoxypropane.

The synthesis and application of MMDA as an internal standard for the determination of MDA has been documented above. In this study, however, the synthesis of 1 mM internal standard solutions of MMDA was achieved by adopting the procedure for the MDA preparation, that is by acid hydrolysis of 3-ethoxymethacrolein in 0.1M HCl, as outlined in Scheme 2.

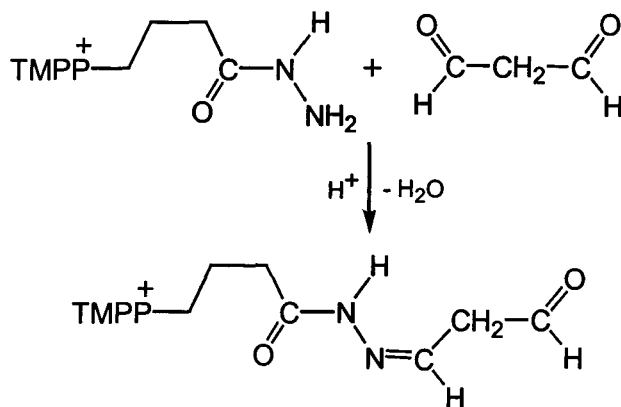


Scheme 2. Formation of MMDA as the internal standard from the hydrolysis of 3-ethoxymethacrolein

Derivatization protocol

All derivatizations were carried out on the solid phase of a polystyrene-divinylbenzene (XAD2) resin with the analyte added to and reacted with the derivatizing agent pre-loaded onto the resin, so that derivatization and isolation occur concurrently [22,23]. Aldehydes react with hydrazide reagents in the presence of an acid catalyst to form a hydrazone linkage [24]. Hence, hydrochloric acid was added to the solution to obtain a pH value of 2.5. The derivatization mixture, containing HTMPP and MDA in a 3 : 1 molar ratio, was then sonicated for 30 min. in an ultrasonic bath at room temperature. The derivative was eluted with 200 μ L of acetonitrile.

The general reaction of an aldehyde with a Girard type reagent is illustrated in Scheme 3 for the reaction of MDA with HTMPP :



Scheme 3. Derivatization of MDA with HTMPP

The acetonitrile solution containing the derivatized compounds was mixed with an equal volume of the matrix solution or pure ethanol. From these solutions 1 μ L aliquots were transferred to the MALDI sample plate.

Estimation of the limits of detection (LOD)

The LOD was estimated by preparing a dilution series of the standard MDA solution and the derivatizing agent mixtures. A 1 μL volume of the derivative was applied to the metal target by the dried droplet method. 300 shots were summed over the entire target spot. The LOD was defined as the molar amount of the analyte in the 1 μL spot that gave a signal to noise ratio (S/N) of > 3 [12,19]. The LOD value in this work was determined through the use of internal standards and calibration curves.

Preparation of the biological samples

Two sets of samples were prepared. The first set of 100 μL of muscle homogenate obtained from mice was mixed with 100 μL 1 M HCl and the second with 0.1M HCl and kept for 2.5 hours with gentle agitation. The homogenate was then centrifuged at 2000g for 2-3 minutes. The supernatant was decanted into tubes and kept at -20°C until further use. In this experiment, four samples were prepared from each set by mixing 20 μL of each sample with 20 μL of HTMPP stock solution (1 mM) and 10 μL of MMDA internal standard solution (1 mM). To each mixture 30 μL of the 5×10^{-3} M HCl catalyst was added and next the mixture was sonicated at room temperature for 30 mins. The derivatives formed were eluted with 50 μL of acetonitrile.

MALDI/MS experiments

The analyses were performed on the Micromass TofSpec 2E MALDI instrument, a time-of-flight mass spectrometer operated in the reflectron mode. Ions were generated by a pulsed nitrogen laser at 337 nm and accelerated to 20 keV. The pressure in the ion source was kept at 1×10^{-6} Torr. All experiments were carried out in a condition where the deflection high voltage (matrix suppressor) was set at 20 kV and the detector voltage at 1.5 kV. The individual mass spectra were generated from the average of 200 to 300 laser shots. A polished stainless steel target plate was used for the analyses. Prior to each set of experiments, the plate was cleaned by soaking it in dichloromethane, followed by hexane, pure formic acid and deionized water and rinsing with acetonitrile.

Results and Discussion

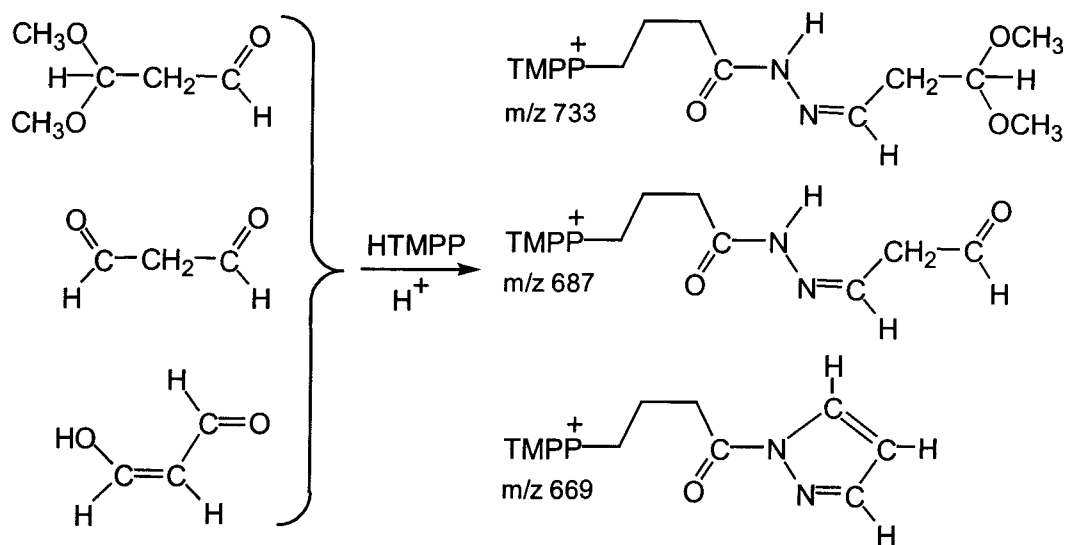
The measurement of low molecular mass compounds by MALDI/MS provides a powerful tool for the investigation of bioanalytical processes. Problems encountered in the analysis of such substances may arise from their volatility, interference with matrix signals or a weak ionization efficiency. Therefore, a straightforward derivatization with a quaternary ion that produces a strong enough signal to eliminate the use of a matrix was investigated. The LOD was estimated and internal standards were applied to measure the performance of the MALDI technique in this analytical procedure. From the data, calibration curves were constructed for the determination of MDA in biological samples. The LOD given refers to the molar amount of the analyte in the mixture applied on the MALDI plate.

MALDI/MS experiments with and without the use of a matrix

Two sets of 12 experiments were performed on a standard mixture of HTMPP and MDA at a molar ratio of 3:1. One set of experiments used DHB as the matrix while the other set contained no matrix at all. A total of 300 laser shots were taken per experiment.

Hydrolysis of the acetal may yield three products, namely the dialdehyde, its enol form and the partially hydrolyzed acetal. Their reaction with HTMPP yields three types of derivatives, see Scheme 4, as indicated by the presence of characteristic ions in the MALDI spectra at m/z 687, 669 and 733 respectively. The latter peak is not always present, compare Figures 1 and 3, but the intensities of all three peaks were summed to derive the MDA content of the samples.

From Fig. 1 and the results presented in Table 1, it follows that the spectra obtained in experiments with and without the matrix are closely similar. This implies that a matrix is not really required in this analytical procedure !



Scheme 4. Hydrolysis of tetramethoxypropane yields HTMPP derivatives of the partially hydrolyzed acetal, malondialdehyde and its enol-keto form that forms a cyclic ion.

Solution	Ions (m/z)	Abundance (average)	HTMPP : MDA (intensity ratio)
HTMPP/ MDA (3:1) with matrix	633	5800	1 : 10
	669	24900	
	687	32200	
	733	None	
HTMPP/ MDA (3:1) without matrix	633	5950	1 : 10
	669	25800	
	687	33600	
	733	None	

Table 1. The results obtained from experiments with and without matrix. The mixture contains only the derivatizing agent HTMPP and the products from the hydrolysis of 1,1,3,3-tetramethoxypropane. The ion at m/z 633 represents the unreacted HTMPP, while ions at m/z 669, 687, and 733 represent the total MDA.

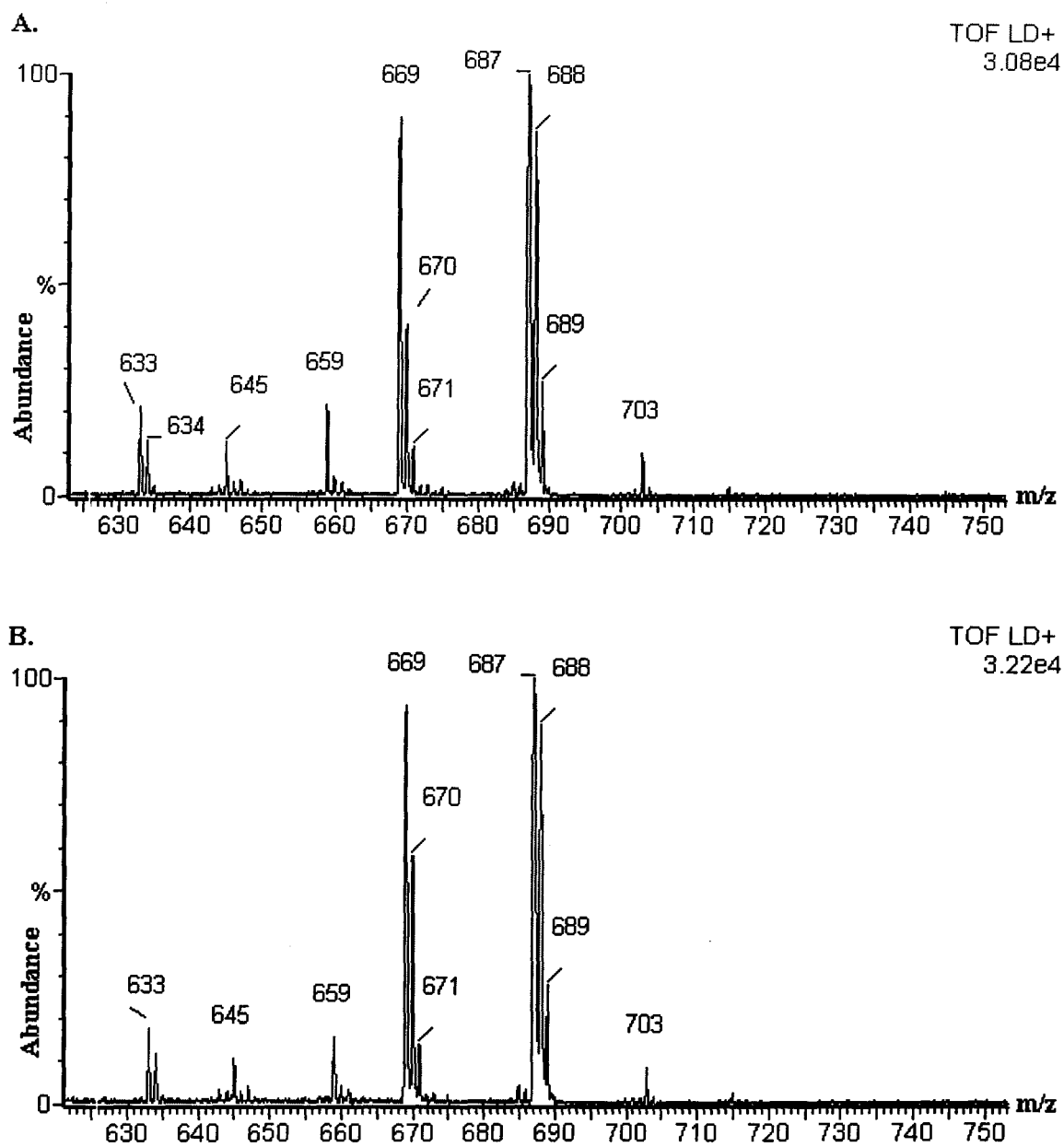


Figure 2.1. MALDI spectra produced from an experiment using DHB as the matrix (item A) and an experiment without any matrix applied (item B).

Limit of detection

The limit of detection (LOD) and the limit of quantitation (LOQ) were calculated from the signal-to-noise ratio of MDA. However, due to the incomplete hydrolysis of the precursor to MDA and its partial enolization, three derivatives are present in the eluate upon reaction with HTMPP, namely the malondialdehyde derivative, the cyclic form of the derivative and the product of incomplete hydrolysis of the acetal, as shown in Scheme 4. The detection limit could therefore not be determined directly from the spectra based only on the intensity of the signal at m/z 687. The fact that the chemical noise varies from one experiment to another, possibly due to varying concentrations of environmental malondialdehyde [25], also requires another method for determining the LOD.

For this purpose, in this project a total of 300 shots was taken per experiment and the noise level was averaged from 10 experiments. A plot of MDA/internal standard vs. MDA concentration was constructed setting the noise level as the intercept. The LOD and the LOQ were then defined as 3 and 10 times the S/N ratios respectively [19]. In the experiment where benzaldehyde was the internal standard, the LOD for MDA was found to be 0.0014 nmol/ μ L and LOQ at 0.0064 nmol/ μ L, whereas in the experiment with methyl malondialdehyde the respective LOD and LOQ were 0.0012 nmol/ μ L and 0.0055 nmol/ μ L.

The plots used for the LOD and LOQ determination are shown in Figure 2. The results of the experiments with MMDA are quite satisfactory. In contrast, those obtained with benzaldehyde appear to be less reliable as the range of error in the intensity ratios was found to be quite large, from 7% to 21% even after repeated experiments. A possible rationale for the deviant behaviour of benzaldehyde is discussed in the next section.

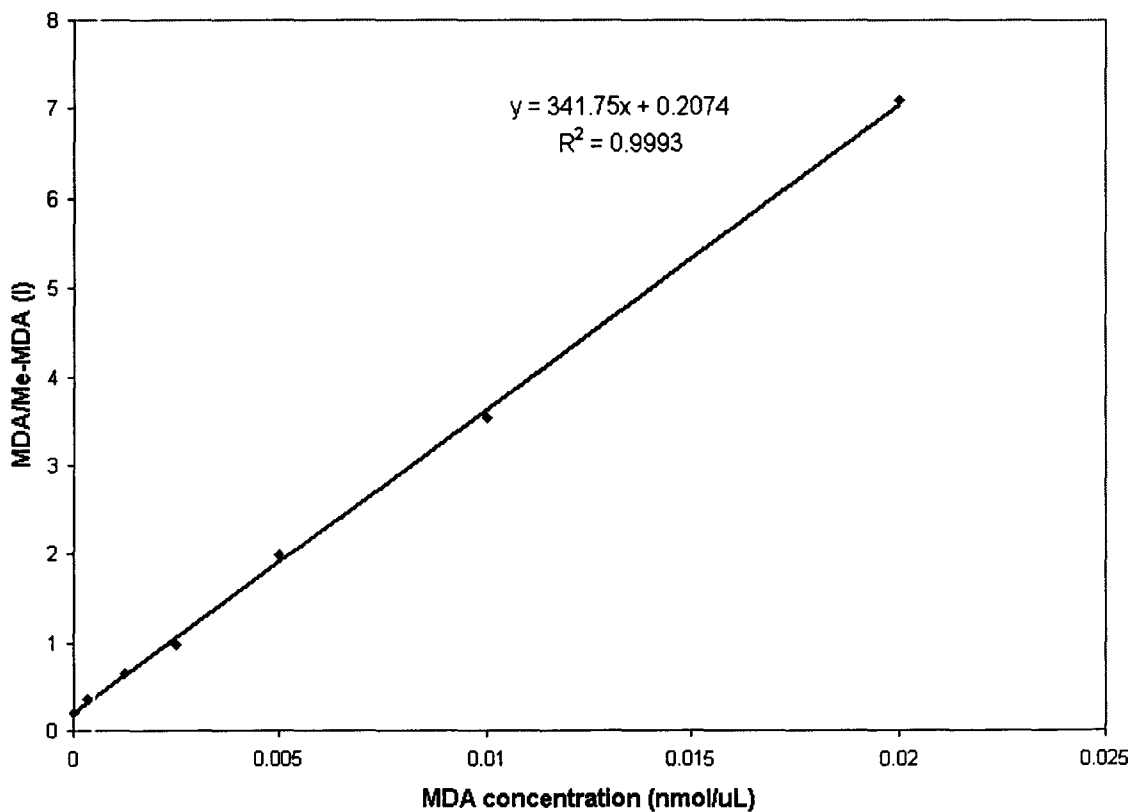
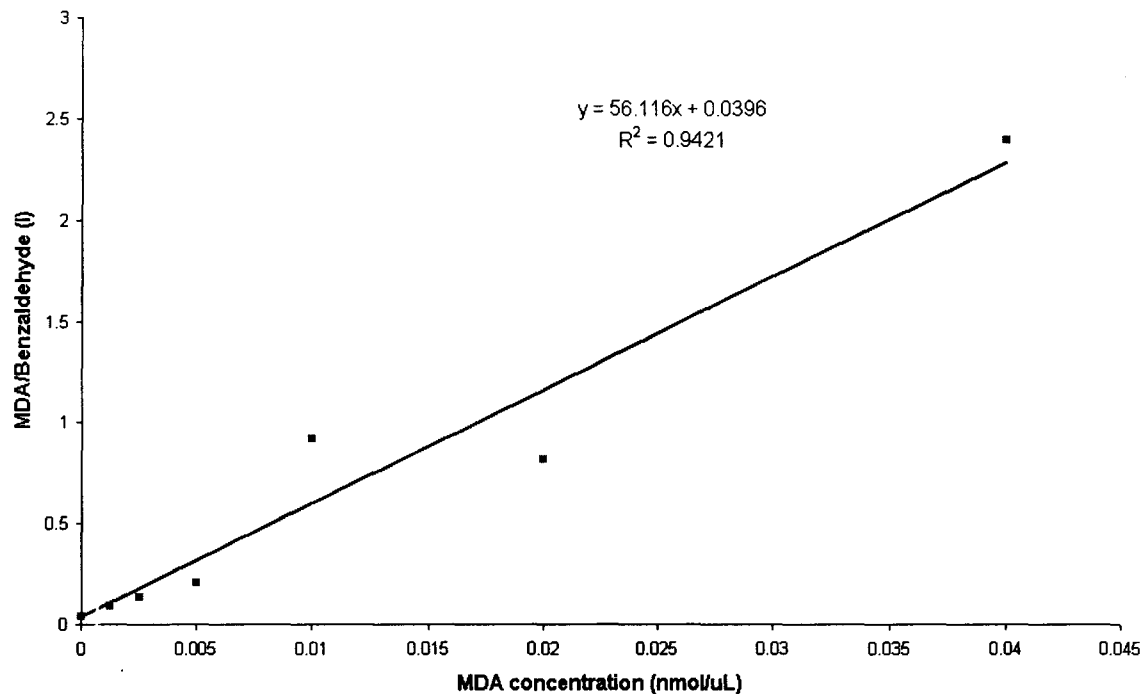
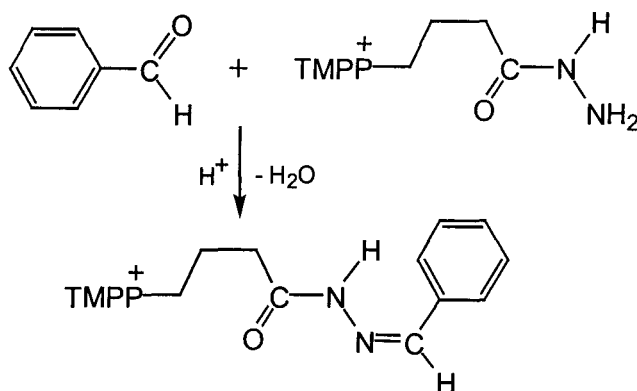


Figure 2.2 Limit of detection of MDA determined from experiments with BzA (top) and MMDA (bottom) as the internal standard.

Application of internal standards for calibration curves

i) The use of benzaldehyde as the internal standard

A dilution series of MDA was added to a standard mixture of HTMPP:BzA at a constant ratio of 20:10. Scheme 5 shows the ions of the underivatized HTMPP and the aldehyde derivative formed.



Scheme 5. The derivative of benzaldehyde and the underivatized HTMPP present in the eluate.

The spectrum of Figure 3 shows the underivatized HTMPP ion at mass 633 and the derivatized BzA at mass 721, while derivatized MDA accounts for the signals at m/z 687 and m/z 669. The partially hydrolyzed acetal generated a derivative at m/z 733.

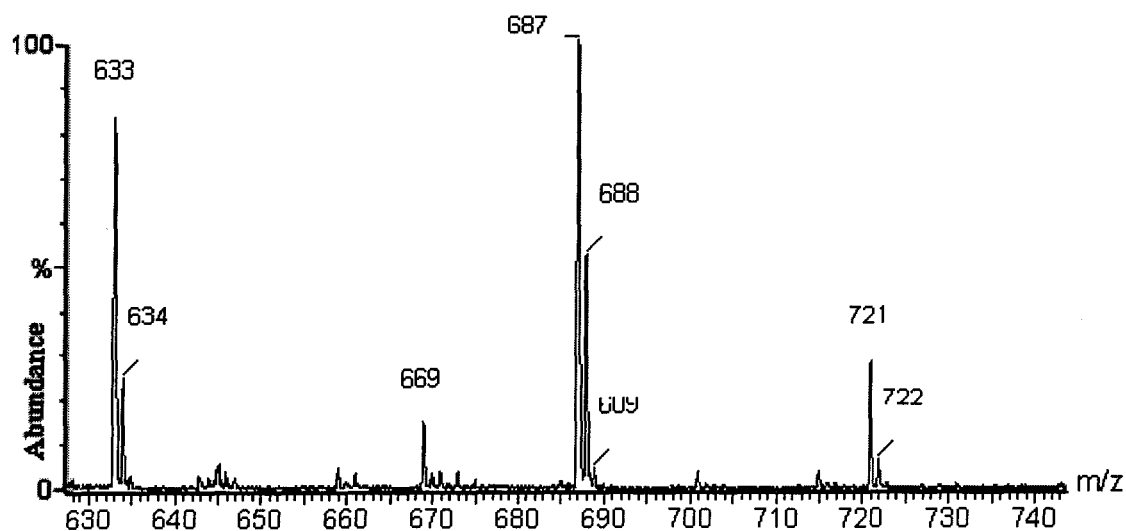


Figure 2.3 MALDI spectra of a mixture containing derivatized MDA (m/z 687 and 669) and BzA (m/z 721).

A calibration curve constructed from the MDA/BzA ratio versus the MDA concentration in Figure 4 produced a linear response from 0.00125 nmol/ μ L to 0.04 nmol/ μ L. The equation for the line was $y = 56.412x - 0.0008$, where y is the intensity ratio and x is the concentration of MDA in nmol/ μ L. The relative standard deviation of the slope (RSD_{slope}) is 12.4 % and $R = 0.9419$. The range of error in the intensity ratio is unexpectedly large : from 7 % to 21 %. These unsatisfactory results could be due to the interference from benzaldehydes released by the resins. This proposal is supported by the observation that occasionally quite an intense signal was present at m/z 721 in spectra of mixtures which did not contain BzA. It should further be noted that benzaldehyde is not structurally close to MDA as compared to MMDA. Hence, a much better results is expected of MMDA as the internal standard.

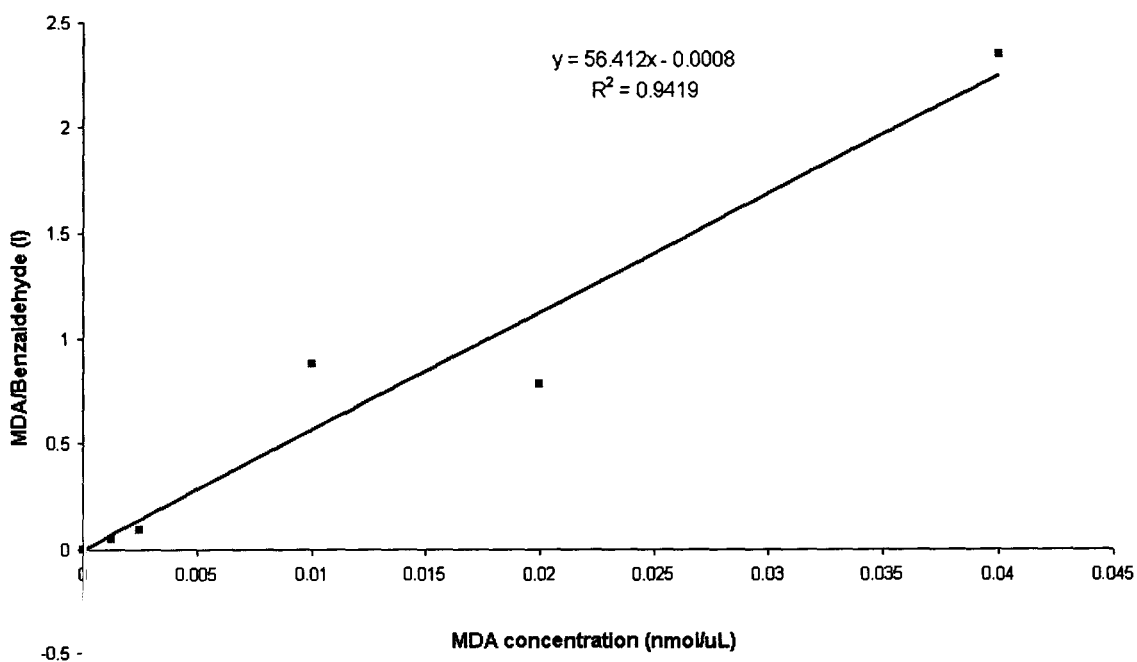
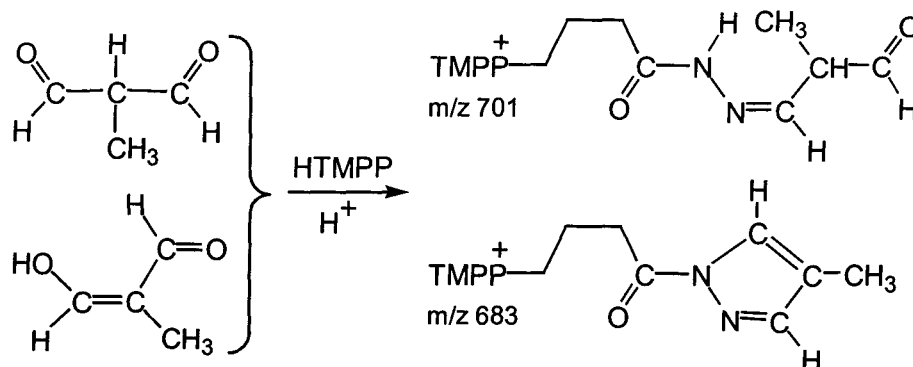


Figure 2.4 The calibration curve for the MDA analysis with BzA as internal standard.

ii) The use of MMDA as the internal standard

Another dilution series of MDA was added to the standard mixture of HTMPP and MMDA at a ratio of 20:10 in an effort to study the application of MMDA as internal standard. The MMDA produced from 3-methoxymethacrolein reacted with the HTMPP reagent to produce derivatives that give rise to signals at mass 701 and at mass 683, which is the cyclic compound shown in Scheme 6. A typical MALDI spectrum is presented in Figure 5.



Scheme 6. Derivatization of MMDA with HTMPP produced compounds at m/z 701 and 683

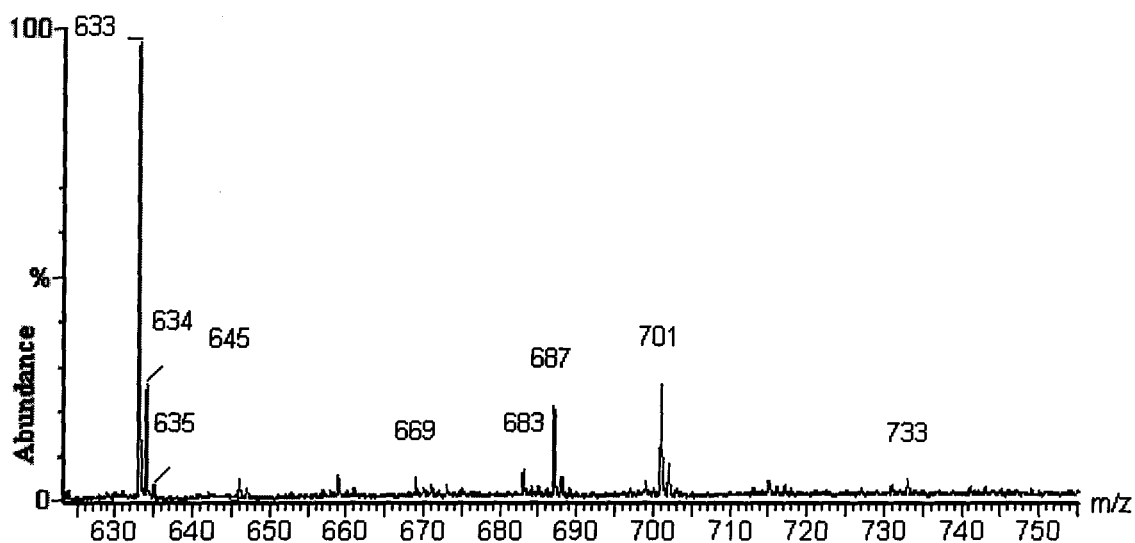


Figure 2.5 MALDI spectra of a mixture containing underivatized HTMPP (m/z 633), derivatized MDA (m/z 669 & 687), MMDA (m/z 683 & 701) and the remaining acetal (m/z 733).

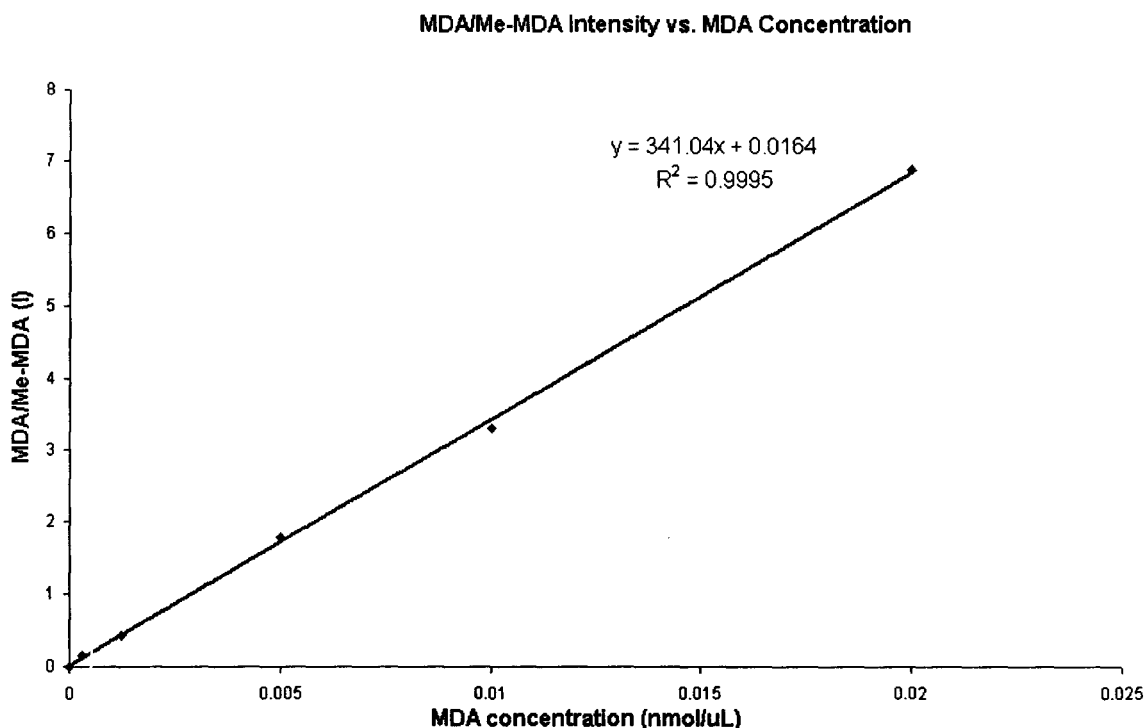


Figure 2.6 The calibration curve for the MDA analysis with MMDA as internal standard.

A plot of the MDA/MMDA ratios versus MDA concentration, see Figure 6, resulted in a linear response from an MDA concentration of 0.0003125 nmol/μL to 0.02 nmol/μL. The equation of the line is $y = 341.04 x + 0.0164$ with the RSD_{slope} value of 1.11 % and $R^2 = 0.9995$. The error in the intensity ratio ranges only from 3 % to 9.4 %.

The observations from the performance of benzaldehyde and methyl malondialdehyde as internal standards in LDI, show that the methyl malondialdehyde is a highly reliable and accurate internal standard for the analysis of malondialdehyde on the MALDI.

Analysis of “real life” biological samples

All four samples were analyzed in 5-8 experiments and the error of the intensity ratios ranges from 6 % to 10 %. The MDA concentration in the samples labeled as Q7, Q43, #43, and #80, was found to be 0.00049 nmol/μL, 0.00028 nmol/μL, below the background, and 0.00011 nmol/μL respectively, see Table 2. The trend of the results in

both the 0.1 M HCl and the 1M HCl sets of samples is found to be consistent. It has been documented that the accurate measurement of MDA content in biological samples depends on several factors which include the subject's environment and activities, the derivatization efficiency and extraction recovery, the mild conditions for sample processing to minimize lipid oxidation, artifact formation that could alter MDA results and the release of bound MDA [13,14].

The results obtained so far show the capability of this method to detect the presence of MDA in "real life" samples but further work is required to confirm the concentrations determined.

Sample	MDA Content (nmol/uL)	
	1M HCl	0.1M HCl
Q7	0.00049	0.00026
Q43	0.00028	0.00005
#48	below background	below background
#80	0.00011	0.00003

Table 2. Results for the biological samples.

Accuracy and Precision

Analytical methods employed for the determination of drugs and metabolites in biological matrices such as urine, plasma and serum are essential throughout drug discovery and development. These data are used to evaluate the bioavailability and pharmacokinetic parameters of a drug to determine if development of the drug should continue, hence the methods that produce the data should be accurate.

The Food and Drug Administration (FDA) has adopted certain guidelines for bioanalytical methods validation to ensure accuracy and precision, sensitivity, selectivity, recovery and stability.

A method is first developed that is capable to determine a reliable concentration of the analyte in the matrix. A calibration curve is then constructed using controlled analyte mixtures. Quality control samples are prepared similarly in terms of method,

conditions and internal standard content and used as a reference to the calibration curve to determine the accuracy and precision of the method.

Method Validation

A calibration curve is created for each analyte in the matrix and in this project, it was constructed specifically for MDA using a series of controlled MDA solutions. As per the FDA guidelines [25], the calibration curve should consist of at least six points in duplicates. The accuracy of each calibration point should be 85-115% except at the lower limit of quantitation (LLOQ) where accuracy may deviate by $\pm 20\%$.

Accuracy

The accuracy of a bioanalytical method is defined as the nearness of a mean of the test results to the true expected value. Accuracy is determined by the analysis of at least five replicate QC samples at three different concentrations spanning the range of the calibration curve. The mean calculated concentration should be within 15% of the intended concentration value except at the LLOQ, where a deviation of up to 20% is allowed. The percent accuracy is calculated as follows: $(C_m/C_i) \times 100$ (Eqn.1), where C_m is the mean of the calculated concentrations and C_i is the intended concentration. Accuracy is generally expressed as a mean of the individual calculated concentrations such as 105 % accuracy.

The accuracy test was performed on seven concentrations spanning the calibration curve with five replicate QC samples. Six samples were within the accurate range of 85-115 % with the lower concentrations, i.e. 0.00125 nmol/ μ L and 0.000625 nmol/ μ L MDA, being close to the 115 % limit.

Precision

The precision of a bioanalytical method illustrates the nearness of tests results upon the repeated analysis of identically prepared QC samples. Precision should be measured using at least five duplicates at each QC concentration. Precision is often calculated as: $SD/C_m \times 100$ (Eqn. 2), where SD is the standard deviation and C_m is the mean of the measured concentration. This value can be translated as the relative standard

deviation of the calculated concentrations (% RSD) or coefficient of variation (CV). The results of the accuracy and precision test are listed in Table 3.

Nominal Concentration (nmol/ μ L)	Accuracy Cm/Ci (%) n=5	Deviation fr. true value (Cm-Ci)/100	Precision (RSD%) n=5
0.000625	112	12.5	3.24
0.00125	115	14.9	13.2
0.00250	94.5	5.48	7.22
0.00500	97.6	2.44	9.07
0.0100	107	7.48	11.8
0.0200	114	13.8	3.29

Table 3. The accuracy and precision of the proposed method.

Conclusion

The newly developed derivitazation reagent HTMPP, in combination with the solid phase analytical derivitazation method allows for the derivitazation, isolation and detection of malondialdehyde, a small volatile and hydrophilic molecule by MALDI/MS.

Furthermore, the use of this derivitazing reagent leads to abundant signals in a MALDI type analysis without a matrix. The selectivity of this reagent towards carbonyl containing compounds and its sensitivity in MALDI/MS provides a possibility for the automation of the solid phase derivitazation technique and enables the routine analysis of malondialdehyde, which is usually present in trace amounts only.

This project also supports the versatility of methyl malondialdehyde as a structurally compatible alternative internal standard for malondialdehyde determinations on mass spectrometric instruments, thus minimizing the cost or complications in synthesizing isotope-labelled compounds for the same purpose. In this project the methyl malondialdehyde was prepared in a similar manner to that of the malondialdehyde standard solution.

Concurrently, this project highlights the need to further investigate the validity of results in bioanalytical methods in which benzaldehyde, a compound not present in a biological matrix, is applied as internal standard in the presence of polystyrene divinylbenzene resins.

In conclusion, the combination of solid phase analytical derivatization, the lipophilic and selective new derivatizing reagent, the non-matrix application on the MALDI/MS and the structurally close but easily synthesized and cheaper alternative of internal standard will make the analyses of malondialdehyde fast and fully automated on a mass spectrometer.

References

1. V. Spikmans, S.J. Lane, B. Leavens, A. Manz, N.W. Smith. *Rapid Commun. Mass Spectrom.* 16 (2002) 1377.
2. J.W. Gouw, P.C. Burgers, M.A. Trikoupis, J.K. Terlouw. *Rapid Commun. Mass Spectrom.* 16 (2002) 905.
3. Tholey A, Wittmann C, Kang M, Bungert D, Hollemeyer K, Heinzle E. *J. Mass Spectrom.* 37 (2002) 963.
4. D.C. Muddiman, A.I. Gusev, K.I. Langner, A. Proctor, D.M. Hercules, P. Tata, R. Venkataramanan, W. Diven. *J. Mass Spectrom.* 30 (1995) 1469.
5. K.K. Mock, M. Davey, J.S. Cottrell. *Biochem. Biophys. Res. Commun.* 177 (1991) 644.
6. M. Steup, B. Stahl, M. Karas, F. Hillenkamp. *Anal. Chem.* 63 (1991) 1463.
7. M.W. Duncan, G. Matanovic, A. Cerpa-Poljak. *Rapid Commun. Mass Spectrom.* 7 (1993) 1090.
8. M.J. Kang, A. Tholey, E. Heinzle. *Rapid Commun. Mass Spectrom.* 15 (2001) 1327.
9. J. Horak, W. Werther, E.R. Schmid. *Rapid Commun. Mass Spectrom.* 15 (2001) 241.
10. E.N. Frankel, W.E. Neff. *Biochim. Biophys. Acta.* 754 (1983) 264.
11. H. Esterbauer, R.J. Schaur, H. Zollner. *Free Radic. Biol. Med.* 11 (1991) 81.
12. B. Karlberg, G. Thorsen, K. J. Claeson, *Chromatogr. B.* 751 (2001) 315.
13. G. Cighetti, S. Debiassi, P. Ciuffreda, P. Allevi. *Free Radic. Biol. Med.* 25 (1998) 818.
14. G. Cighetti, P. Allevi, S. Debiassi, R. Paroni. *Anal. Biochem.* 266 (1999) 222.

15. G. Cighetti, R. Paroni, I. Fermo. *Anal. Biochem.* 307 (2002) 92.
16. G. Cighetti, P. Allevi, L. Anastasia, L. Bortone, R. Paroni. *Clin Chem.* 48 (2002) 2266.
17. A.W. Bull, L.J. Marnet. *Anal Biochem.* 149 (1985) 284.
18. P. Maboudou, D. Mathieu, H. Bachelet, J.F. Wiart, M. Lhermitte. *Biomed. Chromatogr.* 16 (2002) 199.
19. D.C. Muddiman, A.I. Gusev, A. Proctor, D.M. Hercules, R. Venkataramanan, W. Diven. *Anal. Chem.* 66 (1994) 2362.
20. M. Boljan-Leymarie, E. Bruna. *Anal. Biochem.* 173 (1988) 174.
21. A.S. Csallany, M.D. Guan, J.D. Manwaring, P.B. Addis. *Anal. Biochem.* 142 (1984) 277.
22. S.M. Breckenridge, X. Yin, J.M. Rosenfeld, Y.H. Yu. *J. Chromatogr. B.* 694 (1997) 289.
23. J.M. Rosenfeld, *J. Chromatogr. A.* 843 (1999) 19.
24. S.J. Barry, W.J. Leavens, C.O. Manning, R.M. Carr, S. Monte, I. Waterhouse. *Rapid Commun. Mass Spectrom.* 17 (2003) 484.
25. R. Andreoli, P. Manini, M. Corradi, A. Mutti, W.M.A. Niessen. *Rapid Commun. Mass Spectrom.* 17 (2003) 637.
26. S.R. Needham. *American Pharmaceutical Review*

Chapter 3

Analysis of diols in aqueous solutions by their oxovanadium (VO^{++}) complexes using electrospray mass spectrometry

Preamble and summary

The complexation of diols to a metal ion forms the basis of this study where an oxovanadium (IV) complex of ethylene glycol is used as the reagent to study the complexation reaction, equilibrium constant, and competition of other diols for complexation with the vanadyl ion (VO^{++}). The ultimate goal of this study is to develop a fast and reliable method to detect and quantify diols and small polyols in aqueous solutions and biological samples like blood serum and urine with a minimal clean-up.

The analysis is performed using the combination of positive ion electrospray mass spectrometry (ES/MS) for quantitation and tandem mass spectrometry (MS/MS) for structure confirmation. This study builds on the work described by Suzanne Ackloo in Chapter 6 of her PhD thesis: Structure analysis of diols and sugars by their oxovanadium (VO^{++}) complexes using electrospray mass spectrometry [1].

The reagent solution contains the stable [2:1] ethylene glycol : vanadyl ion complex as the internal standard to which the analyte is added prior to the electrospray experiment. The vanadyl complexes formed of interest to this study are: i) the complex with two ethylene glycol molecules, which is the reference complex, ii) the mixed complex of ethylene glycol and the analyte, and iii) the complex with two analyte molecules. The reference complex is used to monitor the efficiency of complexation competition between ethylene glycol and the analytes, hence the complexation tendency of other diols to the vanadyl ion.

The ES mass spectra of the various diols examined produce signals with a high intensity for the mixed and analyte complexes, indicating that effective complexation of the analytes takes place. The peak intensity ratios of the mixed to the reference complex

and that of the analytes to the mixed complex are used in tandem to determine the amount of analyte in an aqueous solution.

The MS/MS experiments can be used to confirm the identity of the diol analyte. These spectra also show differences between stereo isomers of a given diol. However, not all diols studied here showed reliable differences within their isomers.

To study the potential interference of molecules with amino groups, the complexation of oxovanadium to ethanolamine and some diamines was also studied. The analysis reveals that VO^{++} is much more selective for complexation with O-containing than N-containing ligands.

The results of this study indicate that this simple complexation method may be useful to probe the presence and the structure of unknown diols in aqueous solutions. The method is shown to have a detection limit of 6 picomol/ μ L for 1,2-propanediol.

Introduction

Diols have been studied for various reasons. Propylene glycol, for example, is a valuable solvent that finds many uses in food and consumer products such as vanilla extracts and a variety of shampoos. It is also used as a nontoxic antifreeze in breweries and dairy establishments. Ethylene glycol, although widely used in polymer production, is toxic and can cause severe kidney damage or even death [2]. Methods to detect, quantify, and monitor the concentration of diols are continuously being improved as some of these diols are related to our physiological conditions. *meso*-2,3-Butanediol, 1,2-propanediol, and *d,l*-2,3-butanediol, for example, have been associated with alcoholism. Hence, studies are being performed to establish the relationship between their concentration in our body and the development of alcoholism [3]. The investigation on diols has been extended to the study of cis-diol (bio)molecules such as catecholamines and ribonucleosides, which serve as the diagnostic marker for a variety of metabolic disorders. In addition to these (bio)molecules, the detection and quantitation of the diol epoxides formed in the metabolism of polycyclic aromatic hydrocarbons (PAHs) is also important, as this metabolite is carcinogenic [4].

Previous studies of vanadyl complexes using electrospray and atmospheric pressure chemical ionization have shown that protonated neutral complexes $[M+H]^+$ are formed these ionization methods [1]. Based on this observation, and also the boric acid study for the detection of (stereo)isomeric polyols [5], electrospray ionization is chosen as the instrument for the study of diol complexation with the vanadyl ion.

By far the greatest portion of information available on the thermodynamics of coordination is derived from studying competitive processes involving the rivalry of solvent or ligand for a coordination site. In this Chapter we further explore the possibility of using competition for complexation to VO^{++} by other diols against ethylene glycol for the detection of the diols in solution and the analysis of their structures. The study also includes the competition between oxygen and nitrogen-containing ligands for complexation to the oxovanadium ion.

Coordination chemistry involves ligands that are predominately sigma donors with moderate to weak π -acceptor or π -donor tendencies, bound to a metal ion [6]. Vanadium (V) is a $3d^34s^2$ metal which forms π -bonds with ligands, and it exists in a variety of oxidation states ranging from + 5 to - 1. However, the predominant oxidation states of vanadium ions in aqueous solution, are the V(IV) and V(V) ions. VO^{++} forms many stable complexes; although in general it is more stable than the vanadate ion, its stability is enhanced by chelation of ancillary ligands [7,8]. The V(IV)/V(V) redox reaction is also strongly pH dependent. The oxidation of vanadyl salts is slow in acidic solution and can be limited by maintaining the pH below 4 [9].

The chemistry of vanadium is dominated by the formation of oxo species, which have very little tendency to undergo protonation in acidic solution or to interact with other metal ions [10]. It is generally assumed that V(IV) perchlorate in acidic aqueous solution exists in the form of $[VO(OH_2)_5]^{2+}$. The unique feature about this ion is the multiple bond between V(IV) and one of its oxygens, giving a strong axial symmetry to the molecule. This results in three types of oxygens coordinated to a positive center from the four equatorial water molecules and one at the position trans to the yl-oxygen. In a solvent such as water, the axial and equatorial ligands are readily exchanged with water molecules, but the water molecule that replaced the ligand in the trans position to the yl-oxygen usually has a very short residence time of about 10^{-11} seconds. The exchange of equatorial ligands with solvent is fast, with $k = 500 \text{ sec}^{-1}$ compared to $k < 20 \text{ sec}^{-1}$ for the

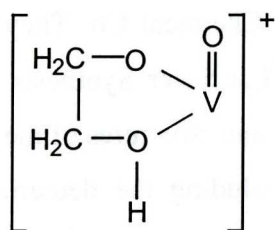
exchange of the yl-oxygen [11]. In the solid state, bis(maltolato)oxovanadium(IV) abbreviated as VO(ma)₂, is five-coordinate with a square pyramidal geometry in which the oxo ligand occupies the axial position, and the two maltol ligands are trans to one another. However, in a polar solvent such as methanol or water, a solvent molecule binds at a position primarily cis to the oxo ligand [12]. The intrinsic rate at which this ligand exchanges with solvent is of fundamental interest from a mechanistic standpoint because of its close relationship to substitution reaction in aqueous V(IV). These observations indicate that ligand exchange in VO⁺⁺ complexes is expected to occur readily under our experimental conditions, and that oxovanadium complexes containing the solvent as a ligand, may also be observed.

Theory predicts that as a hard metal ion, oxovanadium (IV) would prefer coordination of O-donor (bio)molecules, especially those containing a negatively charged O-donor such as carboxylate, phenolate, phosphate or alcoholate [13]. In solution, the vanadyl (IV) ion coordinates with the tartrate anion to give various complexes, depending on the pH of the solution and the relative amounts of vanadyl (IV) and tartrate present [14]. An important feature in the context of this study is the formation of a vanadyl complex containing two tetranegative tartrate ions in which all alcoholic and carboxylic hydrogens are removed. It is also of interest that selective complexation takes place in the presence of the racemic tartrate.

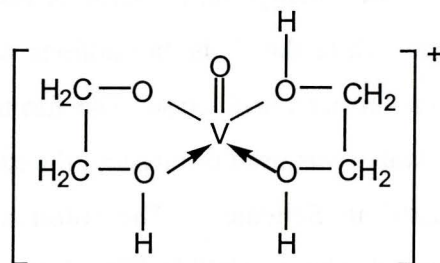
The complexing ability of sugars involves the deprotonation of their hydroxyl groups. In neutral or basic solution, the sugars need an additional donor group to anchor the metal ion at low pH for it to favor the coordination of the hydroxyl groups. The carboxylate acts as the anchoring group in D-galacturonic acid, hence in VO⁺⁺ complexation to D-galacturonic acid, VO⁺⁺ initially binds to the carboxylic group. Once bound to the ligand, deprotonation of the hydroxyl groups occurs so that VO⁺⁺ then coordinates to four of the deprotonated hydroxyls [15]. These observations suggest that simple sugars are able to complex VO⁺⁺ without extra donor groups. Micera et al. support this hypothesis by their finding that VO⁺⁺ complexes with simple sugars, L, yield a structure [VOL_dH]⁺ [#] when the molar ratio of sugar to VO⁺⁺ is 1:1. When the molar ratio is 2:1, the complex [VO(L_d)₂H]⁺ is formed. The formation of 2:1 ligand to metal complex was also observed in the presence of excess ligand in the oxovanadium complex with maltol [12].

Note that the subscript “d’ in L_d refers to a ligand molecule L that has been deprotonated by the loss of one proton

In various analytical studies of vanadyl complexes, the neutral complexes are readily protonated in the electrospray positive ionization mode to yield $(M+H)^+$ ions, which is the technique applied in this study. As shown in the study of Suzanne Ackloo [1], the complexes formed between VO^{++} and a polyol L are the 1:1 complex of $[VOL_dH]^+$ and a 2:1 complex of $[VO(L_d)_2H]^+$, whose structures are shown below. These complexes are referred to as [1M] and [2M] complexes.



VOL_dH^+ or 1M



$VO(L_d)_2H^+$ or 2M

In the context of a study of the interaction of VO^{++} with enzymes, Cornman and co-workers [16] have synthesized and characterized three vanadium (IV)-imidazole complexes. Their techniques produced results that support the presence of imidazole in the complexes and the distribution of oxygen and nitrogen donors [17] in the coordination sphere of the VO^{++} . However, in the study of imidazole mimetic ligands with amino [18], imino [19] and pyrazolyl functional groups, there was only one oxovanadium (IV) complex with imidazole coordinated to the metal center, detected [20]. An important observation from Cornman’s study is that in acid medium the ligands are protonated and replaced by solvent molecules. This prompted us to briefly investigate the complexation tendency of amines to VO^{++} in the presence of oxygen-donor ligands.

The bond lengths at the equatorial position of VO^{++} complexes range from 1.90 to 2.05 Å. An O-donor shows a much shorter bond than an N-donor. This reflects the lower affinity of oxovanadium (IV) to nitrogen donors. Amino groups do not form strong complexes with VO^{++} because they form cationic complexes that lack orbitals that can

form π bonds to the “empty” d_{xz} and d_{yz} orbitals of vanadium. The electron-donating ability of nitrogen may not be the only factor which influences the stability of the vanadium complexes. As shown by Crans and Boukhobza [21], complex coordination numbers, steric hindrance of ligands, and solvation also affect the stability of vanadium complexes.

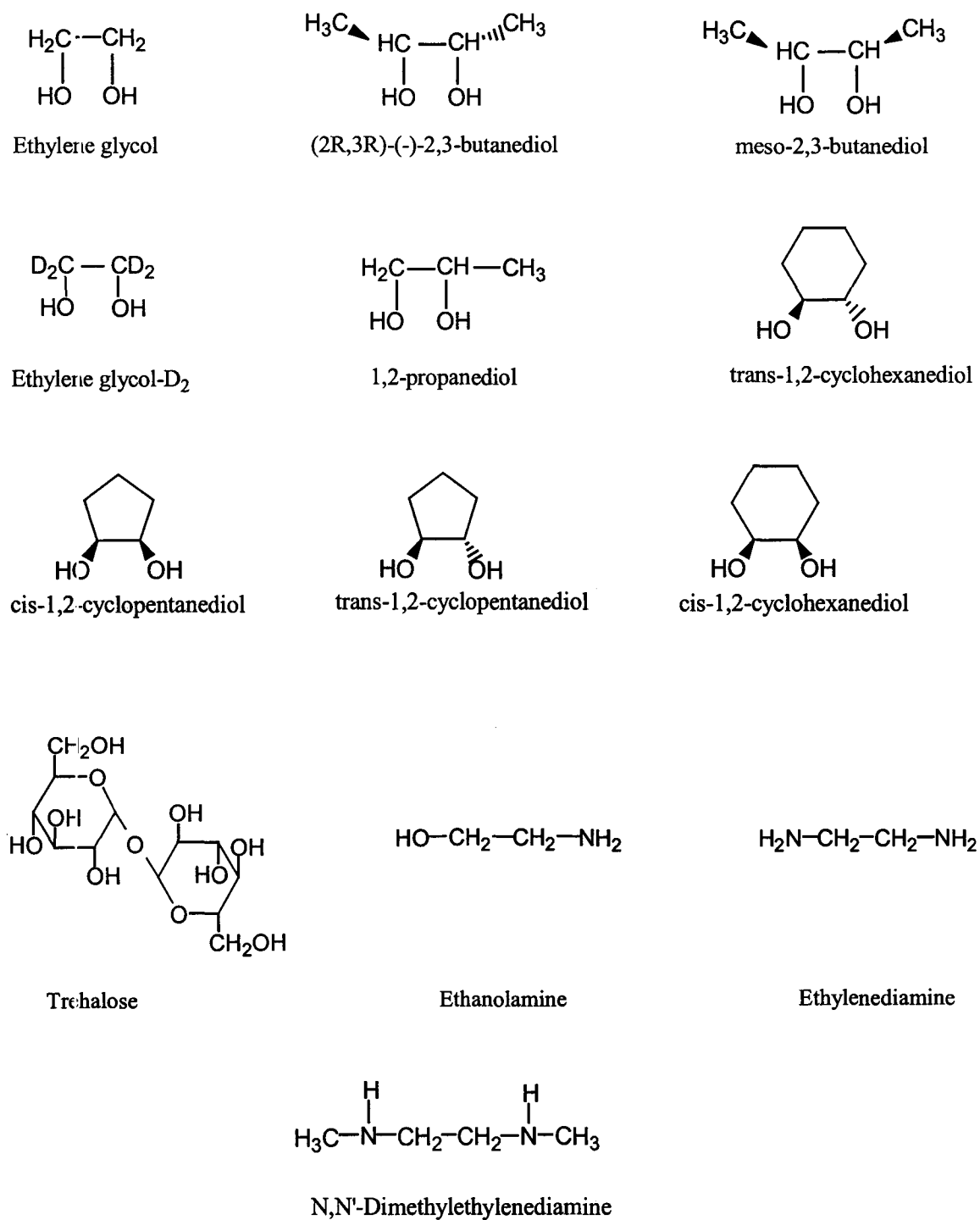
Experimental

The vanadyl sulfate hydrate used in this experiment was purchased from Sigma-Aldrich, while the diols and amines were from Aldrich Chemical Co. They were used without further purification. The formic acid was from Lancaster Synthesis and HPLC grade water was used throughout the experiment. Names and structures of the compound are listed in Scheme 1. The solutions of the diols, including the deuterium labeled ethylene- d_4 glycol ($\text{HOCD}_2\text{CD}_2\text{OH}$), and amines were made at 2.5×10^{-3} M in water. An aqueous solution of formic acid at 2.5×10^{-2} M was used to maintain the pH of the solution below 4.

The mass spectrometric experiments performed involved positive ion electrospray (ES) and MS/MS on the Quattro Ultima instrument (Micromass, England), a Z-spray triple quadrupole instrument. The mass spectra were acquired with the cone voltage set at 35 V, and the capillary at 3.0 kV. The source temperature and desolvation temperature were set at 80 °C and 200 °C respectively and the multiplier voltage was at 450 V to avoid saturation of the detector. The collision gas for the MS/MS experiments was Argon at a gas cell pressure of 2.5×10^{-3} mBar and a collision energy of 10 eV. However, precursor ions that yield only very few ions under these conditions were examined at a higher voltage, 15 eV, and a lower gas cell pressure, 2.5×10^{-4} mBar. The solution was introduced into the electrospray instrument through direct infusion at a rate of 20 $\mu\text{L}/\text{min}$.

It should be noted that the previous study on vanadyl complexes by S.Z. Ackloo. [1] used a different instrument : the Quattro LC (Micromass, England). In that study the cone voltage was set at 15V and the capillary at 3.2 kV. The high voltage lens was set at 0.2 kV and the multiplier at 650 V. Argon was used as the collision gas at a gas cell pressure of 2.5×10^{-3} mBar and a CID voltage of 10 eV. The analyte solution was

introduced into the instrument through a Rheodyne 7010 injector equipped with a 20 μ L injection loop. The mobile phase used throughout the experiment was methanol:water (1:1).



Scheme 1.

Results and Discussion

Complexation of diols

Ethylene glycol (EG) was chosen as the reference diol as it is the simplest polyhydroxy compound that complexes with VO^{++} .

From the study of ref. [1], it follows that ethylene glycol and 1,2-propanediol complex easily with VO^{++} . In theory, a solution containing VO^{++} and an equal amount of EG, and another polyol (L), will form three type of complexes namely the [2M] complexes of $[\text{VO}(\text{EG}_d)_2\text{H}]^+$, $[\text{VO}(\text{EG}_d)\text{L}_d\text{H}]^+$ and $[\text{VO}(\text{L}_d)_2\text{H}]^+$. Should the ES spectrum show signals for the abovementioned [2M] complexes in a ratio of 1:2:1, then EG and the polyol are forming VO^{++} complexes of comparable stability. A much higher intensity of $[\text{VO}(\text{L}_d)_2\text{H}]^+$ in comparison with $[\text{VO}(\text{EG}_d)_2\text{H}]^+$ will indicate the efficient competition of the polyol against EG for complexation to VO^{++} .

In this experiment the molar ratio used for VO^{++} , EG and the polyol is 1:2:1, following the work of S.Z. Ackloo on the complexation of diols to boric acid and oxovanadium [1,5]. The purpose of having excess ethylene glycol in the solution is to avoid memory effects of residual VO^{++} that may be adsorbed in the analyte delivery system.

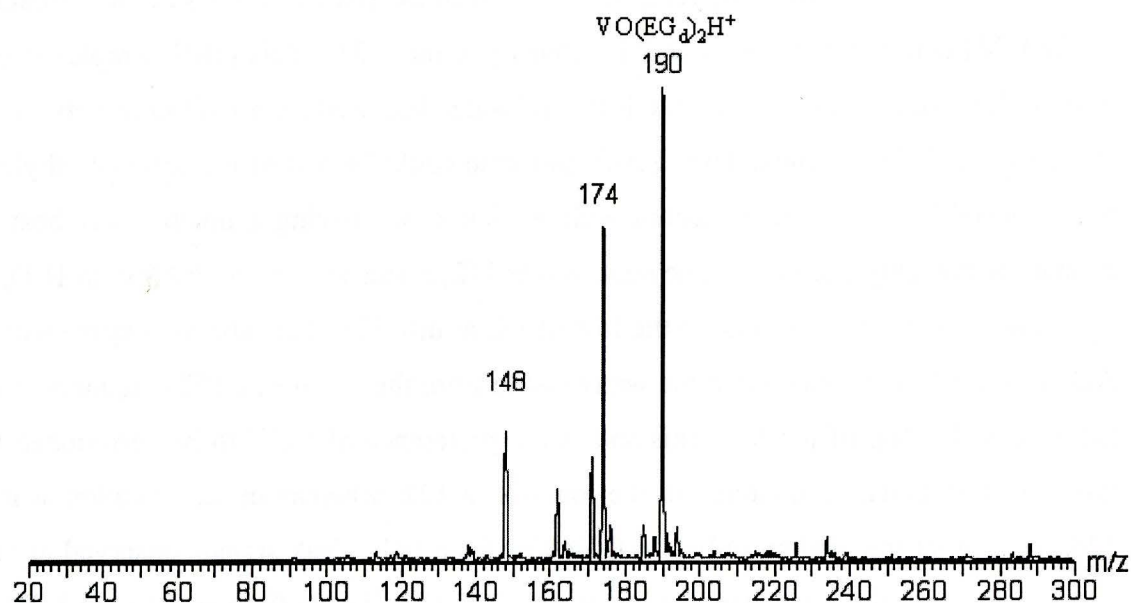
The standard 2.5×10^{-3} M solution of VO^{++} and EG in a 1 : 2 molar ratio was prepared. The polyol of interest was added to the standard solution to form a mixture of VO : EG : polyol in a 1 : 2 : 1 ratio. The pH of the solution was maintained below 4 by adding formic acid of 2.5×10^{-2} M. This was done to prevent the oxidation of Vanadium (IV) to Vanadium (V) [10] and in anticipation of amines that may interfere with oxovanadium-polyol complexation should they be present in the analyte solution. This is based on our preliminary investigation on the complexation of amines to VO^{++} , which showed that in neutral solution the VO/EG/amine mixture readily forms a greyish brown precipitate.

1. Dissociation of the [2M] complex in the reference diol

The ES spectrum of the oxovanadium (IV)-ethylene glycol solution (VO : EG) at 1 : 2 molar ratio is shown in Figure 3-1a. In this spectrum, the peak at m/z 190 belongs to the [2M] complex of EG. The signal at m/z 174 is proposed to be the mixed complex of VO^{++} with EG and formic acid (FA), $[\text{VO}(\text{EG}_d)(\text{FA})\text{H}]^+$, whereas the peak at m/z 148 represents the VO^{++} complex with formic acid and solvent molecules. The ion at m/z 148 is proposed to be $[\text{VO}(\text{FA}_d)(\text{H}_2\text{O})_2]^+$. In the absence of further experimental or computational evidence, the detailed structure of these complexes remains speculative.

The labeling experiment of (VO : EG), using ethylene glycol- d_4 ($\text{HOCD}_2\text{CD}_2\text{OH}$), produced the signals shown in Figure 3.1b. This spectrum confirms the presence of two EG units in the complex at m/z 190 and one in the complex at m/z 174 in the regular experiment. The peak at m/z 148, as predicted, does not contain ethylene glycol as a ligand.

a)



b)

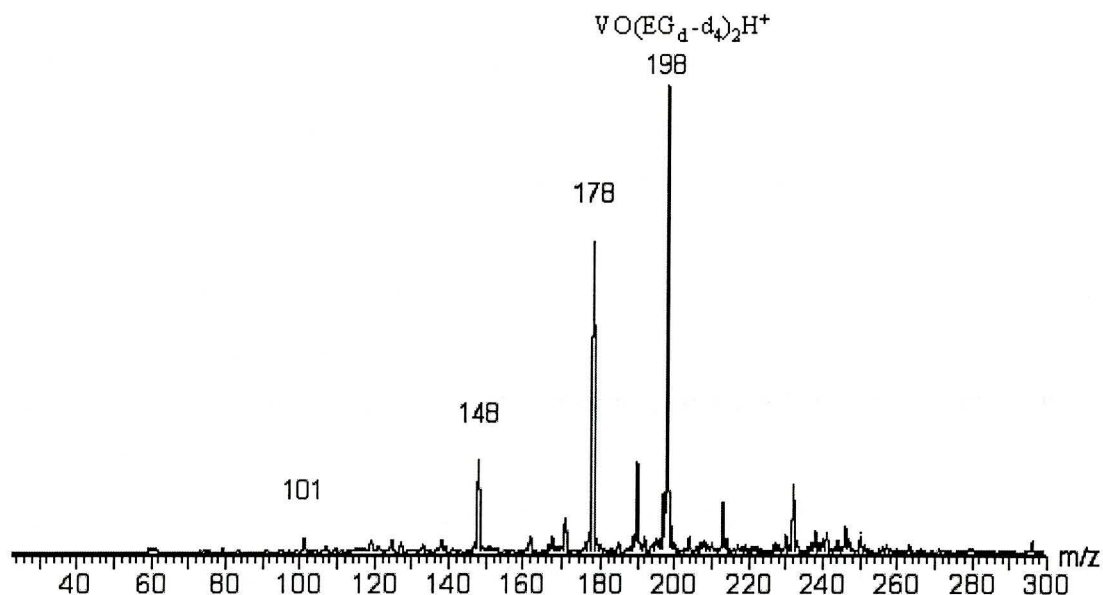
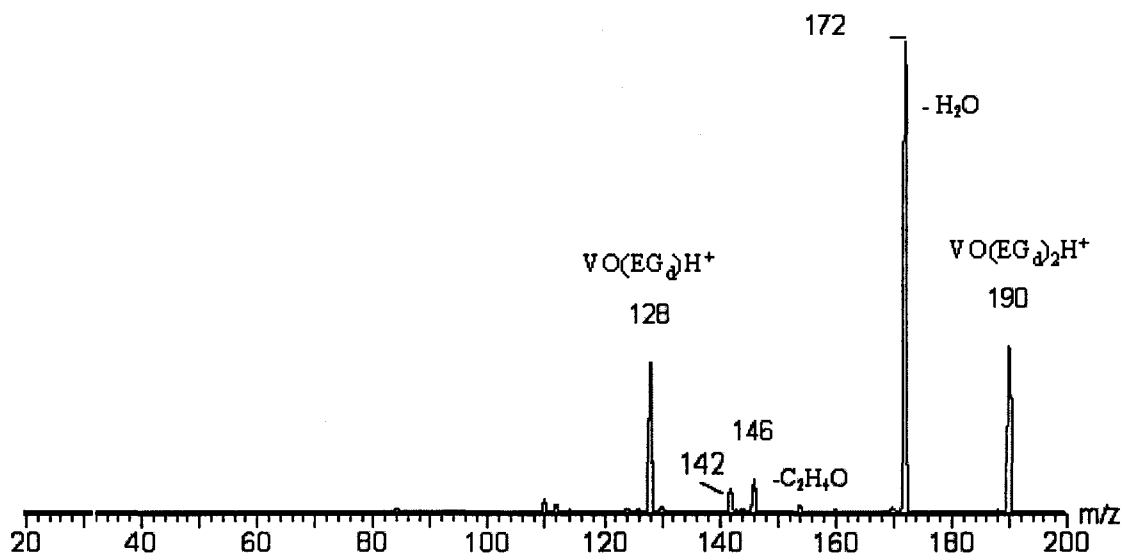


Figure 3.1. a) ES spectrum of VO : EG [1:2] in solution. b) ES spectrum of VO : EG-d₄ [1:2] in solution.

In the MS/MS spectrum of Figure 3.2a, the base peak at m/z 172 corresponds to the loss of water from the [2M] complex. The loss of EG (62 Da) results in the formation of the [1M] complex with considerable intensity at m/z 128. This [1M] complex could also be the result of the consecutive losses of water followed by a C₂H₄O moiety of 44 Da from the [2M] complex. The C₂H₄O molecule could be lost in the form of ethylene oxide, acetaldehyde or vinyl alcohol with the latter two having a much lower heat of formation than ethylene oxide. The peak at m/z 172, corresponding to the loss of H₂O, is more intense than the peak due to the loss of EG at m/z 128. The labeling experiment in Ackloo's work [1] revealed that the water lost to form the ion at m/z 172 originates from the hydroxyl group of the EG. This shows the preference of VO⁺⁺ to be surrounded by three electron-donating O-atoms in the ion at m/z 172, whereas in the complex at m/z 128, VO⁺⁺ is surrounded by only two O-donors from EG. Weak signals observed at m/z 146 and 142 may originate from the losses of a C₂H₄O molecule from m/z 190 and CH₂O of mass 30 Da from m/z 172. The loss of 30 Da to form the complex ion at m/z 142 could also be in the form of the consecutive losses of H₂ and C₂H₄.

a)



b)

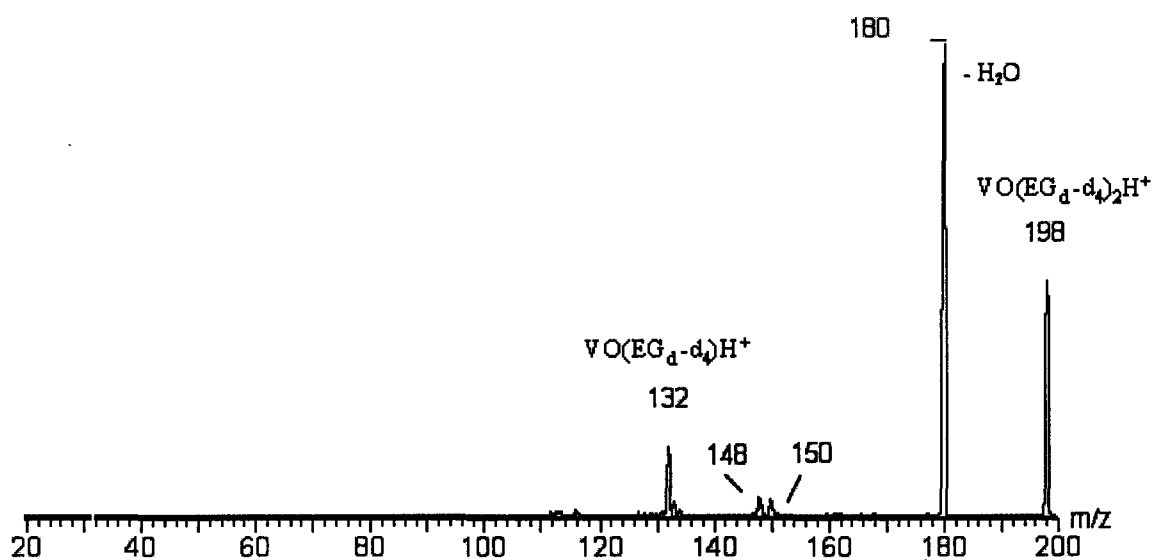


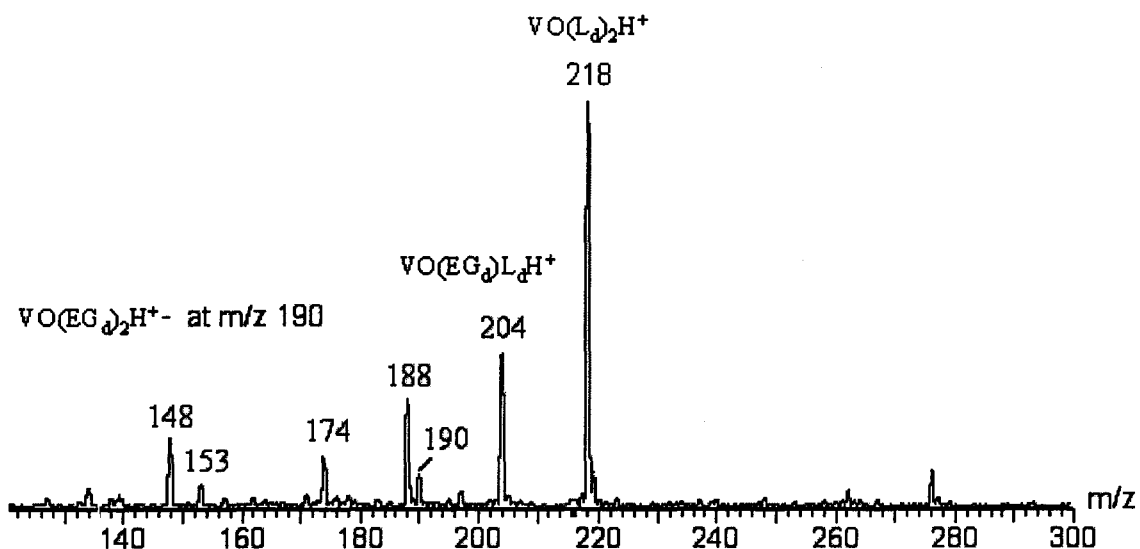
Figure 3.2. a) MS/MS spectrum (Ar, 10 eV) of the [2M] complex of EG, $\text{VO}(\text{EG}_d)_2\text{H}^+$; b) MS/MS spectrum of the [2M] complex of EG-d_4 , $\text{VO}(\text{EG}_d\text{-d}_4)_2\text{H}^+$

The MS/MS spectrum of the ion at m/z 198 in the labeling experiment is shown in Figure 3.2b. The fragment ions at m/z 180, 150, 148 and 132 confirm the presence of EG in the complexes formed at m/z 172, m/z 146, m/z 142 and m/z 128 in the experiment with the unlabelled ion. The ion at m/z 180, loss of 18 Da from the [2M] complex of EG-d_4 , reveals that water is lost in the form of H_2O and that it involves the hydroxyl group of

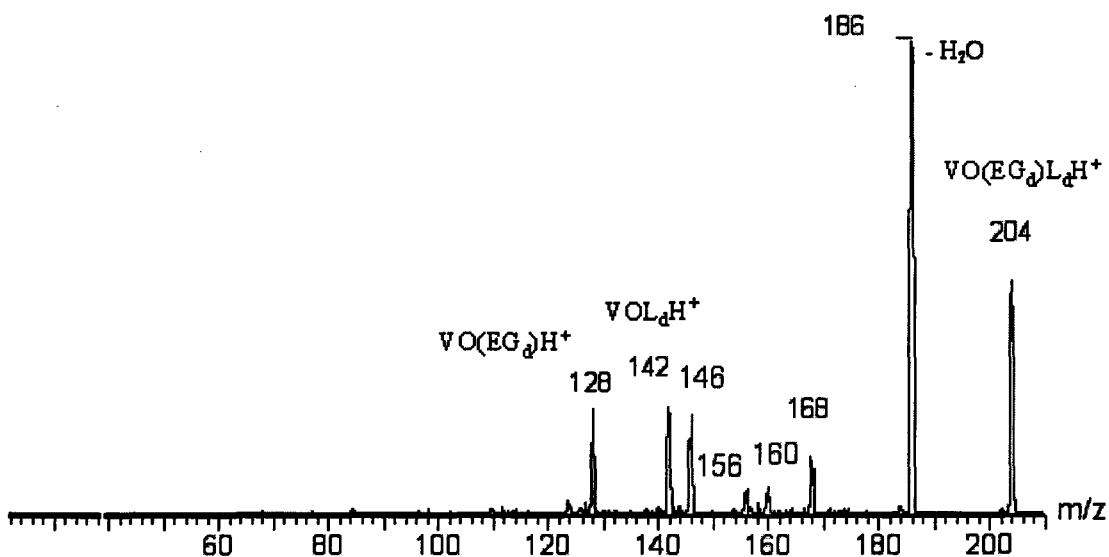
2. Dissociation of the mixed vanadyl complex of EG and 1,2-propanediol

A solution containing VO, EG and 1,2-propanediol in a 1:2:1 molar ratio produced the ES spectrum of Figure 3.3a. At equilibrium, the [2M] complex of EG (m/z 190), the mixed complex (m/z 204), and the [2M] complex of 1,2-propanediol (m/z 218) have an intensity ratio of 1 : 4 : 8. The [2M] complex of 1,2-propanediol is observed to be between 7 - 10 times more intense than the EG [2M] complex within minutes after mixing. Thus, 1,2-propanediol competes effectively with EG in its complexation to VO^{++} .

a)



b)



c)

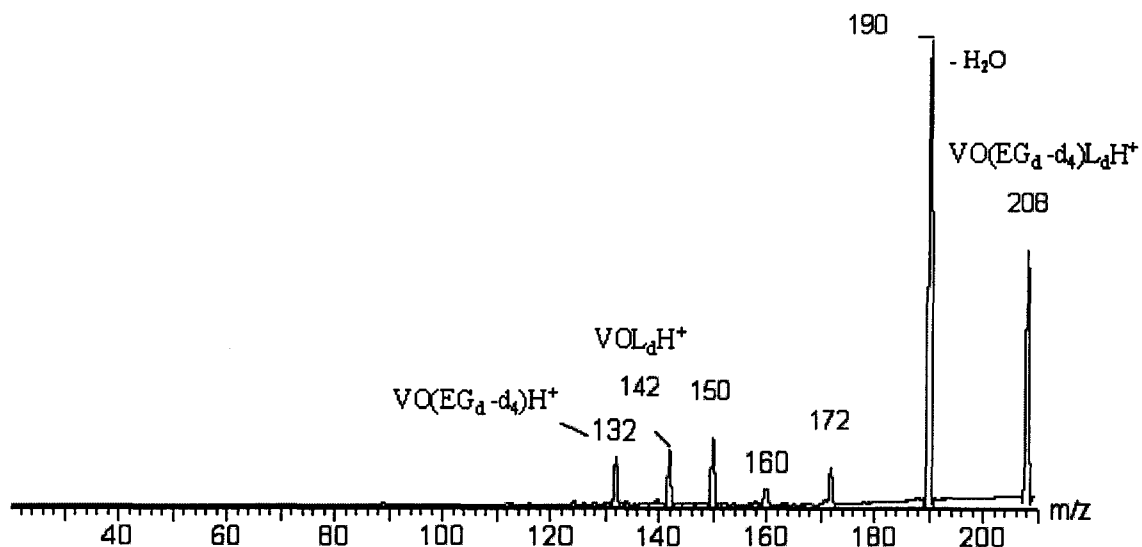


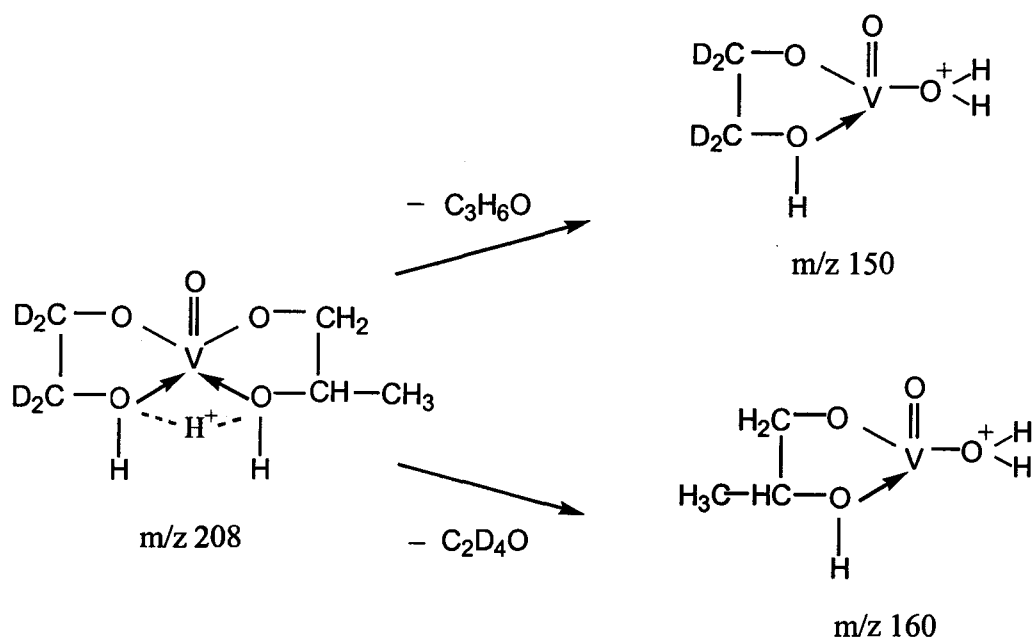
Figure 3.3. a) ES spectrum of VO : EG : 1,2-propanediol [1:2:1] solution. b) MS/MS spectrum of the mixed complex $\text{VO}(\text{EG}_d)\text{L}_d\text{H}^+$ with L = 1,2-propanediol. c) MS/MS spectrum of the mixed complex $\text{VO}(\text{EG}_d\text{-d}_4)\text{L}_d\text{H}^+$ with L = 1,2-propanediol.

The collision-induced dissociation spectrum of the mixed complex at m/z 204 in Figure 3.3b shows peaks of comparable intensity at m/z 142, and 128, corresponding to the loss of EG and 1,2-propanediol, respectively. The peak with the highest intensity, as observed in the dissociation of the reference diol, corresponds to the loss of water. The fact that the m/z 146 peak intensity is higher than that of m/z 160 reveals the higher stability achieved by the mixed complex to lose 58 Da rather than 44 Da to give m/z 160. The mass 58 neutral ($\text{C}_3\text{H}_6\text{O}$) is proposed to be 1,2-propylene oxide, and the mass 44 neutral ($\text{C}_2\text{H}_4\text{O}$), ethylene oxide. The ions at m/z 168 and at m/z 156 are proposed to be the respective losses of H_2O and CH_2O from the ion at m/z 186.

A labeling experiment using ethylene glycol- d_4 yields the MS/MS spectrum of Figure 3.3c. The spectrum shows a mass increase of 4 Da for the fragment ions at m/z 128, 146, 156, 168, 186 in the spectrum of the unlabelled precursor ion, see Figure 3.3a. This observation confirms the presence of one EG unit in these ions. The presence of the ion at m/z 132 supports the proposed loss of the 1,2-propanediol moiety in the formation of the ion at m/z 128, and 1,2-propylene oxide in the formation of the ion at m/z 146. The ion at m/z 190 corresponds to the loss of H_2O from the mixed complex (which occurs

readily in every diol complex studied in these experiments) in Figure 3.3b. It was noted by S.Z. Ackloo [1] that the H atoms in the water molecule lost do not stem from the methylene hydrogen. All water losses observed in this labeling experiment, too, are in the form of H₂O so that the loss of water from the ion at m/z 186 to form m/z 168 may not have involved the methylene hydrogens of the ethylene glycol moiety of the complex. The ions at m/z 142 and m/z 160 do not shift, supporting the proposal that they are generated from the loss of EG and ethylene oxide respectively. It should be noted that the signal at m/z 160 in the labeling experiment could also be an increase of 4 Da from m/z 156 in Figure 3.3b which represents the loss of 30 Da (CH₂O) from the ion at m/z 186. If this is correct, then it suggests that the formaldehyde loss to form the ion at m/z 156 in the experiment with the unlabelled precursor ion originates from the propanediol moiety of the mixed complex.

Scheme 3 represents a tentative proposal for the neutral losses leading to the formation of ions at m/z 150 and 160 in the labeling experiment.

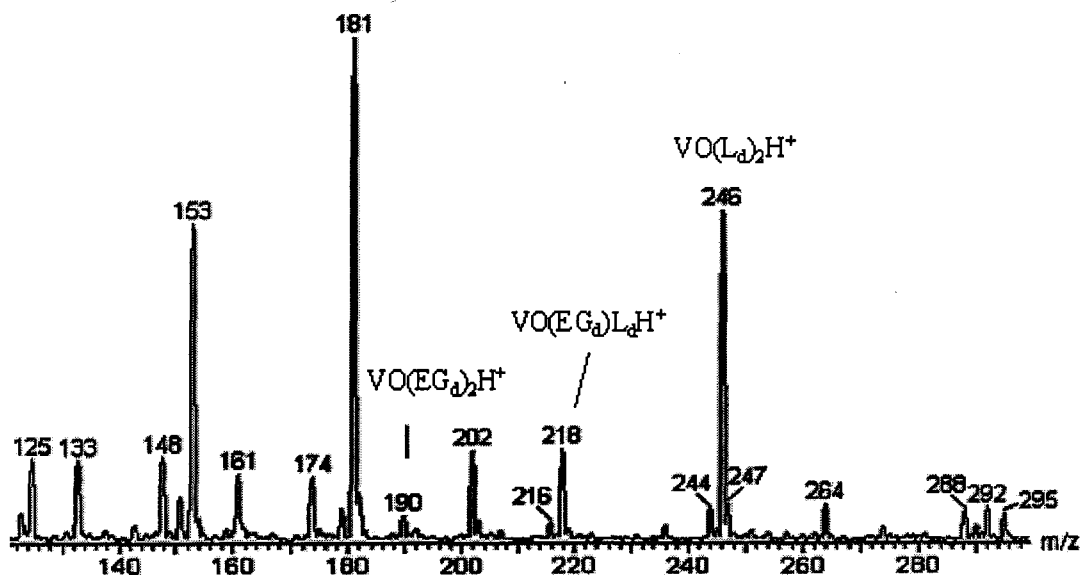


Scheme 3.

3. Dissociations in the vanadyl complexes with stereoisomeric 2,3-butanediols

Figure 3.4 presents the ES mass spectra of solutions containing (2*R*,3*R*)-(-)-2,3-butanediol and its isomer *meso*-2,3-butanediol as the analyte. Generally, the intensity of the [2M] complex of the isomers is more than twice the intensity of the [2M] complex of EG. The full scan mass spectra also show the difference in the intensity ratios of the peaks corresponding to the [2M] complex with (2*R*,3*R*)-(-)-2,3-butanediol, *m/z* 246, to the [2M] complex with EG, *m/z* 190, which is about 3.5 times larger than that observed for the *meso* isomer. This, too, has been observed in S.Z. Ackloo's work [1]. The intensity ratio of the [2M] complex of EG, the mixed complex and the [2M] complex of the (2*R*,3*R*)-diol is 1 : 4 : 14, while for the VO : EG : *meso*-diol system the corresponding ratio is 1 : 2 : 3. From these intensity ratios and the spectra shown in Figure 3.4a and b, it follows that (2*R*,3*R*)-(-)-2,3-butanediol competes more effectively with EG for complexation to VO⁺⁺ than its *meso*-isomer.

a)



b)

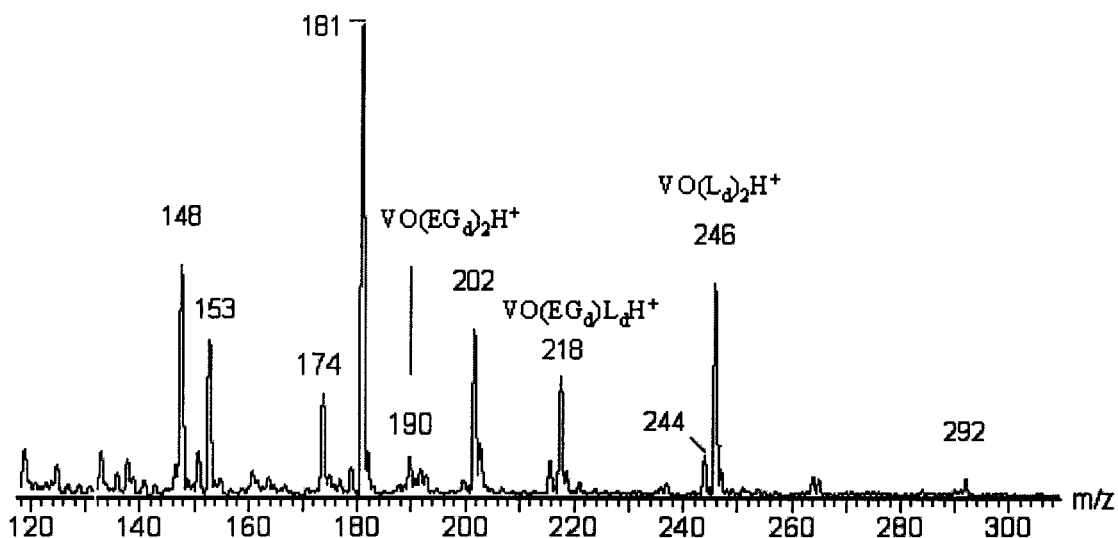


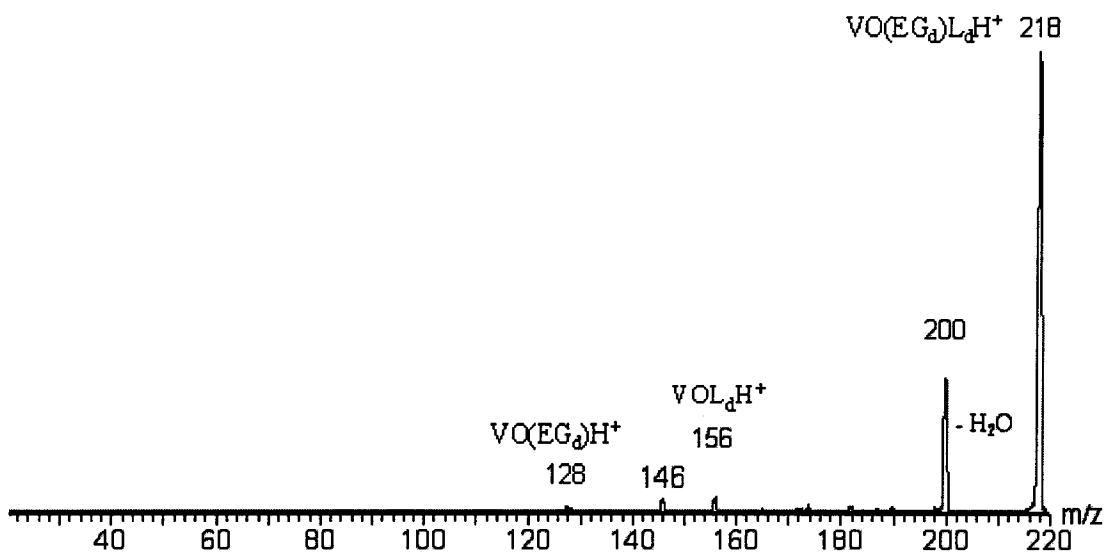
Figure 3.4. a) ES spectrum of VO:EG:2*R*,3*R*-(-)-butanediol [1:2:1] solution. b) ES spectrum of VO:EG:meso-2,3-butanediol [1:2:1] solution.

However, the MS/MS spectra of the mixed complexes of the isomers at m/z 218, taken at a collision energy of 10eV, do not show any appreciable difference except that *meso*-2,3-butanediol shows a stronger daughter ion intensity in general, as observed for the ions at m/z 200, 182, and 156 of Figure 3.5.

S. Z. Ackloo has reported the presence of a weak peak at m/z 188 in the MS/MS spectrum of the isomers, but to a higher extent in the *meso* isomer [1]. In this study, this ion was observed in both isomers but with a much lower intensity, as shown in the spectra of Figure 3.5. The ion at m/z 188 is the result of a formaldehyde loss from the mixed complex.

Another MS/MS experiment was performed at higher collision energy, 15 eV, to study the differences between these two isomers. As seen in Figure 3.6, there is no distinctive fragmentation belonging to any of the isomers. However, beside the presence of new ions in both spectra, the intensity of m/z 140 and 170 is higher in (2*R*,3*R*)-(-)-2,3-butanediol. A consistency observed in the MS/MS spectra acquired at the two collision energies, however, is the fact that *meso*-2,3-butanediol yields more intense peaks at both m/z 146 and m/z 182.

a)



b)

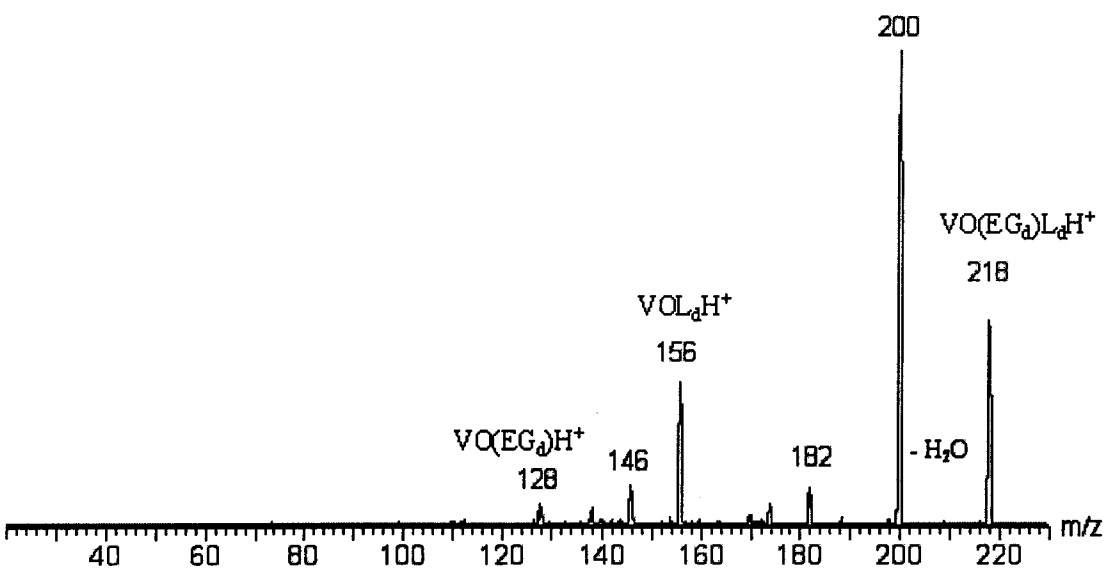
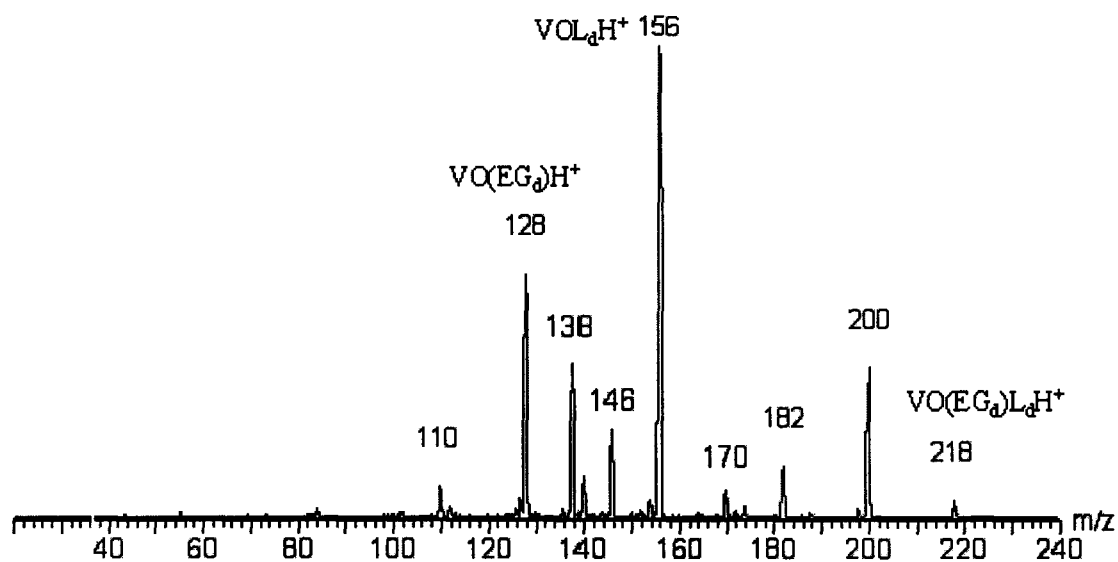


Figure 3.5. a) MS/MS spectrum of the mixed complex of VO : EG : 2R,3R-(-)-butanediol [1:2:1] solution. b) MS/MS spectrum of the mixed complex of VO : EG : meso-2,3-butanediol [1:2:1] solution. MS/MS spectra acquired with Ar at a collision energy of 10eV.

The peak at m/z 146 represents loss of 72 Da, which could be 2,3-butylene oxide (C₄H₈O). The peak at m/z 200 is proposed to be the result of a water loss from the mixed complex and the ion at m/z 182 corresponds to the loss of water from the primary product

ion at m/z 200. The ions at m/z 156 and m/z 128 are formed by the loss of EG and butanediol, respectively.

a)



b)

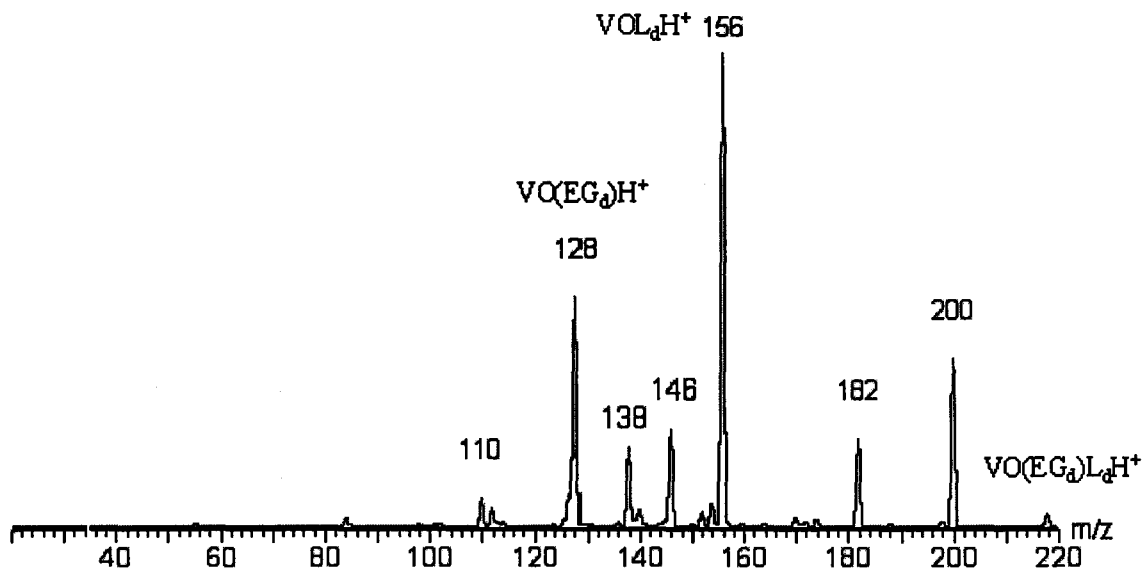


Figure 3.6. a) MS/MS spectrum of the mixed complex of VO : EG : 2*R*,3*R*(-)-butanediol [1:2:1] solution. b) MS/MS spectrum of the mixed complex of VO : EG : *meso*-2,3-butanediol [1:2:1] solution. MS/MS acquired with Ar at a collision energy of 15eV.

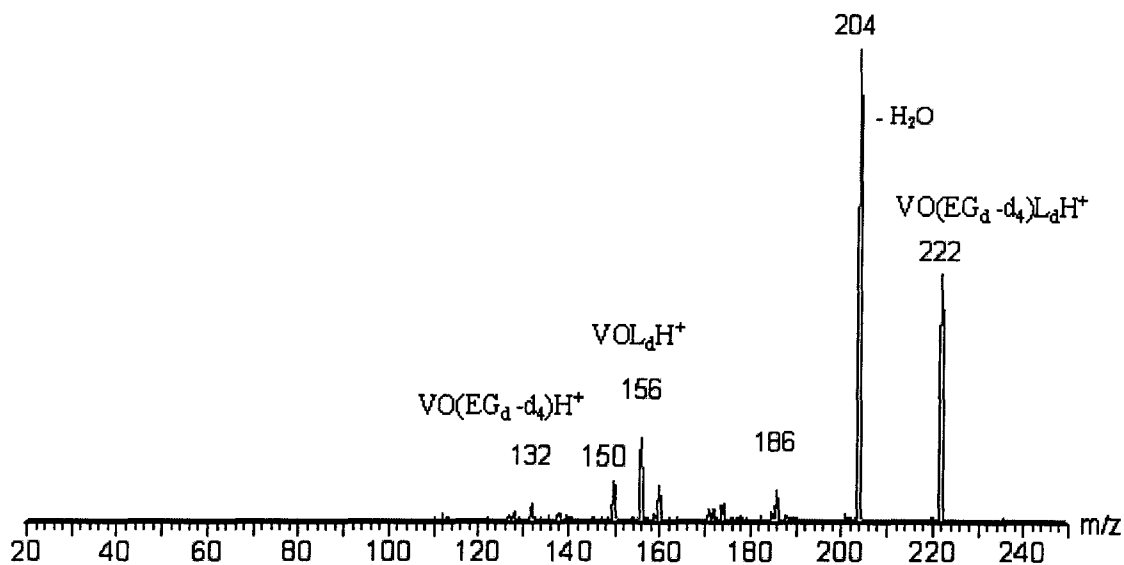


Figure 3.7. MS/MS spectrum of the mixed complex of VO : EG-d₄ : 2R,3R(-)-butanediol [1:2:1] solution at a collision energy of 10eV.

A MS/MS experiment on VO : EG-d₄ : 2R,3R(-)-2,3-butanediol confirms the presence of EG in the ions at m/z 128, 146, 156, 182, 200 and 218 in the experiment with the unlabelled ion. This observation supports the proposal on ions formed at these masses. The ion at m/z 156 was proposed to be the [1M] complex of butanediol but the labeling experiment shows the formation of an ion at m/z 156 and another at m/z 160 which indicates that the peak at m/z 156 in the “unlabelled” experiment, could represent two ions. As the ion at m/z 160 in Figure 3.7 contains an EG unit, the ion at mass 156 in the “unlabelled” experiment could also be the result of a C₂H₄O loss from the ion at m/z 200. Should this be the case, then the C₂H₄O molecule lost comes from the butanediol moiety of the complex. As for m/z 182, the labeling experiment shows that the water molecule lost does not involve the methylene hydrogens of the EG moiety.

In conclusion, the acyclic vicinal diols studied appear to compete efficiently with ethylene glycol for complex formation with VO⁺⁺. Further, 2R,3R(-)-2,3-butanediol competes more effectively against ethylene glycol than its meso isomer. MS/MS experiments on the mixed complexes at m/z 218 at collision energies of both 10 eV and 15 eV, reveal that the *meso*-isomer yields ions at m/z 146 and m/z 182 with a

considerably higher intensity.. This characteristic could possibly be used to differentiate the *meso*-diol from its *2R,3R*-isomer.

4. Vanadyl complexes with cyclic vicinal diols: the *cis*- and *trans*- isomers of cyclopentanediol and cyclohexanediol

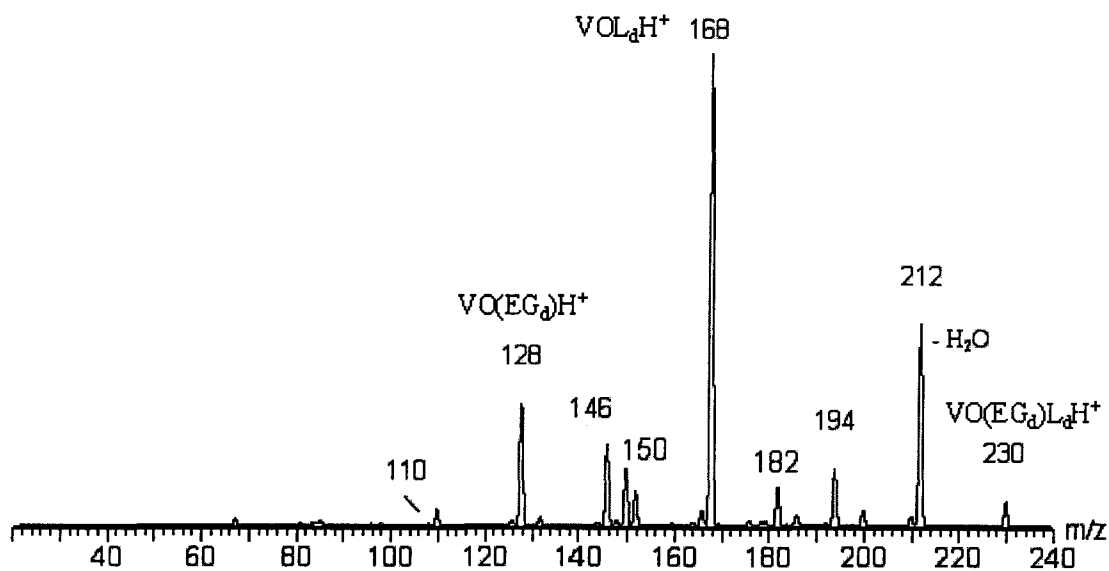
Both cyclic diols readily form a [2M] complex with VO^{++} suggesting an efficient competition against ethylene glycol for complexation to VO^{++} . As observed in the acyclic vicinal diols, the isomers of the cyclic diols also show a different intensity ratio for the [2M] complex of the diol relative to the [2M] complex of EG.

In 1,2-cyclopentanediol, the intensity ratio for the peaks corresponding to the [2M] complex with the *cis*- isomer, relative to that formed with EG, is 7 times greater than that observed with the *trans*- isomer. Ackloo et. al. reported a ratio of 9 times greater in the *cis* isomer than the *trans* isomer [1]. The intensity ratio at equilibrium between the [2M] EG complex, the mixed complex, and the [2M] pentanediol complex is 1 : 4 : 18 for the *cis* isomer and 1 : 4 : 2.5 for the *trans* isomer.

The MS/MS spectra of the mixed complexes with the *cis*- and *trans* isomers at m/z 230 are shown in Figure 3.8. The experiments were performed at a collision energy of 15 eV as the precursor ions did not show much dissociation at 10 eV. The general observation of these spectra is the formation of minor peaks at 2 Da lower than some of the main peaks. These peaks could be the result of the consecutive losses of H_2 .

There are no major differences between the spectra of the 1,2-cyclopentanediol isomers, except that the peaks formed by loss of H_2 are of a higher intensity in the *trans*-isomer. This observation is also documented in the study of Ackloo [1]. The H_2 loss in the *trans* isomer was rationalized as the way to accommodate a more favourable bonding orientation for the hydroxyl groups on the 1,2-cyclopentanediol with VO^{++} . It was also proposed that H_2 loss does not contribute to the peaks observed in the spectrum of the *cis* isomer [1]. Further experiment should be carried out to confirm this proposal.

a)



b)

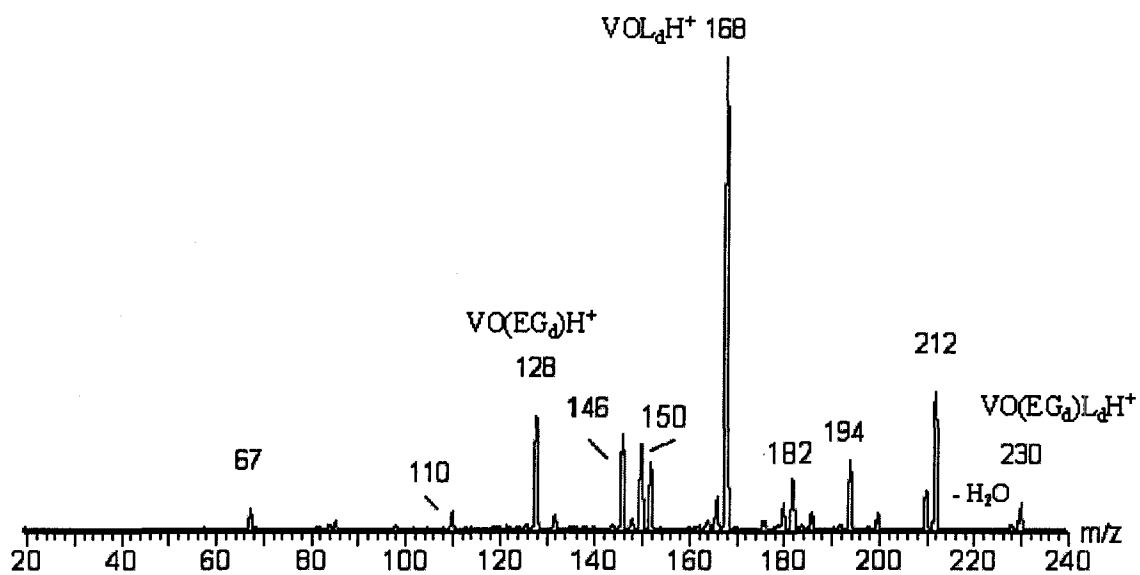


Figure 3.8. a) MS/MS spectrum of the mixed complex of a cis-1,2-cyclopentanediol [1:2:1] solution. b) MS/MS spectrum of the mixed complex of a trans-1,2-cyclopentanediol [1:2:1] solution MS/MS spectra acquired with Ar at a collision energy of 15 eV.

The ions at m/z 168 and m/z 128 are proposed to originate from the respective losses of EG and 1,2-cyclopentanediol from the mixed complex at m/z 230. The high intensity of the ion at m/z 168 indicates, as in the 2,3-butanediols, that the loss of EG is preferred to the loss of the 1,2-cyclopentanediol moiety of the mixed complex. The ion at m/z 212 is proposed to be generated by loss of water, while the ion at m/z 146 represents loss of C_5H_8O from the mixed complex. The peaks at m/z 200 and m/z 182 correspond to the loss of CH_2O from the ions at m/z 230 and m/z 212, respectively. The respective losses of water from the ions at m/z 212, m/z 168, and m/z 128 lead to the formation of the ions at m/z 194, m/z 150 and m/z 110.

The experiment conducted with ethylene glycol- d_4 produced the MS/MS spectrum of Figure 3.9. The spectrum of the trans-isomer shows that the H_2 losses are from the cyclopentanediol moiety of the complex as there are no D_2 losses observed. The spectrum also confirms the presence of EG in the ions at m/z 128, 146, 194, 212 and 230. It supports the proposal that the ion at m/z 146 results from a cyclopentene epoxide (C_5H_8O) elimination from the mixed complex.

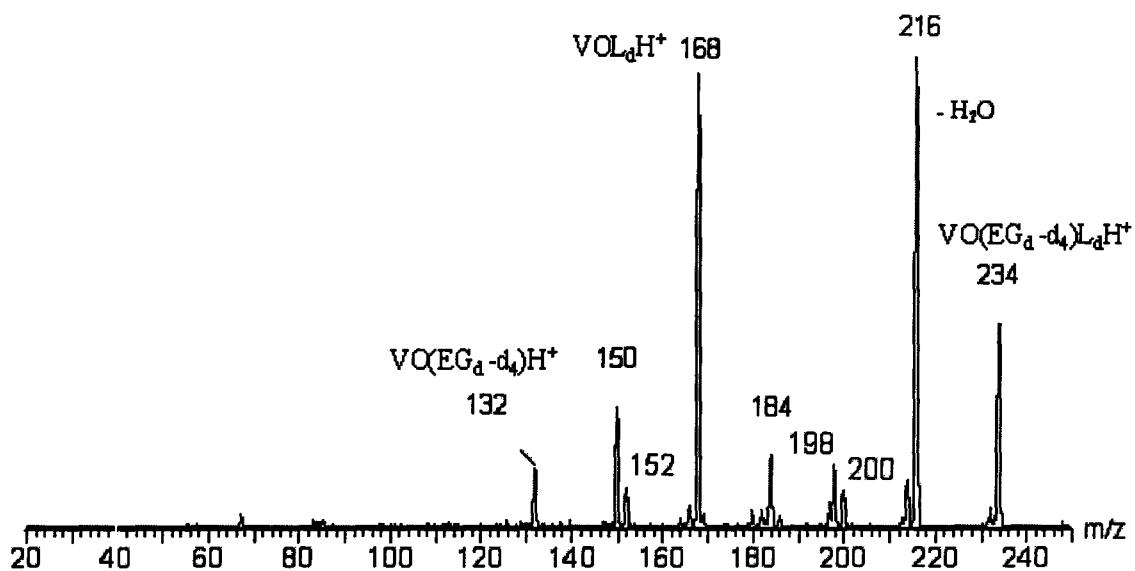


Figure 3.9. MS/MS spectrum of the mixed complex $VO(EG_d-d_4)L_dH^+$ with $L = \text{trans-1,2-cyclopentanediol}$. MS/MS spectrum acquired with Ar at a collision energy of 15eV.

The ion at m/z 184 in the labeling experiment, a 2 Da increase, indicates that the formaldehyde lost to form the m/z 182 ion in Figure 3.8, comes from the EG moiety of the ion at m/z 212. The ion at m/z 200, on the other hand, does not shift in the labeling experiment. The observed losses of 30 Da in the regular experiment and 34 Da in the labeling experiment to form this ion, suggests that it is generated by the consecutive losses of H_2 and C_2H_4 , and not the loss of formaldehyde. It also indicates that the C_2H_4 lost comes from the EG moiety of the mixed complex.

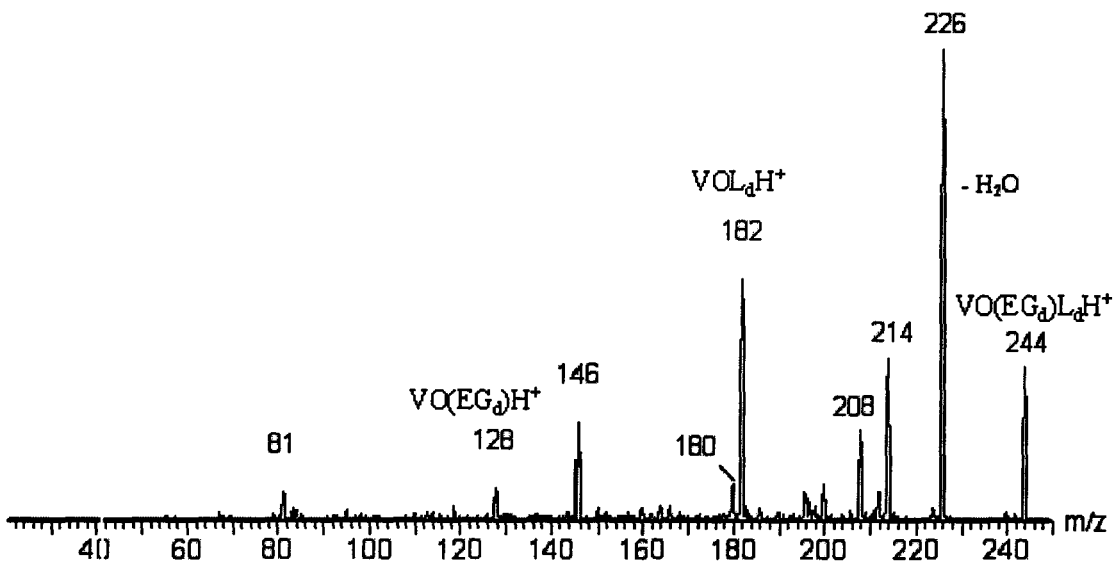
As observed with the cyclopentanediols, *cis*-1,2-cyclohexanediol competes more effectively against ethylene glycol than its *trans* isomer for complex formation with VO^{++} . Unlike 1,2-cyclopentanediol, however, the intensity ratio of the [2M] complex of the analyte to that of the EG in the *cis*-isomer is not significantly higher than that of the *trans*-isomer. The intensity ratio for peaks corresponding to the [2M] complex formed with the *cis*-isomer, relative to that formed with EG, is only about 2 times greater than the ratio observed with the *trans*-isomer.

The MS/MS spectra of the mixed complexes of the isomers are different, as seen in Figure 3.10. The MS/MS experiments were performed on the mixed complexes at m/z 244 at a collision energy of 15 eV. The main difference between the spectra is that the *cis*-isomer forms an ion at m/z 214 which is absent in the spectrum of the *trans*-isomer. This observation was also documented by Ackloo [1]. The ion at m/z 214 is proposed to be generated by loss of CH_2O from the mixed complex. Secondly, apart from the ions at m/z 182 and m/z 200, which correspond to the respective losses of EG and C_2H_4O from the mixed complex, all other ions are formed with a much higher intensity in the *trans*-isomer. The enhanced intensity of the m/z 182 ion in the *cis*-isomer indicates the preference of the mixed complex with the *cis*-isomer to lose EG rather than the 1,2-cyclohexanediol moiety for stability. Thus, the C_2H_4O lost to form the ion at m/z 200 could also be from the EG moiety of the complex.

The ions at m/z 226 and m/z 208 correspond to water losses from the mixed complex and m/z 226 respectively. The ion at m/z 128 is generated by the loss of 1,2-cyclohexanediol, while the ion at m/z 146 could represent the loss of cyclohexene epoxide ($C_6H_{10}O$) from the mixed complex. All these ions are of higher intensity in the *trans*-isomer indicating the preference of the *trans*-isomer to lose the 1,2-cyclohexanediol moiety. Loss of water from the ion at m/z 208 could account for the ion at m/z 190.

The m/z 164 ion could be generated by loss of 44 Da from the m/z 208 ion, or else by loss of 62 Da from m/z 226. These losses could be in the form of C_2H_4O and EG, respectively. The peak at m/z 81, which represents the 1,2-cyclohexene ion, also displays a much higher intensity in the spectrum of the trans-isomer.

a)



b)

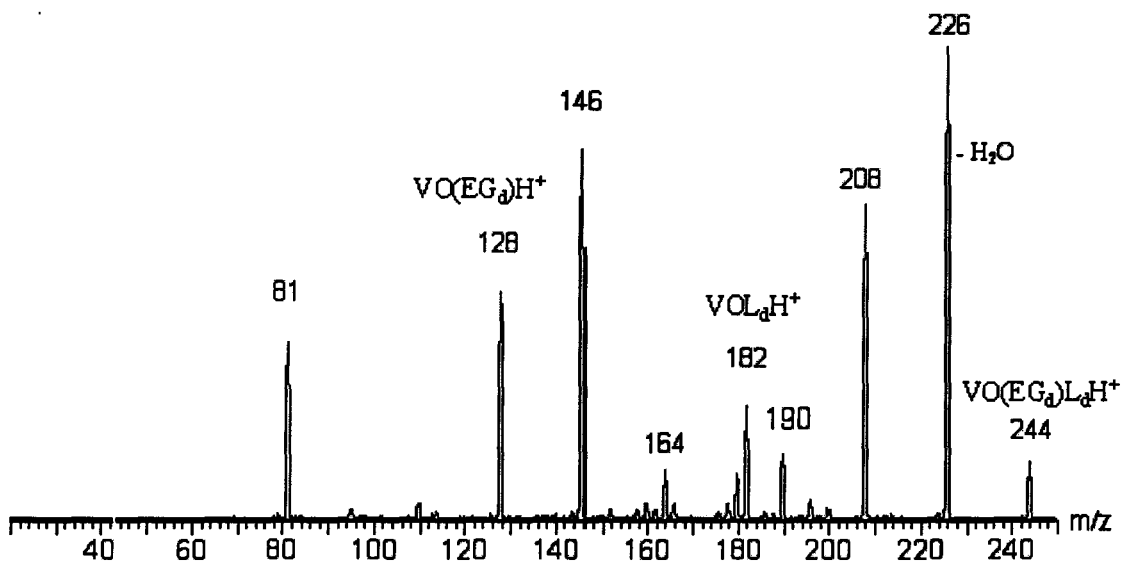


Figure 3.10. a) MS/MS spectrum of the mixed complex of a cis-1,2-cyclohexanediol [1:2:1] solution. b) MS/MS spectrum of the mixed complex of a trans-1,2-cyclohexanediol [1:2:1] solution. MS/MS spectra acquired with Ar at a collision energy of 15 eV.

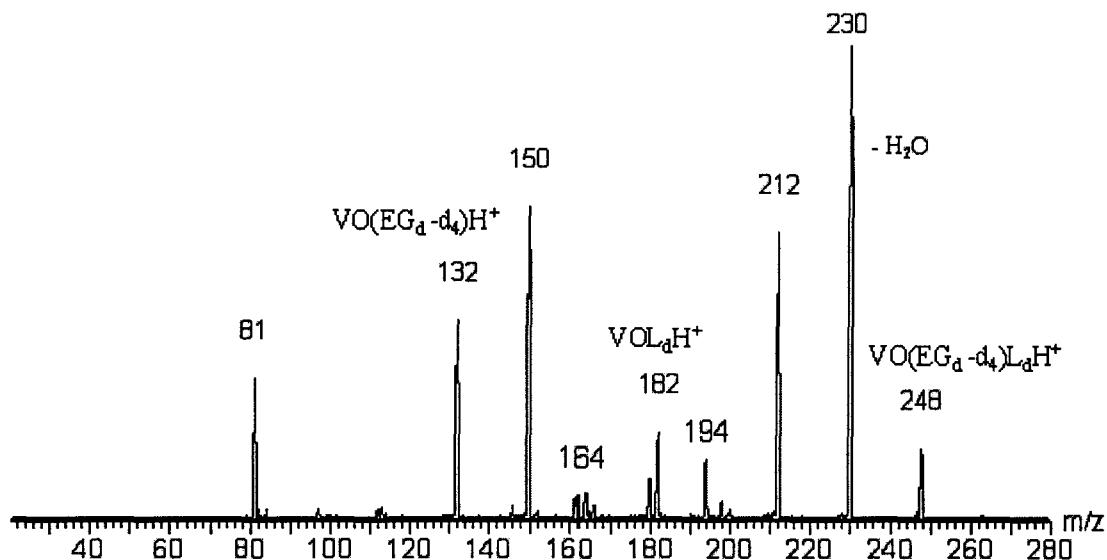


Figure 3.11 MS/MS spectrum of the mixed complex of VO(EG_d-d₄)L_dH⁺ with L = trans-1,2-cyclohexanediol. MS/MS spectrum acquired with Ar at a collision energy of 15eV.

The EG-d₄ labeling experiment performed on the mixed complex with trans-1,2-cyclohexanediol produced the spectrum of Figure 3.11. The ions at m/z 81, m/z 164, and m/z 182, do not shift, which supports the proposal that they contain only the 1,2-cyclohexanediol moiety. However, further labeling experiments would be required to determine whether the neutral lost to form the ion at m/z 164 is in the form of ethylene oxide or ethylene glycol.

The spectrum also confirms the presence of the EG unit in the ions at m/z 128, 146, 190, 208, 226 and 244 in the spectrum of the unlabelled precursor ion. This observation supports the proposed composition of the complexes formed at these masses. It also indicates that if water was lost from m/z 208 to form m/z 190, then it must have involved the hydrogen of the 1,2-cyclohexanediol moiety.

The complexes formed with the cyclohexanediols produced more characteristic MS/MS spectra than the cyclopentanediols. The trans-isomer of the 1,2-cyclohexanediol in general, dissociates more readily than the cis-form as witnessed by the higher intensity of the product ions in its MS/MS spectrum. The formation of higher intensity ions at m/z 146 and m/z 128 in the trans-isomer reflects the stability achieved by losing the cyclohexanediol moiety. The cis-isomer, on the other hand, loses EG more readily to

form the ion at m/z 182, highlighting the stability of the oxovanadium complexation with a cis-1,2-cyclohexanediol ligand as opposed to the trans form. The obvious difference between the cis- and the trans-isomer is the formation of the m/z 214 ion in the cis-isomer.

The only difference observed between the cyclopentane diols are the H_2 losses in the trans-isomer. However, without further experiments, it is difficult to propose that the losses observed in the cis-isomer of the cyclopentane diols are not related to H_2 .

5. Disaccharides

S.Z.Ackloo's study on sugars [1] showed that melibiose, a galactose/glucose disaccharide, contains a pair of hydroxyl groups in the cis-orientation on the galactose residue. Another pair of hydroxyl groups on the glucose residue, though not in the cis orientation, is capable of mutarotation, which results in an effective complexation with VO^{++} . Gentiobiose, like trehalose, is a glucose disaccharide. However, gentiobiose undergoes effective complexation to VO^{++} because it has a pair of hydroxyl groups that is capable of mutarotation.

An experiment was performed on a disaccharide, trehalose, for a comparison with the results obtained with the diols. Trehalose is a glucose disaccharide with an α -1,1-O-glycosidic linkage and glucose sugars have all their hydroxyl groups in the trans orientation. Trehalose, as opposed to gentiobiose, does not have hydroxyl groups that can undergo mutarotation. Therefore, it is expected to compete less efficiently with ethylene glycol for complexation to oxovanadium.

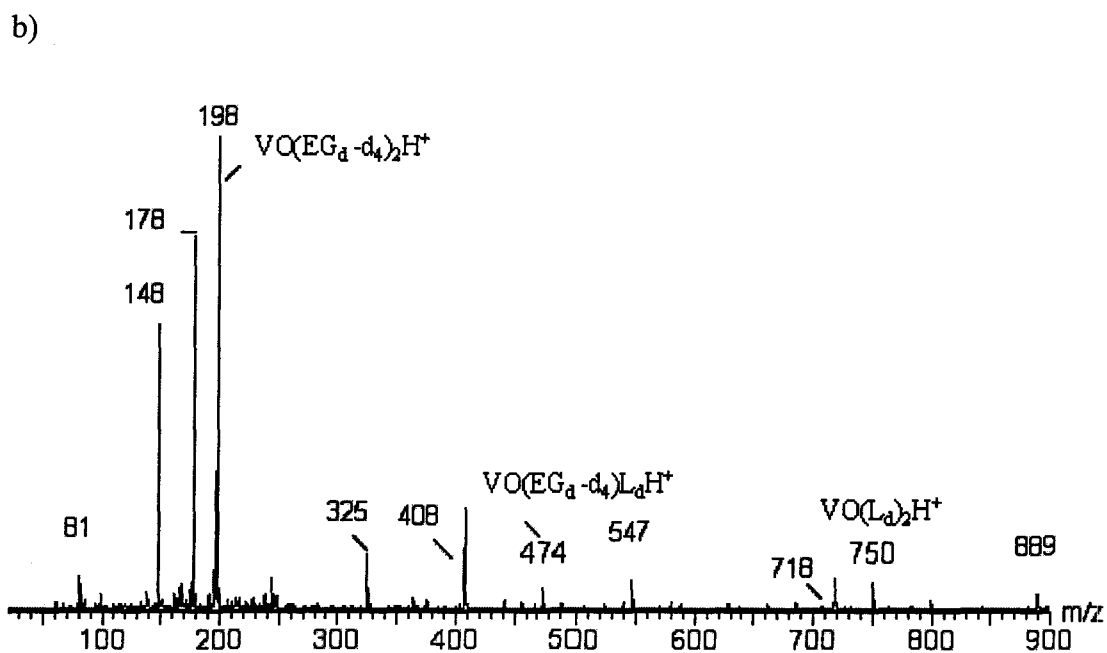
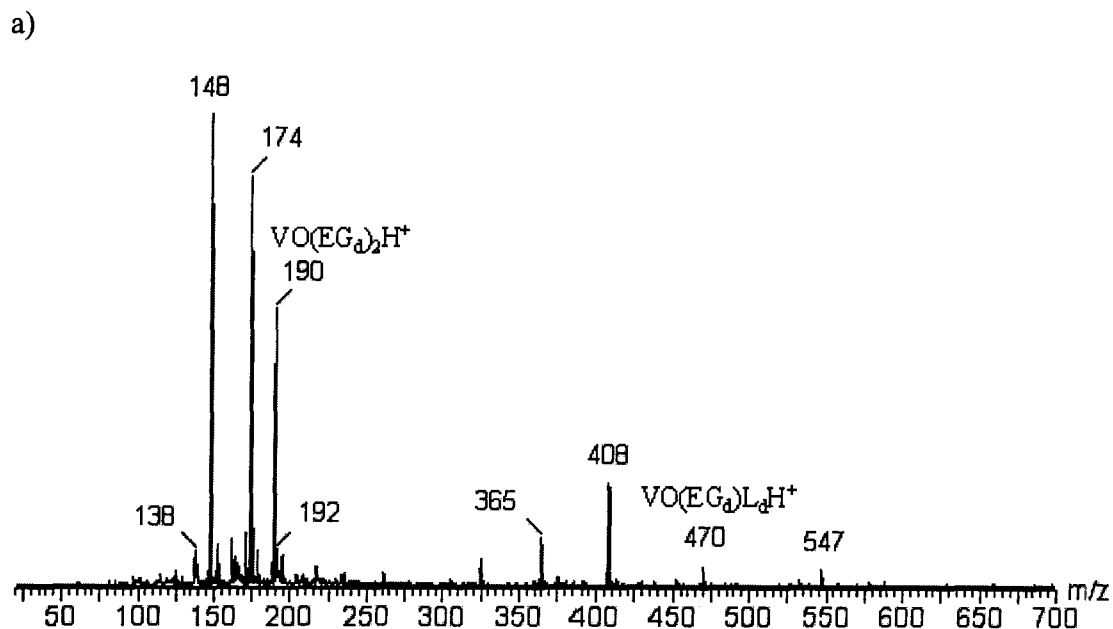


Figure 3.12 . a) ES spectrum of a VO : EG : trehalose [1:2:1] solution. b) ES spectrum of a VO : EG- d_4 : trehalose [1:2:1] solution

Figure 3.12a shows the ES spectrum produced for the VO : EG : trehalose solution in 1 : 2 : 1 molar ratio. The intensity of the [2M] EG complex at m/z 190 is relatively high compared to that of the mixed complex at m/z 470. The formation of the [2M] trehalose complex at m/z 750 is too minimal that the signal of this ion is seldom seen in the spectra of this solution. It was also observed that the intensity for the

oxovanadium-trehalose complex at m/z 408 is present in the ES spectrum and is always higher than that of the mixed complex. This indicates the higher tendency for sugars to form a [1M] complex with oxovanadium than to form the mixed complex in solution. This observation is further confirmed by the ES spectrum of the labeling experiment with ethylene glycol- d_4 in Figure 3.12b. The shift of 8 Da and 4 Da is observed only in the ions at m/z 190 and m/z 470 respectively. The results indicate that trehalose competes less efficiently with ethylene glycol for complexation to VO^{++} .

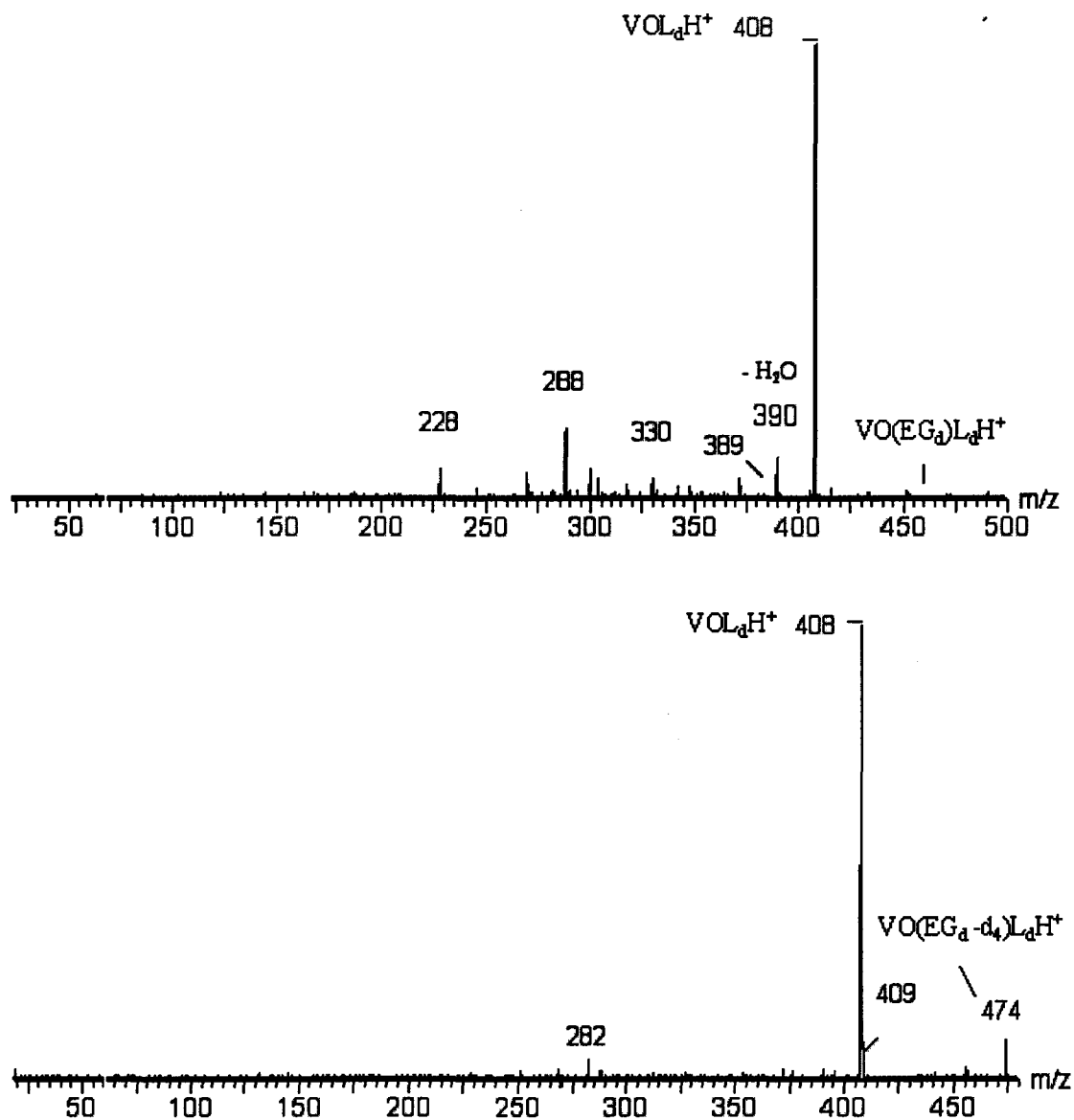


Figure 3.13. MS/MS spectrum of the mixed complex of VO : EG : trehalose (top) ; MS/MS spectrum of the mixed complex of VO : EG- d_4 : trehalose (bottom). MS/MS spectra acquired with Ar at a collision energy of 15 eV.

The MS/MS spectrum in Figure 3.13a shows that the mixed complex readily loses EG to form a stable ion at m/z 408. The analyte complex at m/z 408 dissociates further by the loss of H_2O and $C_4H_8O_4$ to form the respective ions at m/z 390 and m/z 288. It has been reported [22] that the losses of 60 Da ($C_2H_4O_2$), 90 Da ($C_4H_{10}O_2$) and 120 Da ($C_4H_8O_4$) are characteristic of the O-glycosidic linkage type. The ^{18}O -labelling studies of Leary et al. suggest that the $C_4H_8O_4$ loss involves the O-atom at C_1 and that its fragmentation pathway involves both C_1 and C_2 . The complexation behaviour of trehalose with oxovanadium is also in line with the observations on the diol isomers discussed above in that a trans orientation of the hydroxyl groups is less favourable for complexation.

Complexation competition between amines and diols

1. Ethanolamine ($H_2NCH_2CH_2OH$)

An acidified aqueous solution with a 1 : 2 : 1 molar ratio of VO, EG and ethanolamine produced the spectrum of Figure 3.14 (top). In theory, an effective competition of ethanolamine against ethylene glycol for complexation to oxovanadium, will result in the formation of ethanolamine [2M] and mixed complex ions, at m/z 188 and 189 respectively. These signals are not observed. It is seen that the spectrum is dominated by peaks at m/z 190, 174 and 148, which belong to the [2M] complex of EG and the associated oxovanadium-solvent molecule complexes. This is confirmed by the MS/MS spectra of these ions and the results of a labeling experiment using ethylene glycol- d_4 , see the bottom spectrum of Figure 3.14. Ethanolamine clearly does not complex to VO^{++} in the presence of ethylene glycol in acidic solution, but instead forms a protonated ion producing a weak signal at m/z 62.

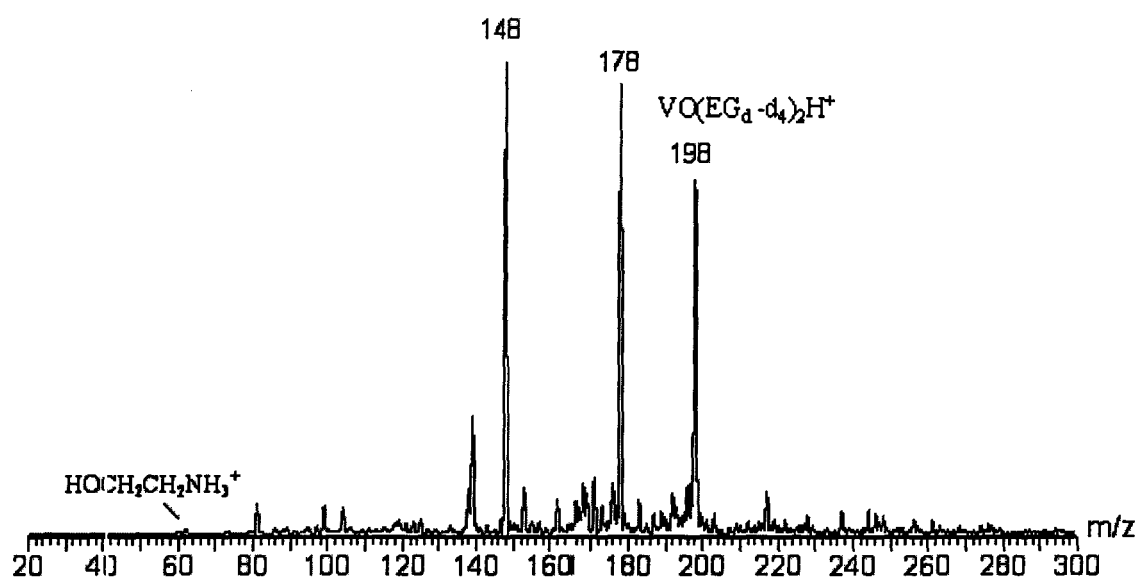
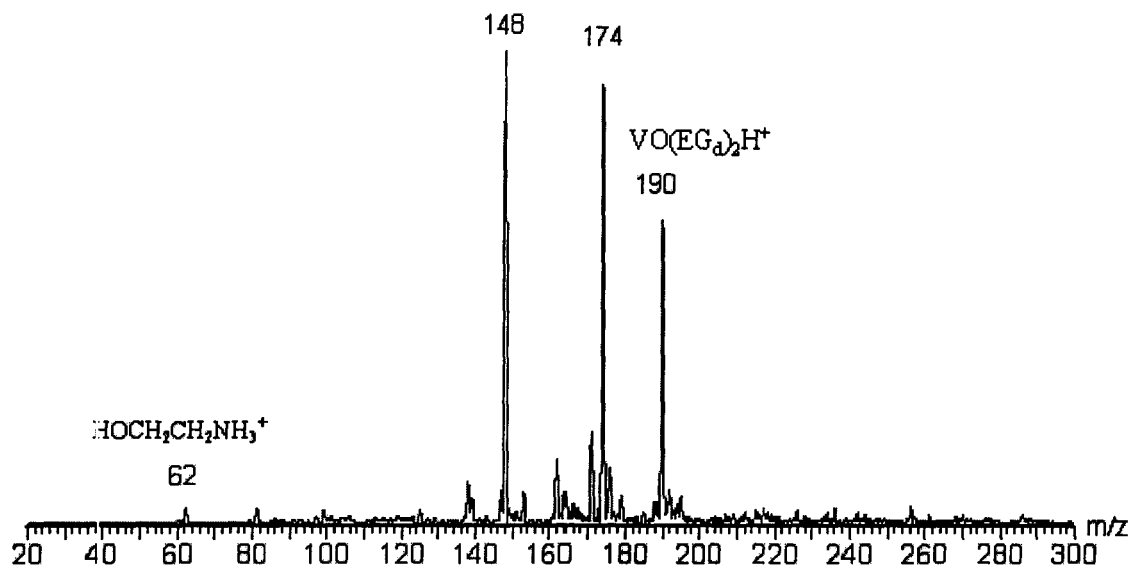


Figure 3.14 ES spectra of VO : EG : ethanolamine [1:2:1] (top) and VO : EG-d₄ : ethanolamine [1:2:1] (bottom).

2. Ethylenediamine ($\text{H}_2\text{NCH}_2\text{CH}_2\text{NH}_2$)

The strong signals in the ES spectrum of the VO : EG : ethylenediamine solution of a 1:2:1 molar ratio, correspond to the oxovanadium(IV)-ethylene glycol complex ions at m/z 190 and m/z 174, see Figure 3.15a. The m/z 148 ion represents the oxovanadium-formic acid-water complex discussed in the previous section. This interpretation is

supported by the results of an EG-d₄ labeling experiment, whose MS/MS spectrum confirms the presence of EG in the former two ions.

Ions for the mixed complex and the [2M] ethylenediamine complex, at m/z 188 and m/z 186 respectively, are not observed. A weak signal for the protonated diamine is produced at m/z 61, as seen in Figure 3.15b. Ethylenediamine obviously does not form a stable complex with VO⁺⁺ in the presence of ethylene glycol.

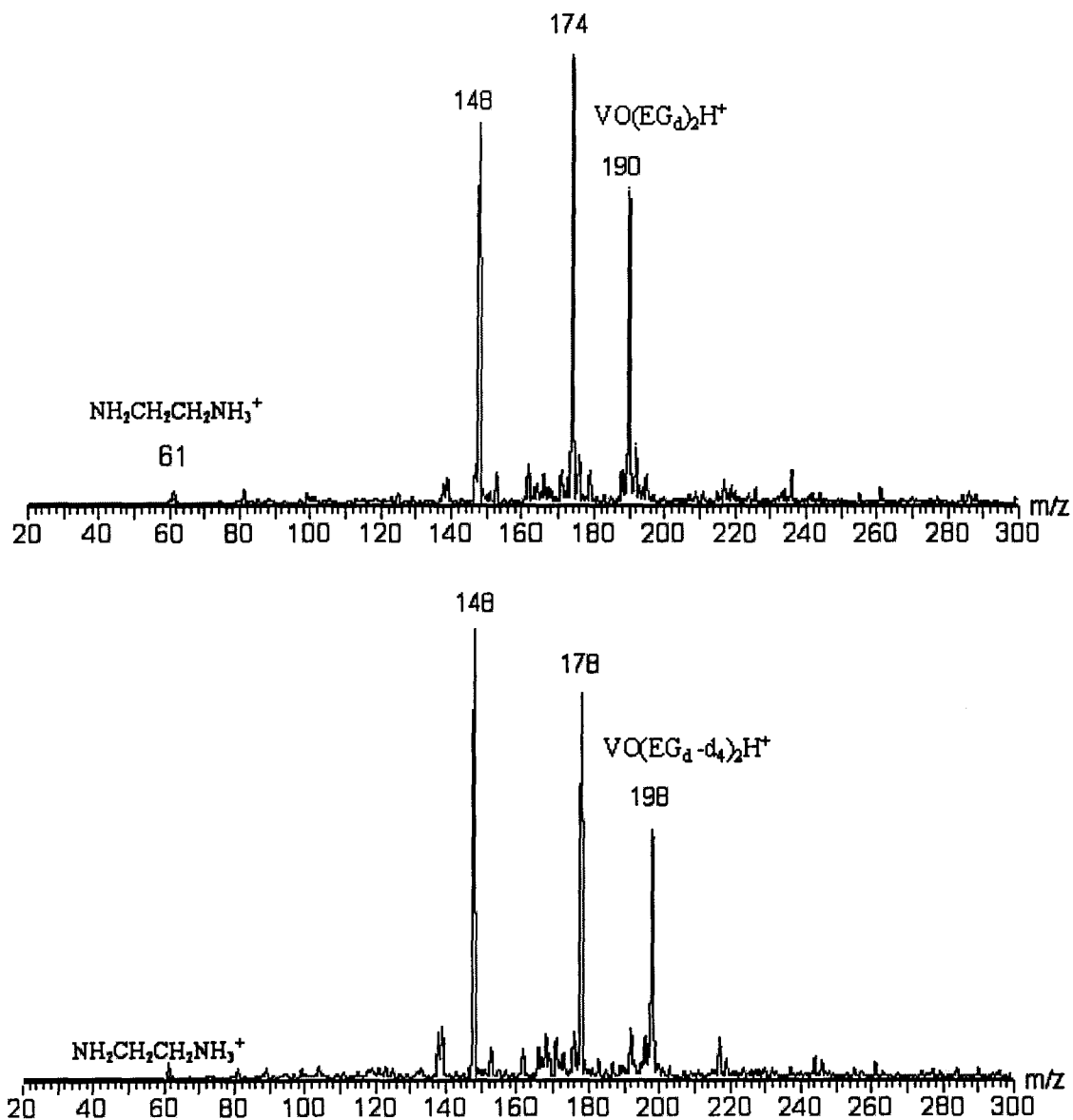


Figure 3.15 ES spectra of VO:EG:ethylenediamine [1:2:1](top) and VO:EG-d₄: ethylenediamine [1:2:1] (bottom).

3. *N,N'*-Dimethylethylenediamine ($\text{CH}_3\text{NHCH}_2\text{CH}_2\text{NHCH}_3$)

The complexation tendency of a secondary amine to VO^{++} was also investigated using a 2.5×10^{-3} M solution of dimethylethylenediamine.. This amine does not form a complex with oxovanadium (IV)-ethylene glycol either. It is seen that the amine has a high tendency to form protonated ions rather than that it forms complexes with VO^{++} in the acidic solution.

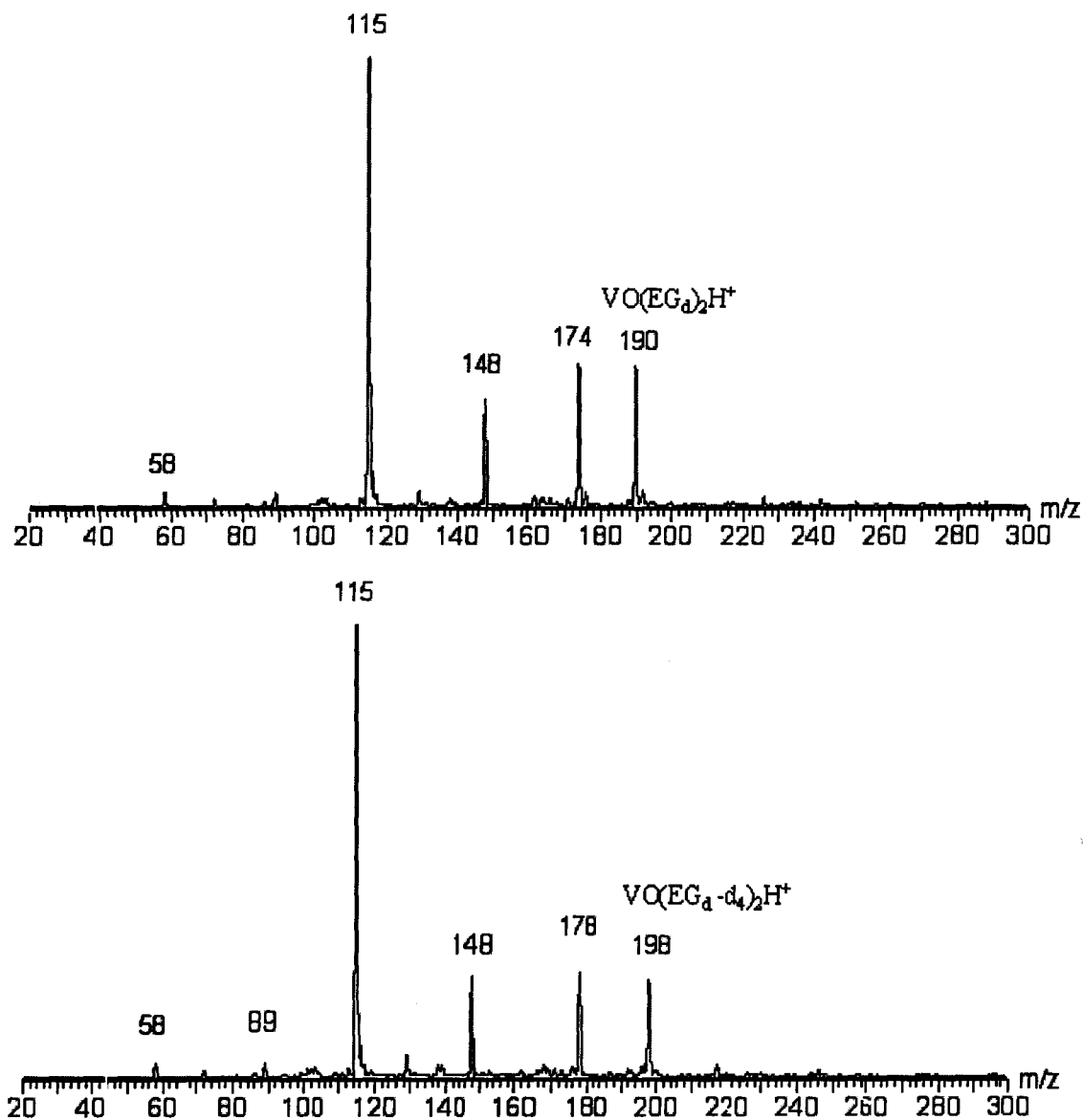


Figure 3.16 ES spectra of VO:EG:dimethylethylenediamine [1:2:1] (top) and of VO:EG-d₄:dimethylethylenediamine [1:2:1] (bottom).

A comparison of the ES spectra presented in Figures 3.16a and b shows that the ions at m/z 115, 89 and 58 do not contain EG. The spectra also show that dimethylethylenediamine, as opposed to the other amines investigated, forms a strong ion at m/z 115 whose structure and origin is not known. Other ions present are the protonated diamine, $\text{CH}_3\text{HNCH}_2\text{CH}_2\text{NH}_2\text{CH}_3^+$, and $\text{CH}_2\text{CH}_2\text{NH}_2\text{CH}_3^+$, at m/z 89 and m/z 58 respectively.

Being a weak base, the tendency of an amine to become protonated increases in an acidic solution. As discussed in the Introduction, the first step in the vanadyl ion complexation is the deprotonation of the ligand. This is quite difficult to achieve with an amine in an acidic solution. Hence, the absence of complexation by amines in this study could be due to both incompetitiveness with the oxygen-donating ligand, and the requirement of a relatively high pH. In this context it is worth noting that the numerous complexation studies of amines to metal ions have all been performed in a basic environment.

The equilibrium constant of oxovanadium(IV)-ethylene glycol complexes with diols

As mentioned above, the complexation of a diol to oxovanadium (IV)-ethylene glycol in aqueous solution yields two species, namely the mixed complex, and the [2M] complex of the diol. An experiment to determine the equilibrium constant (formation constant) of the diol's complexation reaction to VO^{++} was carried out in acidic solution at room temperature. The pH was kept below 4 to minimize the oxidation of the vanadyl ion. The intensity of the signals for the [2M] complex of EG ($\text{VO}(\text{EG}_d)_2\text{H}^+$), the mixed complex, ($\text{VOEG}_d\text{L}_d\text{H}^+$), and the [2M] complex of the diol, ($\text{VO}(\text{Ld})_2\text{H}^+$), was measured four minutes after mixing and then every two minutes for about an hour. It was found that equilibrium is reached almost immediately. The equilibrium constant for the formation of the mixed complex K_1 :



$$K_1 = \frac{[\text{VO}(\text{EG}_d)\text{L}_d\text{H}^+][\text{EG}]}{[\text{VO}(\text{EG}_d)_2\text{H}^+][\text{L}]}$$

And K_2 for the formation of the [2M] complex of the diol :



$$K_2 = \frac{[\text{VO}(\text{L}_d)_2\text{H}^+][\text{EG}]}{[\text{VO}(\text{EG}_d)\text{L}_d\text{H}^+][\text{L}]}$$

The overall equilibrium constant K_{eq} for the complexation was then determined from the K_1 and K_2 values measured from the curve of intensity ratio of the complexes as a function of time:

$$K_{\text{eq}} = K_1 \times K_2 \quad 3$$

1. 1,2- Propanediol

The intensity ratio of the complexes was calculated four minutes after 1,2-propanediol was added to the reagent mixture. The intensities were recorded every 2 minutes for 40 to 50 minutes.

Equilibrium constant for oxovanadium-ethylene glycol complex reaction with 1,2-propanediol

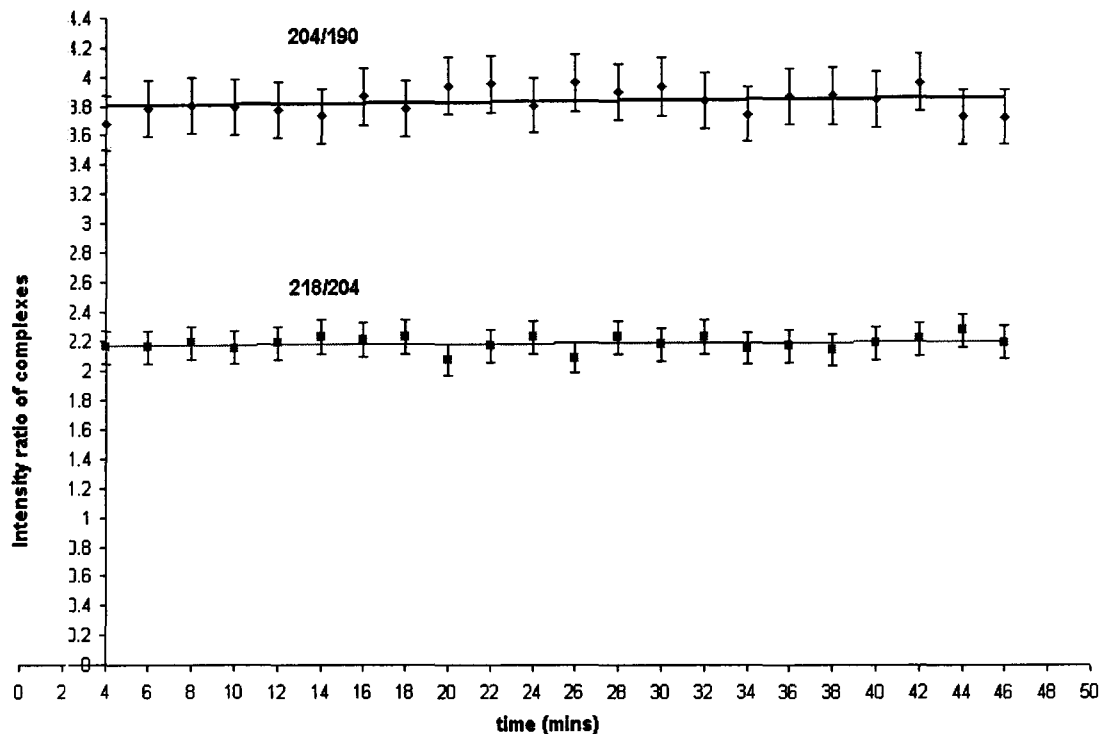


Figure 3.17. The formation constant K_1 for the mixed complex at m/z 204 and K_2 for the [2M] complex of 1,2-propanediol at m/z 218 as a function of time.

From the plot of K_1 and K_2 versus time in Figure 3.17, it can be concluded that the equilibrium for the complexation reaction is reached almost immediately. The K_1 value for the formation of the mixed complex $\text{VOEG}_d\text{L}_d\text{H}^+$ for 1,2-propanediol is 3.84 ± 0.39 , while the K_2 value is 2.19 ± 0.06 . The range of error in the K_1 measurement is between 5 to 14 %, while it is only 0.5 to 7 % in K_2 .

The equilibrium constant (K_{eq}) value of 8.40 ± 0.21 is high, indicating the preference of the overall reaction for the complexation with 1,2-propanediol. This supports our previous discussion on 1,2-propanediol's efficient competition against ethylene glycol for complexation to the oxovanadium (IV) ion. The relative standard deviation of the K_{eq} in this experiment is 2.5%.

2. 2R,3R-(-)-2,3-Butanediol

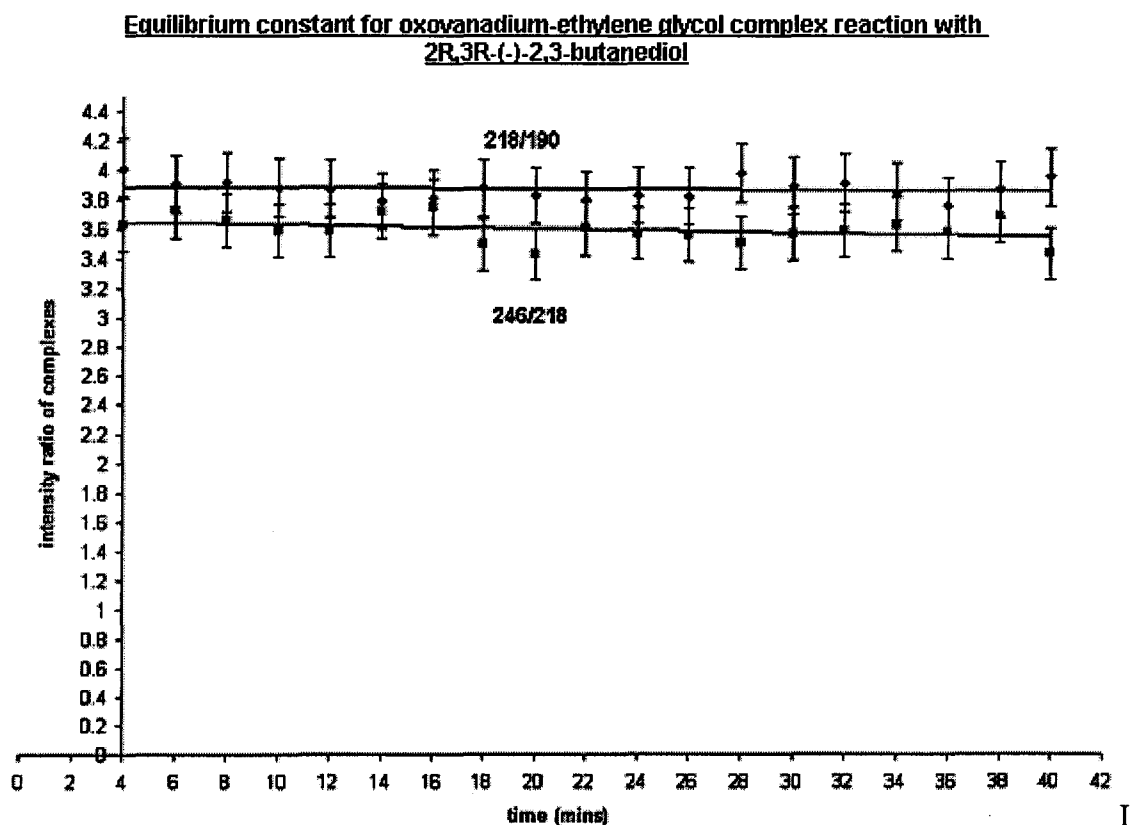


Figure 3.18. The formation constant K_1 for the mixed complex at m/z 218 and K_2 for the [2M] complex of 2R,3R-(-)-2,3-butanediol at m/z 246 as a function of the reaction time.

In this compound, the formation constant K_1 for the mixed complex from the reference complex, and K_2 for the formation of the [2M] complex of 2*R*,3*R*-(-)-2,3-butanediol from the mixed complex, are comparable. K_1 is 3.87 while the K_2 value is 3.60 with the error in the measurement of the values ranging only from 0.4 % to 7.3 %. Analogously to 1,2-propanediol, the 2,3-butanediol also has a large K_{eq} value, 13.95 ± 0.38 , which indicates that the position of the equilibrium lies more towards the formation of the [2M] complex of the 2,3-butanediol. This result also supports the observation that the 2,3-butanediol competes effectively against ethylene glycol for complexation to VO^{++} .

3. cis-1,2-Cyclopentane-1,2-diol

cis-1,2-Cyclopentane-1,2-diol's K_1 value of 4.48 ± 0.15 is slightly higher than its K_2 value of 3.94. The range of errors in the value of K_1 and K_2 measured using this method is relatively small, between 1 % to 7 %.

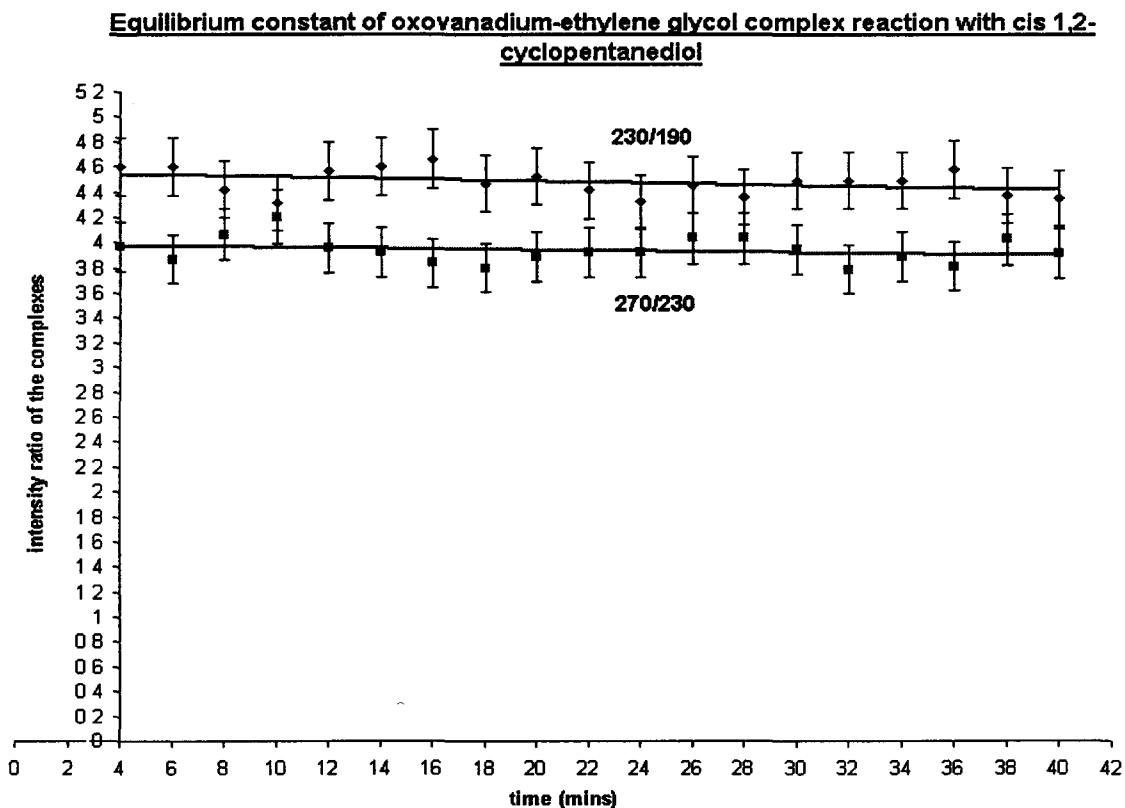


Figure 3.19. The formation constant K_1 for the mixed complex at m/z 230 and K_2 for the [2M] complex of cis-1,2-cyclopentane-1,2-diol at m/z 270 as a function of the reaction time.

The value of K_{eq} is 17.63 ± 0.4 for this compound. In line with the 1,2-propanediol and 2,3-butanediol experiments, the K_{eq} value of this cyclic diol also indicates that the formation of the oxovanadium (IV) complex $VOLd_2H^+$, is favored over that with ethylene glycol. The RSD of the K_{eq} determined is 2.4%.

4. cis-1,2-Cyclohexanediol and trans-1,2-cyclohexanediol

The experiment to determine the formation constant was performed on both the cis- and trans- isomers of 1,2-cyclohexanediol. The graph in Figure 3.20 shows that the measured K_1 and K_2 values in the 'cis' isomer are 5.10 and 3.90 respectively, while the values in the 'trans' isomer are lower, with a K_1 value of 4.76 and a K_2 value of 2.26 as derived from from the graph of Figure 3.21.

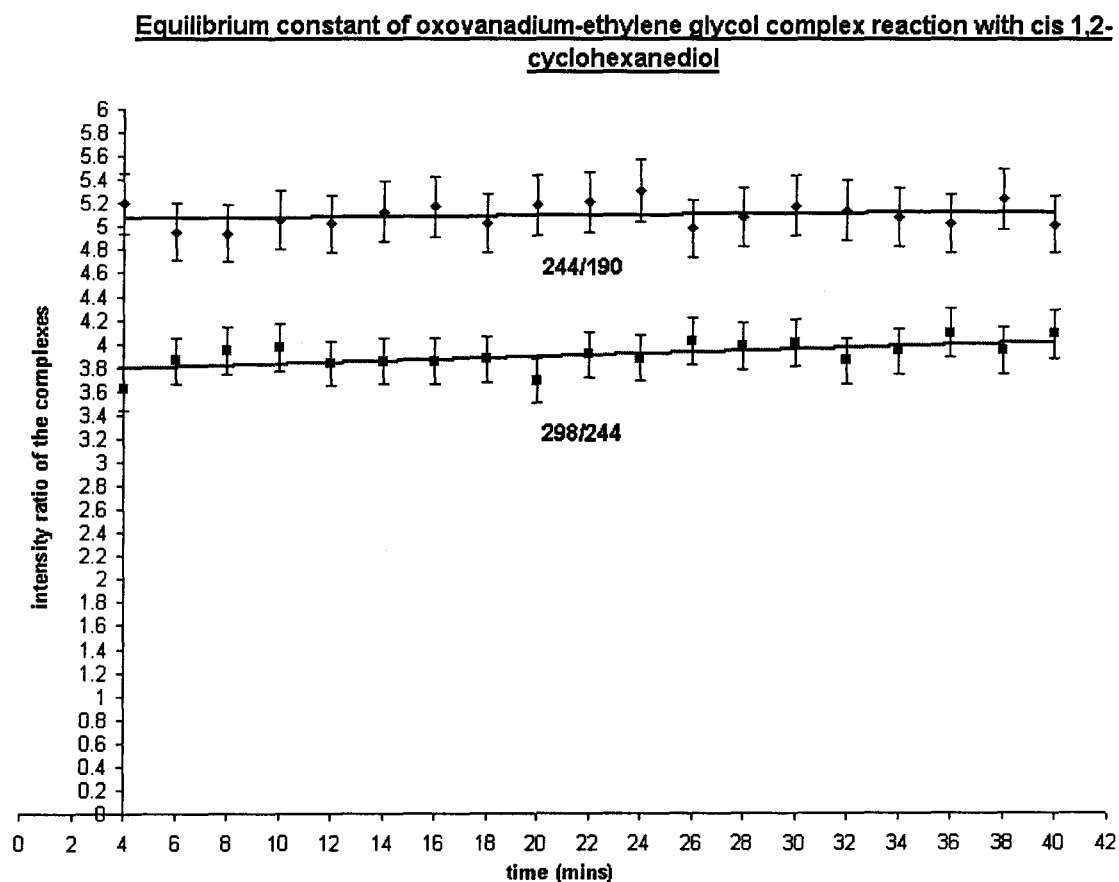


Figure 3.20. The formation constant K_1 for the mixed complex at m/z 244 and K_2 for the [2M] complex of cis-1,2-cyclohexanediol at m/z 298 as a function of time.

Equilibrium constant of oxovanadium-ethylene glycol complex reaction with trans-1,2-cyclohexanediol

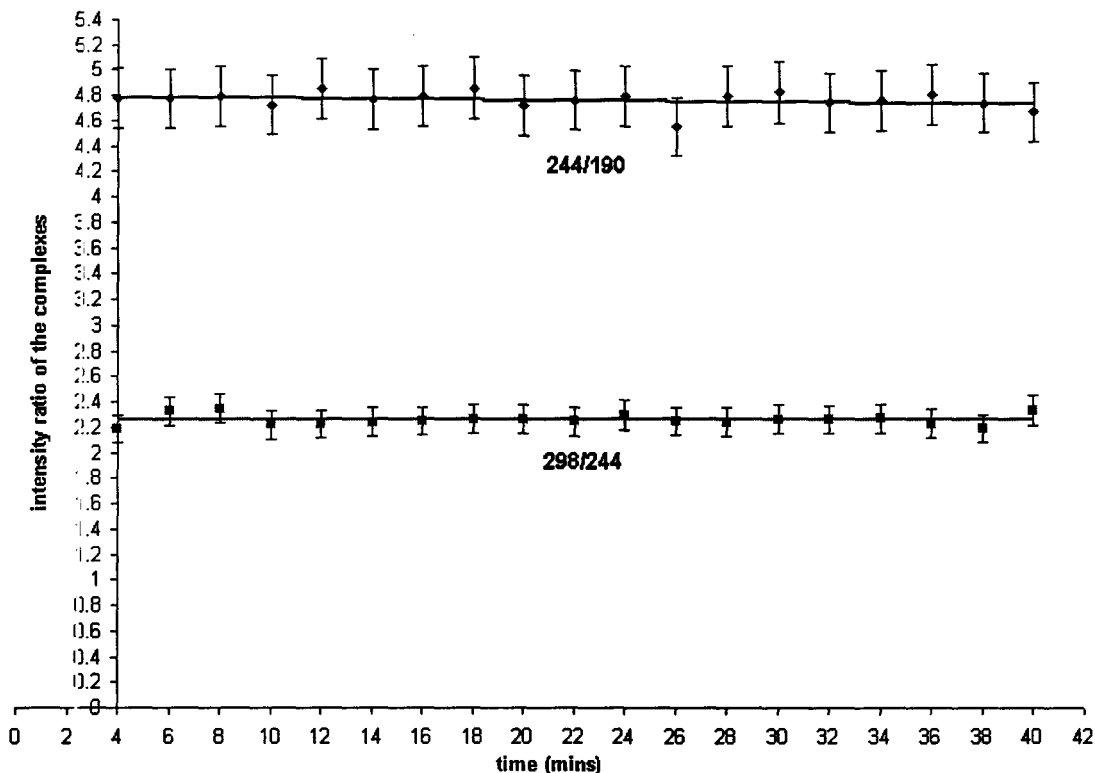


Figure 3.21. The formation constant K1 for the mixed complex at m/z 244 and K2 for the [2M] complex of trans-1,2-cyclohexanediol at m/z 298 as a function of time.

The high K_{eq} value of the 'cis' isomer at 19.94 ± 0.58 as compared to the K_{eq} of the 'trans' isomer at 10.74 ± 0.25 confirms the earlier observation that the 'cis' isomer competes more efficiently with ethylene glycol to form a complex with oxovanadium (IV). The RSD for the K_{eq} values determined for the two isomers were below 3 %.

Estimate of the limit of detection

A series of VO:EG reagent solutions was prepared to monitor the strength of the $\text{VO}(\text{EG}_d)_2\text{H}^+$ complex signal as a function of the concentration. The bottom spectrum of Figure 3.21 is that of the reagent at the standard concentration of 2.5×10^{-3} M, which is the concentration used throughout this study. This spectrum serves as a comparison to study the relative intensity of $\text{VO}(\text{EG}_d)_2\text{H}^+$ complex ion at lower concentrations.

It is seen from the top spectrum of Figure 3.22 that at a 2.5×10^{-5} M concentration, the $\text{VO}(\text{EG}_d)_2\text{H}^+$ complex signal at m/z 190 lies within the chemical background noise. Thus, this concentration is too low for a meaningful analysis.

The middle spectrum of Figure 3.22 refers to a 2.5×10^{-4} M reagent solution. The signal intensity of the ion at m/z 190 is still sufficiently strong at this concentration so that the reagent can be reliably applied to detect a diol present at a low concentration in an aqueous solution. However, an experiment at this concentration with 1,2-propanediol added at a 0.1 : 1 diol to reagent ratio, produced inconsistent intensity ratios for the complexes of interest. This follows from the measured intensity ratios, which are not in agreement with the calibration curves shown in Figure 3.26. This point is further illustrated by the difference in the ratios observed in the spectra of Figure 3.23. These spectra both refer to VO:EG:1,2-propanediol solutions of a diol to reagent molar ratio of 0.1 : 1. The top spectrum represents a 2.5×10^{-4} M VO:EG concentration, while the bottom spectrum was obtained with the standard reagent concentration of 2.5×10^{-3} M. It is seen that for the same mol ratio, the $\text{VOEG}_d\text{L}_d\text{H}^+$ to the $\text{VO}(\text{EG}_d)_2\text{H}^+$ intensity ratio measured for the ions at m/z 204 and m/z 190, is higher in the diluted solution than that observed with the standard solution.

The inconsistency in the intensity ratios could be due to interference from the background chemical noise ions having the same mass to charge ratio as those of the mixed complex and the 1,2-propanediol [2M] complex. Chemical backgrounds intensities are usually inconsistent, thus affect the accuracy of measurements at such a low concentration of diol.

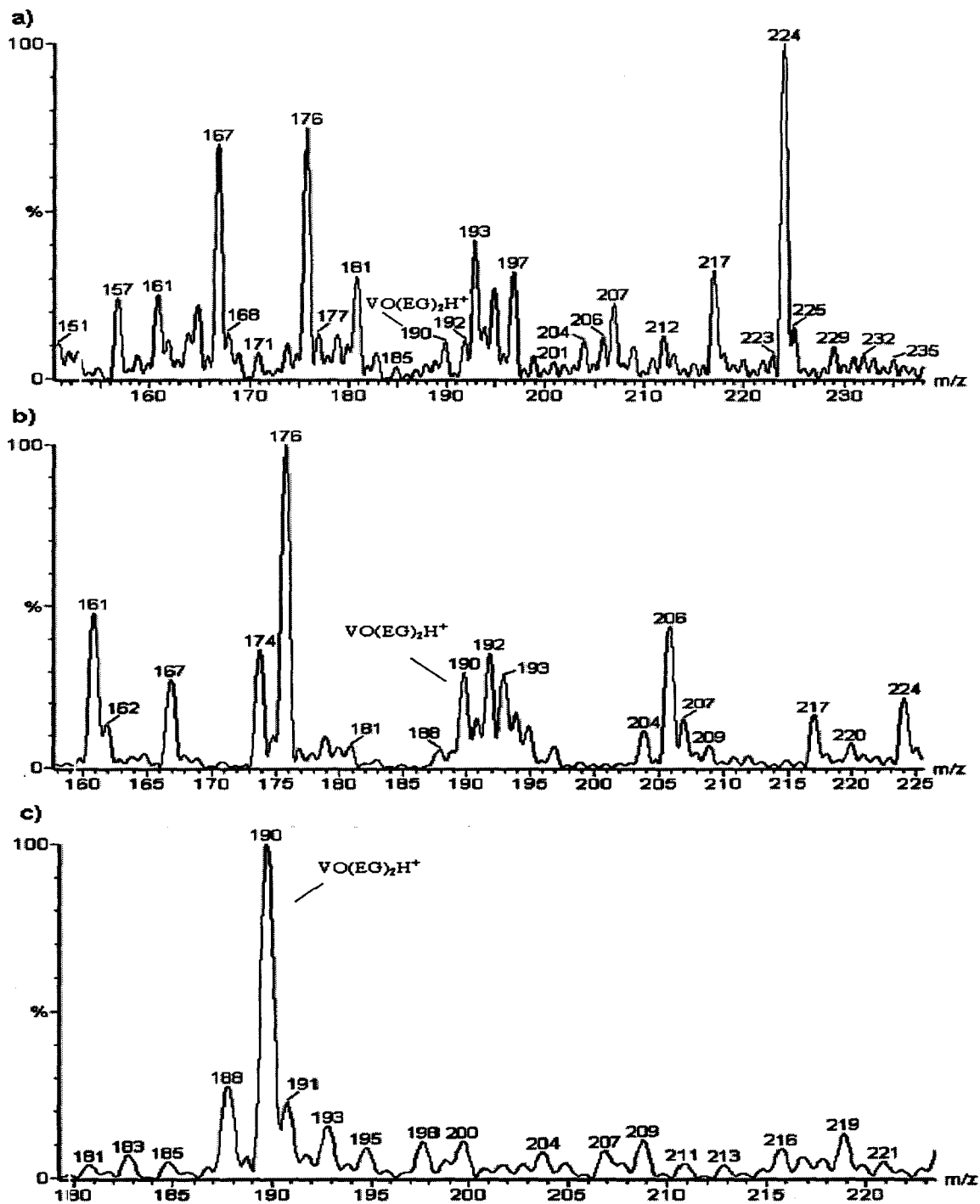


Figure 3.22. Partial ES spectra of the VO:EG reagent as a function of its concentration : top spectrum : $2.5 \times 10^{-5} \text{ M}$; middle : $2.5 \times 10^{-4} \text{ M}$; bottom : $2.5 \times 10^{-3} \text{ M}$.

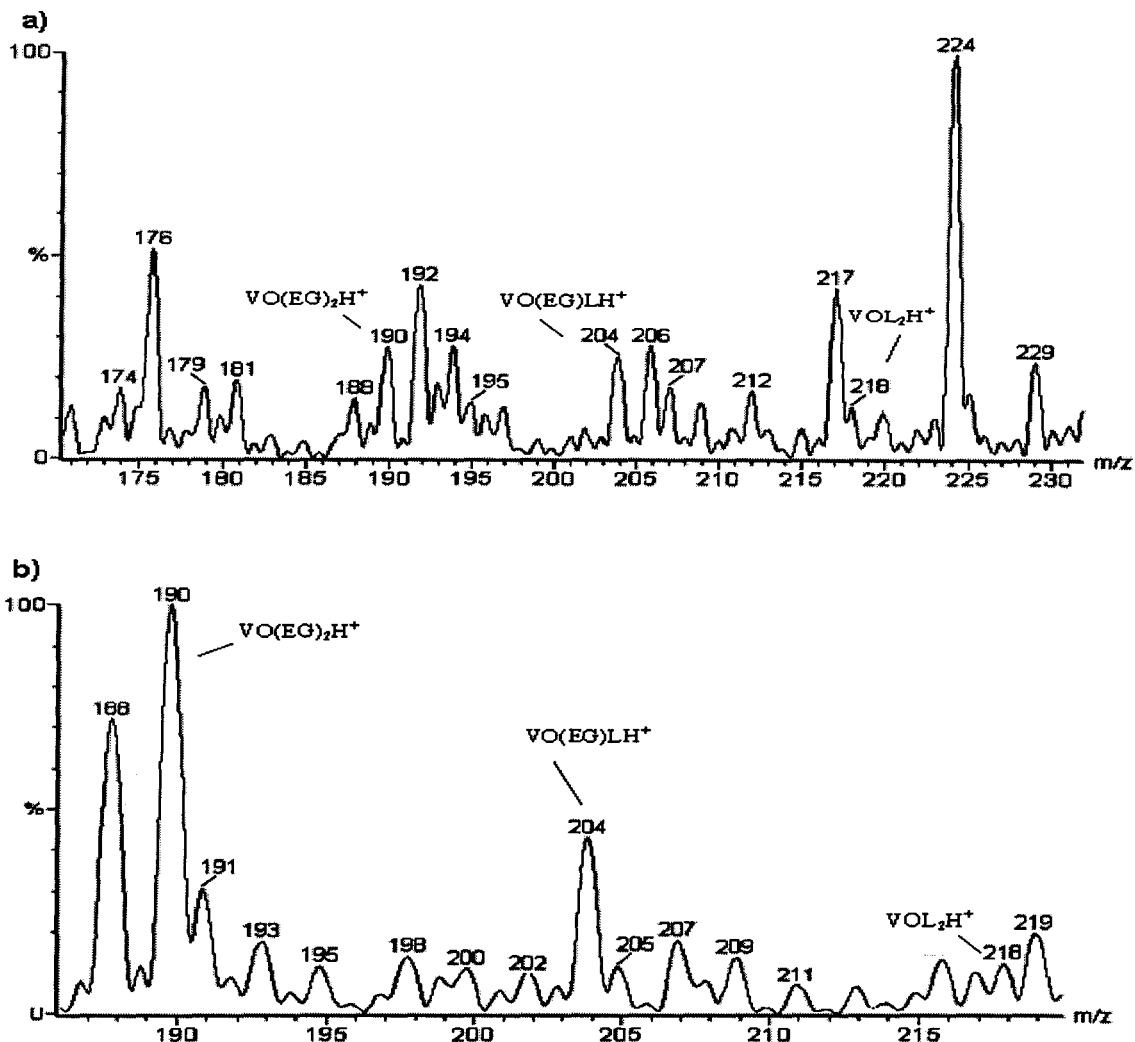


Figure 3.23. Partial ES spectra showing the complex ions $\text{VO}(\text{EG}_d)_2\text{H}^+$, $\text{VO}(\text{EG}_d)\text{L}_d\text{H}^+$ and $\text{VO}(\text{L}_d)_2\text{H}^+$ at a 1,2-propanediol to reagent ratio of 0.1 : 1 and a VO : EG concentration of 2.5×10^{-4} M (top spectrum) and 2.5×10^{-3} M (bottom spectrum).

At the 2.5×10^{-4} M reagent concentration, the lowest quantity of 1,2-propanediol that produced intensity ratios of the complexes of interest consistent with the calibration curves, corresponds to a diol to reagent mol ratio of 0.2 : 1. This solution produced the spectrum of Figure 3.24 ; the ratio of the mixed complex at m/z 204 to the reference complex at m/z 190, and the [2M] complex of 1,2-propanediol at m/z 218 to the mixed complex, produced mean values of 0.6 and 0.3, respectively. This scenario is taken to estimate the detection limit of 1,2-propanediol. It represents a diol concentration of 1.25×10^{-10} mol per 20 μL injection and translates into a practical detection limit of 6 picomol/ μL .

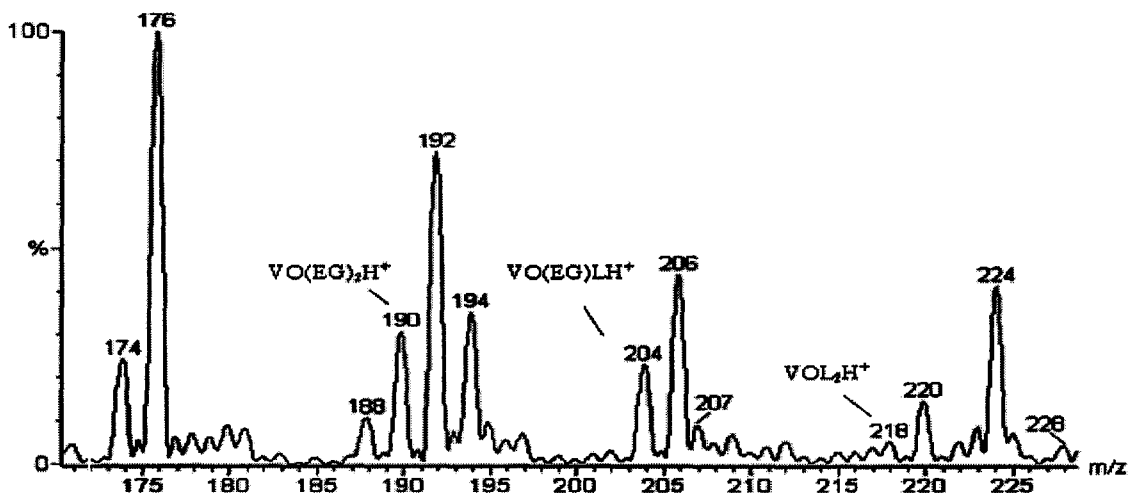


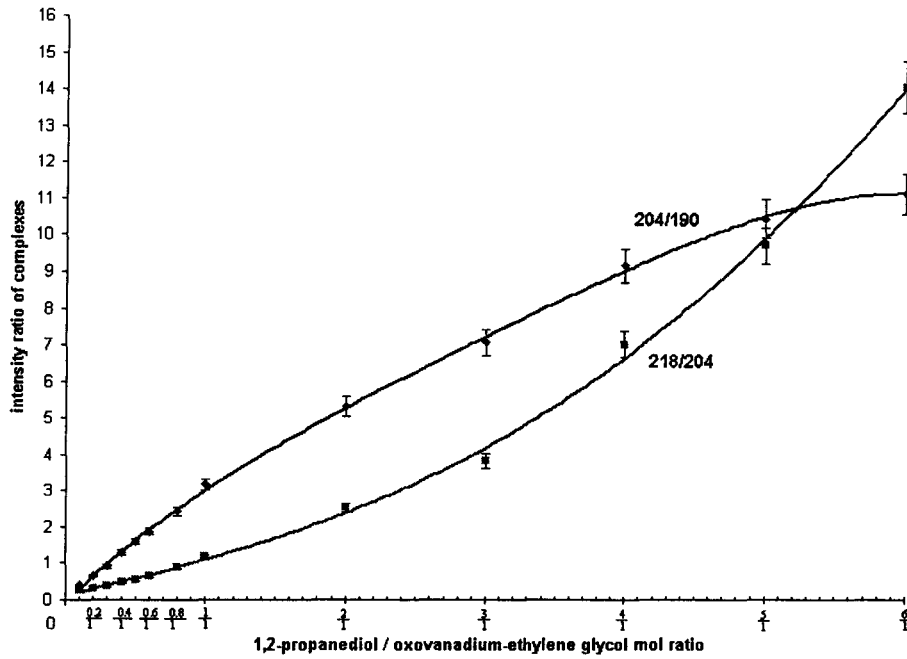
Figure 3.24. Partial ES spectrum showing the complex ions $\text{VO}(\text{EG}_d)_2\text{H}^+$, $\text{VO}(\text{EG}_d)\text{L}_d\text{H}^+$ and $\text{VO}(\text{L}_d)_2\text{H}^+$ at a VO : EG concentration of 2.5×10^{-4} M and a mol ratio of 1,2-propanediol to reagent of 0.2 : 1.

Calibration curves for the quantitative analysis of diols

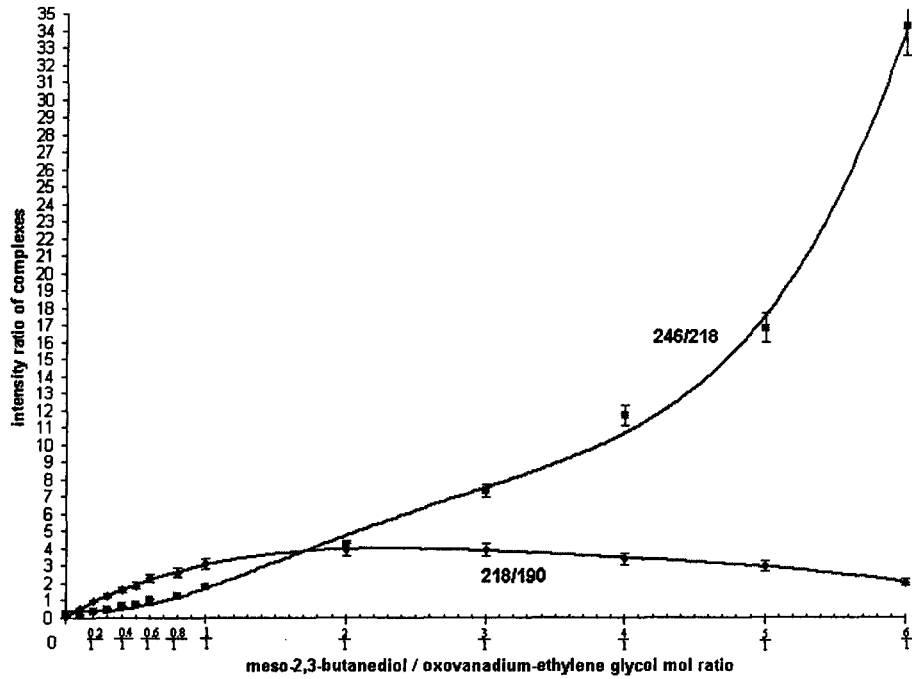
A series of reagent solutions at a concentration of 2.5×10^{-3} M was prepared to which a diol was added in a range of concentrations. This series of mixtures was used to record the change in intensity ratio of the diol complexes to the reagent complex. The diol to reagent mol ratio ranged from 0.1 : 1 to 6 : 1 and represents a diol concentration of 5×10^{-7} mol up to 3×10^{-5} mol per 20 μL injection ($0.25 \mu\text{mol}/\mu\text{L}$ to $1.5 \mu\text{mol}/\mu\text{L}$). The intensity ratios of the [2M] complex of the diol to the mixed complex, and that of the mixed complex to the [2M] complex of EG, were calculated and the graphs of intensity ratios versus mol ratios were constructed.

The graphs for 1,2-propanediol, *meso*-2,3-butanediol, *cis*-1,2-cyclopentanediol and *cis*-1,2-cyclohexanediol, are presented in Figure 3.25. These graphs show an exponential increase in the intensity of the [2M] complex of the diols when the diols are present beyond the 1:1 mol ratio to the reagent.

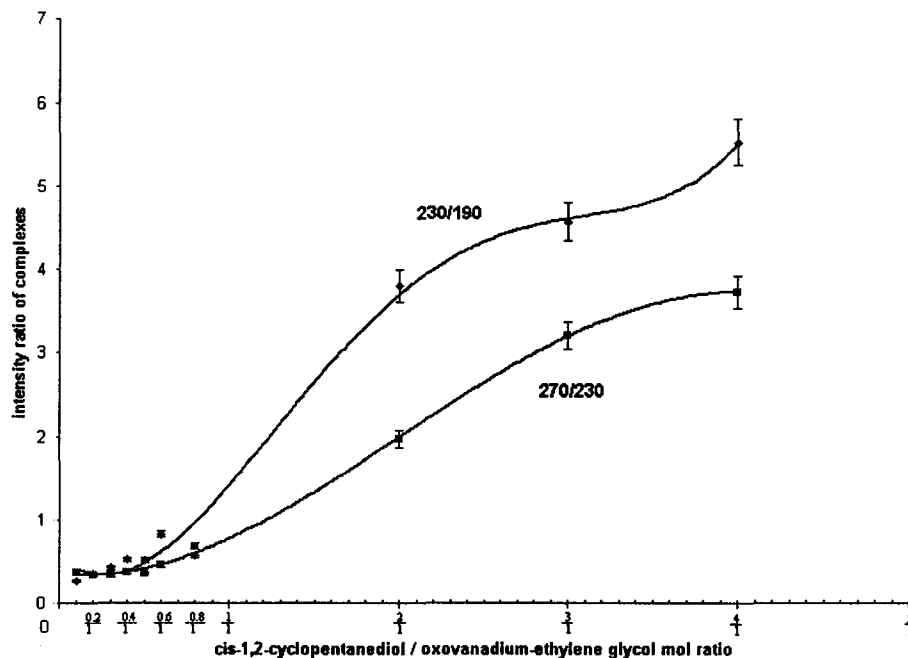
Calibration curve for oxovanadium-ethylene glycol complex reaction with 1,2-propanediol



Calibration curve for oxovanadium-ethylene glycol complex reaction with meso-2,3-butanediol



Calibration curve for oxovanadium-ethylene glycol complex reaction with cis-1,2-cyclopentanediol



Calibration curve for oxovanadium-ethylene glycol complex reaction with cis-1,2-cyclohexanediol

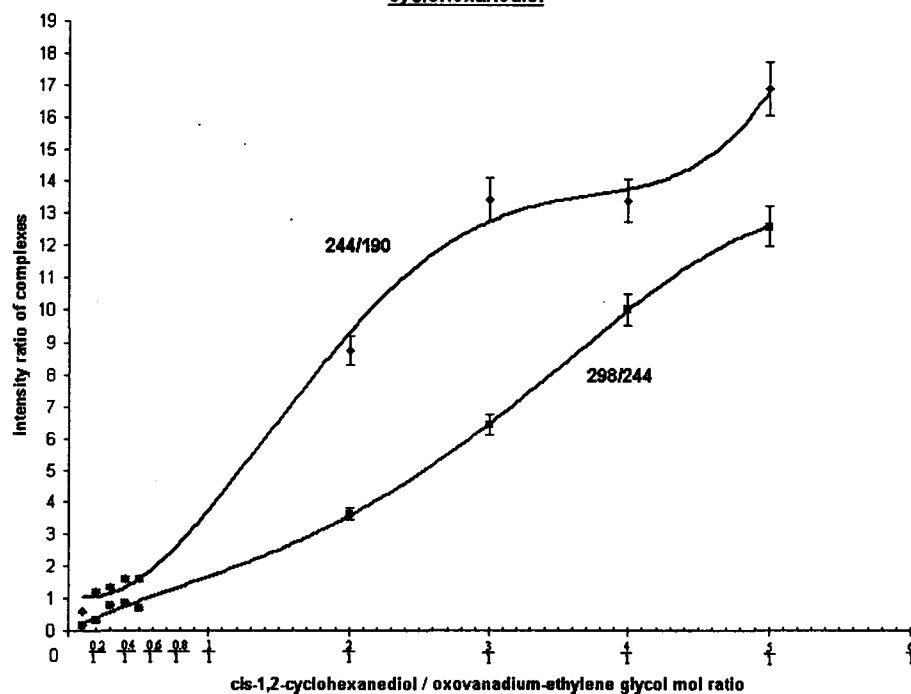


Figure 3.25 Plots of the intensity ratios of the mixed complex to the reagent complex and the diol [2M] complex to the mixed complex versus the diol to reagent mol ratio.

The graphs of Fig. 3.25 provide a useful tool for a preliminary analysis of the diol content of a given solution. At high diol concentrations the intensity of the reagent complex is reduced to such an extent that background chemical noise may make the quantitative analysis unreliable. If this is the case for a given sample, the value derived from the graph can be used as a guide to dilute or concentrate the unknown diol solution so that the measured ratios fall within the calibrated range of concentrations. The calibration curves for the diols are shown below.

It was found that the signal intensity of the [2M] complex of EG is reliably above the noise level only up to a diol : reagent mol ratio of 2 : 1 in almost all of the diols used in the calibration curve experiment. This represents a concentration of 0.025 μmol per 20 μL injection. The calibration curves of the diols were then constructed based on the concentration range that gives rise to a consistent and reliable signal intensity ratio of the [2M] complex of EG, the mixed complex and the [2M] complex of the diol up to a diol : reagent mol ratio of 2 : 1.

1. The calibration curve for 1,2-propanediol

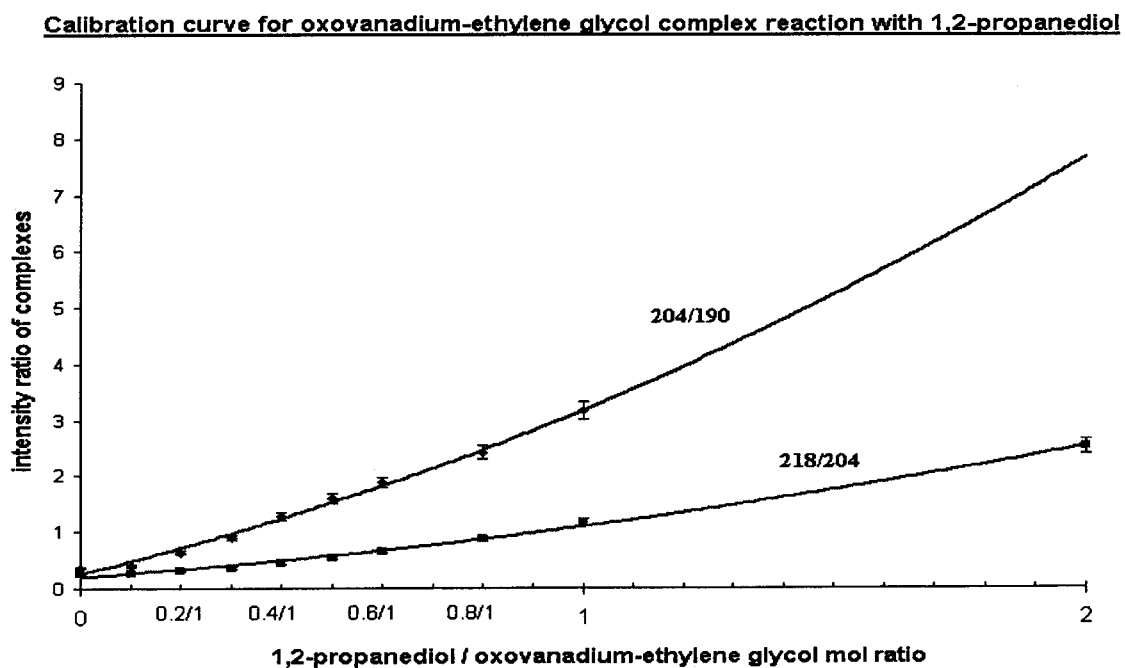


Figure 3.26. Calibration curve for 1,2-propanediol : [218/204] - diol [2M] complex to mixed complex, [204/190] - mixed complex to EG [2M] complex.

The calibration curve constructed for 1,2-propanediol is based on the intensity ratio of the mixed complex at m/z 204 to the [2M] complex of EG at m/z 190, and the [2M] complex of 1,2-propanediol at m/z 218 to the mixed complex. These two ratios yield two lines with the equations $y = 0.7943 x^2 + 2.1235 x + 0.2568$ for 204:190 and $y = 0.2808 x^2 + 0.6111 x + 0.1971$ for 218:204 as shown in Figure 3.26, with $R = 0.9943$ and $R = 0.996$ respectively. The range of error in the measured ratios varied only from 1 % to 6 %. These two intensity ratios can concurrently be used to calculate the concentration of 1,2-propanediol present in the unknown solution.

2. The calibration curve for *meso*-2,3-butanediol

Calibration curve for oxovanadium-ethylene glycol complex reaction with *meso*-2,3-butanediol

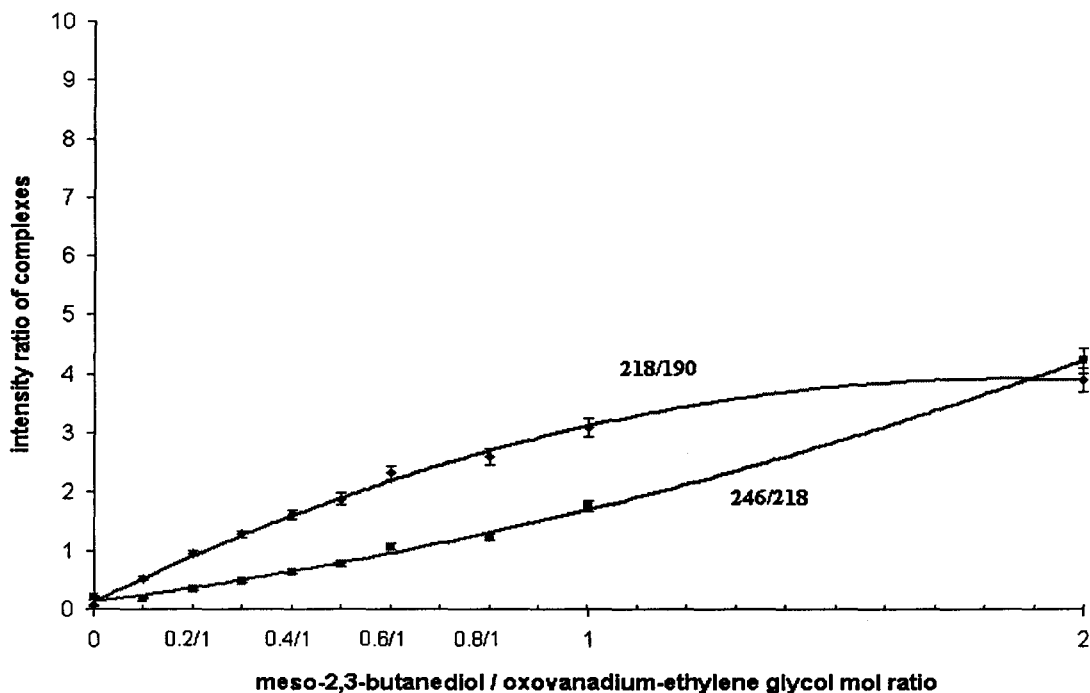


Figure 3.27. Calibration curve for *meso*-2,3-butanediol: [246/218] - diol [2M] complex to mixed complex, [218/190] - mixed complex to EG [2M] complex.

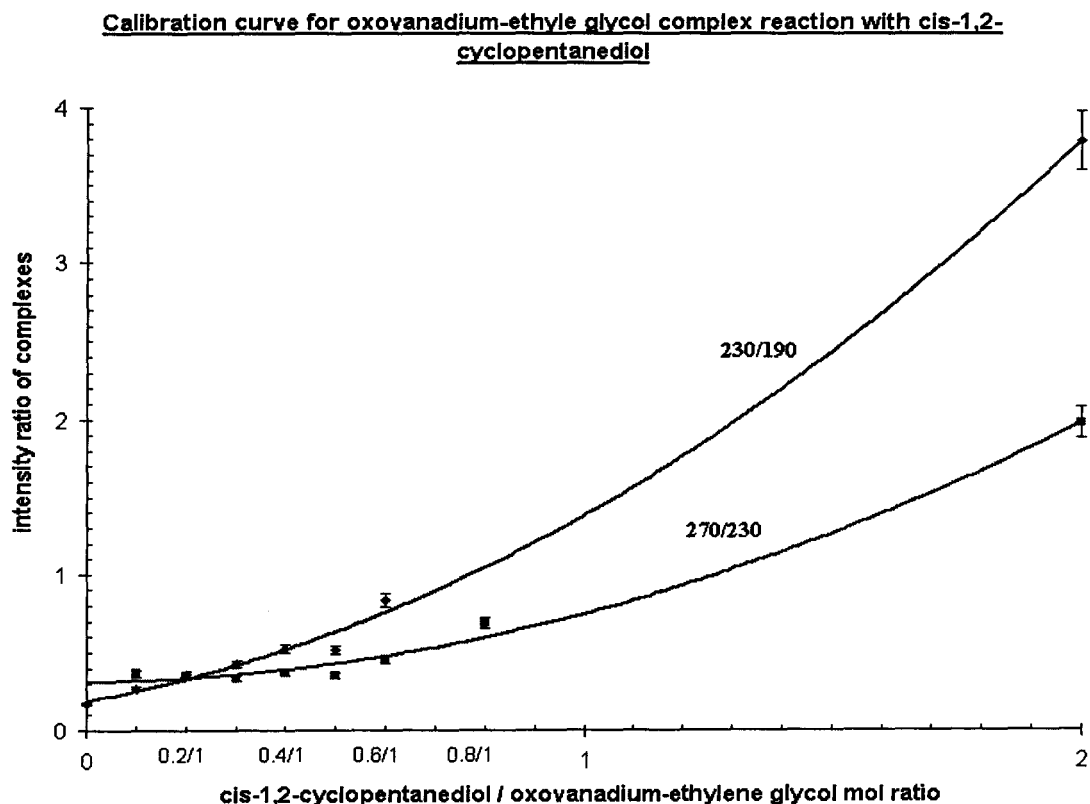
The calibration curves for *meso*-2,3-butanediol were constructed based on the intensity ratios of the [2M] complex of EG, the mixed complex and the [2M] complex of the *meso*-2,3-butanediol, against the diol to reagent mol ratio, following the procedure for

1,2-propanediol. The mixed complex and the reagent complex ratio (218:190) yields a line with an equation of $y = -1.117 x^2 + 4.1182 x + 0.1267$ with $R = 0.9974$, while the [2M] complex : mixed complex ratio (246:218) yields the calibration curve at $y = 0.4653 x^2 + 1.1308 x + 0.1225$ of $R = 0.9978$. The errors in the intensity ratios for both curves range from 1 % to 5 %. The curves are shown in Figure 3.27.

3. Calibration curves for cis-1,2-cyclopentanediol and cis-1,2- cyclohexanediol

The calibration curves for the cis-isomer of the cyclic diols were also prepared up to a diol to reagent molar ratio of 2 : 1. For cis-1,2-cyclopentanediol, the intensity ratio of the mixed complex at m/z 230 to the reagent,(230:190), produced a line with an equation of $y = 0.6347 x^2 + 0.5177 x + 0.2118$. The [2M] complex of cis-1,2-cyclopentanediol to the mixed complex (270:230) produced the curve at $y = 0.3984 x^2 + 0.0363 x + 0.311$, as shown in Figure 3.28a.

a)



b)

Calibration curve for oxovanadium-ethylene glycol complex reaction with cis-1,2-cyclohexanediol

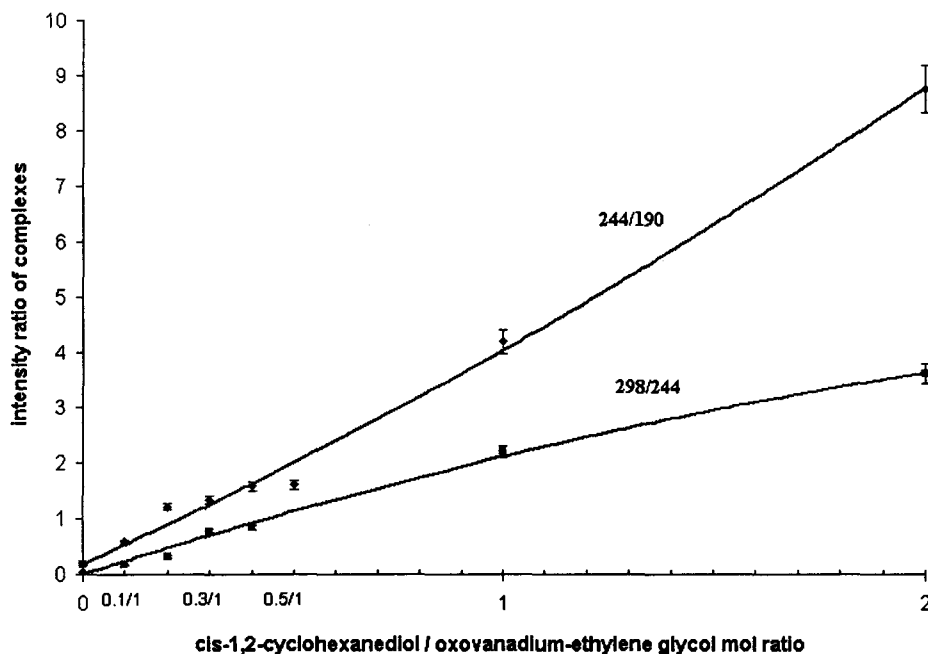


Figure 3.28 a) Calibration curve for cis-1,2-cyclopentanediol : [270/230] - diol [2M] complex to mixed complex, [230/190] - mixed complex to EG [2M] complex; b) Calibration curve for cis-1,2-cyclohexanediol: [298/244] - diol [2M] complex to mixed complex, [244/190] - mixed complex to EG [2M] complex.

The two calibration curves for the cyclopentanediol have acceptable regression values of 0.998 and 0.9917 respectively. However, the range of errors for this diol is quite large (between 1 % to 13 % of the mean).

On the other hand, cis-1,2-cyclohexanediol produced data with a better precision - comparable to that of 1,2-propanediol and *meso*-2,3-butanediol, see above – as reflected by an RSD value of 0 to 8 %. The intensity ratio of the mixed complex to the reagent (244:190), and the [2M] cis-1,2-cyclohexanediol complex to the mixed complex (298:244), yield calibration curves of $y = 0.4339 x^2 + 3.42 x + 0.1938$ and $y = -0.2946 x^2 + 2.4037 x + 0.0084$ respectively, as shown in Figure 3.28b.

Conclusions

The ease of diol complex formation and the extent of their competition with ethylene glycol for complexation to oxovanadium can be assessed by the relative intensity of the [2M] complex of the diols and the [2M] complex of EG, and the value of their formation constants, when a measured quantity of the diols is added to an aqueous solution of a preformed ethylene glycol/oxovanadium (IV) complex..

An ES/MS experiment is capable of differentiating the isomers by the intensity ratios of the [2M] complex of the EG, the mixed complex, and the [2M] complex of the diols. However, the MS/MS experiment provides more characteristic spectra of the isomers and should be used in combination with the ES spectra for the identification of the diols in solution.

The MS/MS experiments on the cyclic diols show that the trans-isomer characteristically loses the diol moiety of the complex, while the cis-isomer generates high intensity ions corresponding to the formation of the oxovanadium-diol complexes. This reflects the stability achieved for the cis-isomer by the formation of oxovanadium-diol complexes rather than complexation to EG, and vice versa for the trans isomer. The cis-isomer of the cyclohexanediols produced a distinctive peak at m/z 214, which corresponds to the loss of a formaldehyde. The cyclopentanediols, on the other hand, are not as easily differentiated by their MS/MS spectra. However, loss of H_2 is observed to be more prominent for the trans-isomer.

The difference between the *meso*-2,3- and (2*R*,3*R*)-(-)-2,3-butanediols is the tendency of the *meso*-isomer to consistently form fragments ions of higher intensity than its optically active counterpart, at m/z 146 and m/z 180. This is observed at collision voltages of 10 eV and 15 eV.

The sugar trehalose whose hydroxyl groups are in the trans position, as shown in S.Z.Ackloo's work [1], does not compete efficiently with ethylene glycol for complexation to oxovanadium, and the MS/MS spectrum shows that the dissociation of the mixed complex occurs mainly by the loss of water and a neutral of mass 120 Da.

The formation constants obtained for the complexation reaction of the diols to oxovanadium support the proposal that the diols compete effectively with ethylene glycol

for complexation to oxovanadium. Amines, however, do not form any complex with oxovanadium in the presence of ethylene glycol. This implies that amines and other nitrogen bases in biological matrices will not interfere with the analysis of polyols.

It is not possible to reliably differentiate the isomers of 2,3-butanediol and 1,2-cyclopentanediol because the CID spectra of the complexes are virtually the same.

Finally, it should be noted that the use of the oxovanadium complex with ethylene glycol- d_4 may provide a fast and reliable alternative method for the analysis of ethylene glycol in blood or urine samples [23].

References

1. S.Z. Ackloo. *Ph. D. Thesis*. McMaster University. 2001. p. 181.
2. a) Z. Zhang, J.E. Jackson, D.J. Miller. *Applied Catalysis A: General*. 219 (2001) 89;
b) R.L. Peterson, D.O. Rodgers. *Clinical Chemistry*. 20 (1974) 7.
3. L.L. Needham, R.H. Hill, D.L. Orti, M.E. Felver, J.A. Liddle. *J. Chromatog.* 233 (1982) 9.
4. a) K.S. Boos, B. Wilmers, E. Schlimme, R. Sauerbrey. *J. Chromatog.* 456 (1988) 93; b) B.W. Day, S. Naylor, L.S. Gan, Y. Sahali, T.T. Nguyen. *J. Chromatog.* 562 (1991) 563.
5. S.Z. Ackloo, P.C. Burgers, J.K. Terlouw, B.E. McCarry. *Rapid Commun. Mass Spectrom.* 13 (1999) 2406.
6. K.F. Purcell, J.C. Kotz. *Introduction to Inorganic Chemistry*. Saunders College. Philadelphia. 1980. p. 307.
7. C. Orvig, G.R. Hanson, Y. Sun. *Inorg. Chem.* 35 (1996) 6507.
8. N.D. Chasteen. *Vanadyl (IV) EPR Spin Probes Inorganic and Biochemical Aspects*. *In: Biological Magnetic Resonance*. V.3. L.J. Berliner and J. Reuben (Eds.). Plenum Press. New York. 1981. p. 53.
9. C. Orvig, P. Caravan, L. Gelmini, N. Glover, F.G. Herring, H. Li, J.H. McNeill, S.J. Rettig, I.A. Setyawati, E. Shuter, Y. Sun, A.S. Tracey, and V.G. Yuen. *J. Am. Chem. Soc.* 117 (1995) 12759.

10. a) F.A. Cotton and G. Wilkinson. *Advanced Inorganic Chemistry*. 3rd Ed. John Wiley & Sons, Inc. New York. 1972. p. 818; b) J. Selbin. *Chem. Rev.* 65 (1965) 153.
11. R.K. Murmann. *Inorg. Chim. Acta.* 25 (1977) L43.
12. Y. Sun, B.R. James, S. J. Rettig, C. Orvig. *Inorg. Chem.* 35 (1996) 1667.
13. P. Buglyo, E. Kiss, I. Fabian, T. Kiss, D. Sanna, E. Garribba and G. Micera. *Inorg. Chim. Acta.* 306 (2000) 174.
14. R.E. Tapscott and R.L. Belford. *Inorg. Chem.* 6 (1967) 735.
15. a) G. Micera, A. Dessi, H. Kozlowski, B. Radomska, J. Urbanska, P. Decock, B. Dubois and I. Olivier. *Carbohydr. Res.* 188 (1989) 25; b) M. Branca, G. Micera, A. Dessi and H. Kozlowski. *J. Chem. Soc. Dalton Trans.* (1989) 1283; c) M. Branca, G. Micera, A. Dessi and D. Sanna. *J. Inorg. Biochem.* 45 (1992) 169; d) M. Branca, G. Micera, A. Dessi, D. Sanna and H. Kozlowski. *J. Chem. Soc. Dalton Trans.* (1990) 1997.
16. C.R. Cornman, J. Kampf, M.S. Lah, V. L. Pecoraro. *Inorg. Chem.* 31 (1992) 2035.
17. E. de Boer, K. Boon, R. Wever. *Biochem.* 27 (1988) 1629.
18. a) K. Wiegardt, U. Bossek, K. Volckmar, W. Swiridoff, J. Weiss. *Inorg. Chem.* 23 (1984) 1387; b) K. Wiegardt, B. Nuber, W.S. Sheldrick, J. Weiss. *Inorg. Chem.* 29 (1990) 363.
19. X. Li, M.S. Lah, V.L. Pecoraro. *Inorg. Chem.* 27 (1988) 4657.
20. L. Xioping, Z. Kangjing. *J. Crystallogr. Spectros. Res.* 16 (1986) 681.
21. a) M.R. Asam, G.L. Glish. *J. Am. Soc. Mass Spectrom.* 8 (1997) 987; b) Z. Zhou, S. Ogden, J.A. Leary. *J. Org. Chem.* 55 (1990) 5444.
22. D.C. Crans, I. Boukhobza. *J. Am. Chem. Soc.* 120 (1998) 8069.
23. M. Balikova. *J. Chrom. Biomed. Appl.* 434 (1988) 469.

SUMMARY

Mass spectrometry is one of the most sensitive and widely applied instrumental techniques in analytical chemistry. In this thesis, the focus is on the application of two soft ionization techniques, namely electrospray and matrix-assisted laser desorption, to study small biomolecules.

Chapter 2 describes the application of a newly synthesized reagent, 4-hydrazino-4-oxobutyl tris(2,4,6-trimethoxyphenyl) phosphonium bromide for the derivatization of malondialdehyde using the solid phase analytical derivatization technique. The specific and in situ derivatization shortens the sample preparation time and minimizes interference. The reagent also produces a strong signal in the MALDI, with or without the application of a matrix. The elimination of the matrix further minimizes interference and provides an opportunity for the development of a fully automated methodology for the analysis of malondialdehyde.

The complexation of diols to oxovanadium ion is used as the basis to study the complexation competition between diols in Chapter 3, where the oxovanadium (IV) complex of ethylene glycol is used as the reagent. The aim of the study is to develop a fast and reliable method for the detection and quantitation of diols in aqueous solutions and in biological samples. The analysis is performed using the electrospray ionization technique. Tandem mass spectrometry is used to obtain the structural information and as a confirmation of the complexes formed. The MS/MS spectra may also provide additional information on the differences between the isomers of the diols studied.

The results of the studies promise fast and highly reliable methods for the study of aldehydes as a measure of oxidative stress, and the detection of diols in aqueous solutions or biological samples. These developments positively contribute to analytical and biomedical research.